

## Plane Waves in Lossless Media

Our study of waves has been limited so far to those depending upon only one space dimension. Most of the field aspects of the problem have been suppressed by our use of the voltage and current concepts. It is now our task to consider waves in more than one space dimension, and to pay more attention to the fields.

The *uniform* plane wave provides a simple and important special case of wave motion in space, at the same time retaining, from one point of view, many features characteristic of transmission-line waves. From another point of view, however, uniform plane waves lead to a consideration of the more general *nonuniform* plane waves, and to the whole question of guided waves.

The subject of plane waves is simplest when the medium in which they propagate is lossless. We treat this case in the present chapter, and the effects of loss in the next.

### 7.1 Uniform Plane Waves in the Time Domain

#### 7.1.1 Introduction

In Chapter 2, we encountered time-varying solutions of Maxwell's equations with electric and magnetic fields, each having only two components. These solutions are in a class we shall subsequently examine further, called TEM waves (transverse electromagnetic waves), so named because the field vectors lie completely in planes *transverse* to the direction of wave propagation. In Chapter 2, Sec. 2.3, moreover, we used the simplest form of such TEM waves to meet the boundary conditions imposed by parallel, perfectly conducting

planes. This solution had the second special property that, at any instant of time, neither  $\mathbf{E}$  nor  $\mathbf{H}$  varied with position in the transverse plane containing them. This type of solution is known as a *uniform plane wave* (or sometimes an infinite plane wave). It will be compared later with other TEM waves—like those on an open-wire line—in which the strength and direction of  $\mathbf{E}$  and  $\mathbf{H}$  do vary with position in the transverse planes containing them (see Chapter 9).

In the solution in Chapter 2, the direction of  $\mathbf{E}$  in space was chosen normal to the metal planes to meet the boundary conditions they imposed. However, it is clear that, if the planes were drawn apart indefinitely, the entire field in space would remain a solution to Maxwell's equations. Similarly, a uniform plane wave propagating in any direction in free space is also a solution of Maxwell's equations, inasmuch as

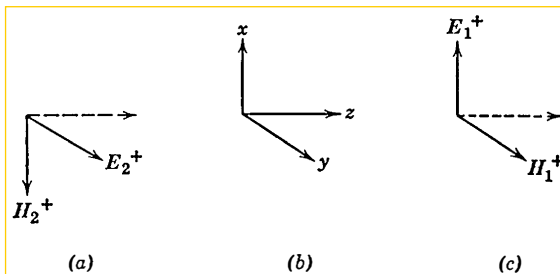


**Fig. 7.1.** Schematic pictures of two independent uniform plane waves propagating in the  $+z$  direction.

the direction of propagation may always be taken as the  $z$ -axis to conform with our previous results.

Since Maxwell's equations, as we have agreed to consider them, are linear vector equations, any sum of vector solutions is also a solution. Therefore a superposition of many uniform plane waves traveling in different directions in space is a valid electromagnetic field. Moreover, it is apparent that one uniform plane wave cannot be obtained as a linear combination of others propagating in different directions. Hence there are at least as many linearly independent uniform plane wave solutions to the field equations as there are different directions in space. More than this, even for a given direction of propagation, there are *two* linearly independent uniform plane-wave solutions to Maxwell's equations. Figure 7.1 and the following discussion are addressed to this matter.

### 7.1.2 Details of the Solution

In terms of the coordinate system of Fig. 7.1b, we shall write Maxwell's equations (Eqs. 1.24b, 1.25, and 1.31) for a lossless, linear, homogeneous medium with constant parameters ( $\sigma = 0$ ,  $\epsilon$ ,  $\mu$ ) and without sources. We shall consider the case of uniform plane waves, for which, by our definition,

$$(a) \quad E_z = H_z \equiv 0 \quad (7.1)$$

$$(b) \quad \frac{\partial}{\partial x} \equiv \frac{\partial}{\partial y} \equiv 0$$

There remain only the following equations, rearranged for convenience

$$(a) \quad \left. \begin{aligned} \frac{\partial E_x}{\partial z} &= -\mu \frac{\partial H_y}{\partial t} \\ \frac{\partial H_y}{\partial z} &= -\epsilon \frac{\partial E_x}{\partial t} \end{aligned} \right\} \text{Set 1}$$

$$(c) \quad \left. \begin{aligned} \frac{\partial E_y}{\partial z} &= \mu \frac{\partial H_x}{\partial t} \\ \frac{\partial H_x}{\partial z} &= \epsilon \frac{\partial E_y}{\partial t} \end{aligned} \right\} \text{Set 2} \quad (7.2)$$

$$(d) \quad \left. \begin{aligned} \frac{\partial E_y}{\partial z} &= \mu \frac{\partial H_x}{\partial t} \\ \frac{\partial H_x}{\partial z} &= \epsilon \frac{\partial E_y}{\partial t} \end{aligned} \right\} \text{Set 2}$$

There are two *independent* pairs of equations: equations 7.2a and 7.2b relate *only*  $E_x$  and  $H_y$ , whereas Eqs. 7.2c and 7.2d relate *only*  $E_y$  and  $H_x$ . Each pair is formally identical with the equations of a lossless transmission line. The solutions can be written immediately.

For Eqs. 7.2a and 7.2b, aside from the obvious d-c solutions, we have

$$(a) \quad E_x = f_+ \left( t - \frac{z}{v} \right) + f_- \left( t + \frac{z}{v} \right) \quad (7.3)$$

$$(b) \quad H_y = \frac{1}{\eta} \left[ f_+ \left( t - \frac{z}{v} \right) - f_- \left( t + \frac{z}{v} \right) \right]$$

where

$$(a) \quad \eta = + \sqrt{\frac{\mu}{\epsilon}} \equiv \text{characteristic wave impedance (ohms)} \quad (7.4)$$

$$(b) \quad v = \frac{1}{\sqrt{\epsilon\mu}} \equiv \text{velocity of light}$$

Considering the (+) and (-) waves separately, we have

$$(a) \quad E_x^+ = \eta H_y^+ = f_+ \left( t - \frac{z}{v} \right) \quad (7.5)$$

$$(b) \quad E_x^- = -\eta H_y^- = f_- \left( t + \frac{z}{v} \right)$$

If subscript 1 is used to denote the solution of Eq. 7.2, Set 1, we have

$$(a) \quad E_1 = a_x E_x = a_x E_x^+ + a_x E_x^- = E_1^+ + E_1^-$$

$$(b) \quad H_1 = a_y H_y = a_y H_y^+ + a_y H_y^- = H_1^+ + H_1^- \quad (7.6)$$

Equations 7.5 become

$$(a) \quad E_1^+ = \eta H_1^+ \times a_z$$

$$(b) \quad E_1^- = -\eta H_1^- \times a_z \quad (7.7)$$

Equation 7.5a is represented schematically by Fig. 7.1c, in which the dotted line shows the direction of propagation (+z).

For Eqs. 7.2c and 7.2d, the obvious modification of algebraic sign yields

$$(a) \quad E_y = g_+ \left( t - \frac{z}{v} \right) + g_- \left( t + \frac{z}{v} \right)$$

$$(b) \quad H_x = -\frac{1}{\eta} \left[ g_+ \left( t - \frac{z}{v} \right) - g_- \left( t + \frac{z}{v} \right) \right] \quad (7.8)$$

The functions  $g_{\pm}$  are in no way related to the functions  $f_{\pm}$  in Eqs. 7.3 as far as Eqs. 7.2 are concerned, because Eqs. 7.2c and 7.2d are completely independent of Eqs. 7.2a and 7.2b. In place of Eqs. 7.5, we now have

$$(a) \quad E_y^+ = -\eta H_x^+ = g_+ \left( t - \frac{z}{v} \right)$$

$$(b) \quad E_y^- = \eta H_x^- = g_- \left( t + \frac{z}{v} \right) \quad (7.9)$$

If subscript 2 is used to denote the solution of Eq. 7.2, Set 2, we have

$$(a) \quad E_2 = a_y E_y = a_y E_y^+ + a_y E_y^- = E_2^+ + E_2^-$$

$$(b) \quad H_2 = a_x H_x = a_x H_x^+ + a_x H_x^- = H_2^+ + H_2^- \quad (7.10)$$

Equations 7.9 become

$$(a) \quad E_2^+ = \eta H_2^+ \times a_z$$

$$(b) \quad E_2^- = -\eta H_2^- \times a_z \quad (7.11)$$

Equation 7.9a is represented schematically by Fig. 7.1a.

Equations 7.7 and 7.11 prove that  $E_{1,2}^{+,-}$ ,  $H_{1,2}^{+,-}$ , and the direction of propagation are mutually perpendicular for each of the four

separate waves. Their relative orientations are such that the Poynting vector  $S_{1,2}^+$  is at every instant in the direction of propagation.

$$(a) S_{1,2}^+ = E_{1,2}^+ \times H_{1,2}^+ = \eta |H_{1,2}^+|^2 a_z = \frac{1}{\eta} |E_{1,2}^+|^2 a_z \quad (7.12a)$$

$$(b) S_{1,2}^- = E_{1,2}^- \times H_{1,2}^- = -\eta |H_{1,2}^-|^2 a_z = -\frac{1}{\eta} |E_{1,2}^-|^2 a_z \quad (7.12b)$$

We conclude that every uniform plane wave propagating in a given direction (the  $+z$  direction, for example) can always be decomposed into two waves having the same direction of propagation but with mutually perpendicular electric (and magnetic) fields. Therefore any such solution  $E_T^+$  and  $H_T^+$  is expressible in the form

$$(a) E_T^+ = a_x E_x^+ + a_y E_y^+ = E_1^+ + E_2^+ \quad (7.13a)$$

$$(b) H_T^+ = a_x H_x^+ + a_y H_y^+ = H_1^+ + H_2^+ \quad (7.13b)$$

where the subscript  $T$  stipulates that  $E$  and  $H$  lie in planes transverse to the direction of propagation. A similar conclusion applies to  $(-)$  waves.

### 7.1.3 Power Considerations and Orthogonality

Having assured ourselves that every uniform plane wave may be expressed as a linear combination of the preceding four solutions, we must now consider some general properties of the energy flow, or Poynting vector, for such linear combinations.

First, the power carried by the general  $(+)$  wave (Eq. 7.13) is the algebraic sum of the  $(+)$  wave powers carried by each component wave separately. To prove this, note that

$$\begin{aligned} S^+ &= E_T^+ \times H_T^+ = (E_1^+ + E_2^+) \times (H_1^+ + H_2^+) \\ &= E_1^+ \times H_1^+ + E_2^+ \times H_2^+ + E_1^+ \times H_2^+ \\ &\quad + E_2^+ \times H_1^+ \end{aligned} \quad (7.13c)$$

But

$$E_1^+ \times H_2^+ = E_2^+ \times H_1^+ \equiv 0 \quad (7.13d)$$

because  $E_1^+$  and  $E_2^+$  are parallel to  $H_2^+$  and  $H_1^+$  respectively. Therefore, as stated above,

$$S^+ = S_1^+ + S_2^+ \quad (7.13e)$$

Similarly, for the  $(-)$  waves:

$$S^- = S_1^- + S_2^- \quad (7.13f)$$

The fact that the power in a  $(+)$  [or  $(-)$ ] wave of Set 1 adds *without cross terms* to the power in a  $(+)$  [or a  $(-)$ ] wave of Set 2, to give the total  $(+)$  [or  $(-)$ ] wave power when waves of Sets 1 and 2 are present together, is one example of a more general condition known as *orthogonality* of two solutions of a set of differential equations. The usual statement of such a condition involves an integration. For instance, suppose that in a region  $R$  of space (or time)  $\phi_i$  and  $\phi_j$  are two different scalar solutions of the same differential equation. Then these functions are said to be orthogonal if

$$\int_R \phi_i \phi_j dR = 0 \quad \text{when } i \neq j$$

If  $\phi_i$  and  $\phi_j$  are vector functions, the multiplication under the integral would be either a dot- or cross-product. Sometimes the integration need not cover the whole region  $R$  but may involve only a line or plane in it. In the present case of uniform plane waves, the fields do not vary with position at all over planes normal to the direction of propagation. Accordingly, a result like Eq. 7.13d may be integrated over any area in the plane of the fields. Indeed, it may most conveniently be regarded as an orthogonality condition *per unit area*.

As indicated above, the orthogonality of two functions makes sense only if they are different. By this, we mean that one is not simply a (nonzero) constant times the other ( $\phi_j \neq a\phi_i$ ). When they are different in this sense, the functions are said to be *linearly independent*. Evidently, orthogonality is not simply a consequence of the linear independence of the two functions in question. Additional conditions are necessary. For example, in the present field problem, the solutions  $E_1$  and  $E_2$  are orthogonal specifically because of their perpendicular relation in real space. Such a relationship is by no means implied in the word "orthogonality," as used in the general theory of orthogonal functions, and we shall shortly see examples of orthogonality arising for quite different reasons.

To proceed still further with these ideas, consider the complete combination of  $(+)$  and  $(-)$  waves of Sets 1 and 2 (Eqs. 7.6 and 7.10). The Poynting vector is

$$\begin{aligned} S &= (E_1 + E_2) \times (H_1 + H_2) \\ &= E_1 \times H_1 + E_2 \times H_2 + (E_2 \times H_1 + E_1 \times H_2) \\ &= S_1 + S_2 + (E_2^+ \times H_1^- + E_2^- \times H_1^+ \\ &\quad + E_1^+ \times H_2^- + E_1^- \times H_2^+) \end{aligned} \tag{7.13g}$$

in which we have already used Eq. 7.13d and its analog for  $(-)$  waves.

Once again, however,

$$\mathbf{E}_{2,1}^+ \times \mathbf{H}_{1,2}^- = \mathbf{E}_{2,1}^- \times \mathbf{H}_{1,2}^+ \equiv 0 \quad (7.13h)$$

because  $\mathbf{E}_{2,1}^+$  and  $\mathbf{E}_{2,1}^-$  are parallel respectively to  $\mathbf{H}_{1,2}^-$  and  $\mathbf{H}_{1,2}^+$ . It follows that the (+) waves of one solution type are orthogonal to the (-) waves of the other and that

$$\mathbf{S} = \mathbf{S}_1 + \mathbf{S}_2 \quad (7.13i)$$

Finally, the similarity of Eqs. 7.3 and 7.8 to those of a lossless transmission line reminds us that the power carried by combined (+) and (-) waves of either Set 1 or Set 2 is also simply the algebraic sum of those carried separately by the (+) and (-) waves alone:

$$\mathbf{S}_{1,2} = \mathbf{S}_{1,2}^+ + \mathbf{S}_{1,2}^- \quad (7.13j)$$

although the reason for this fact is quite different from that underlying Eqs. 7.13e, 7.13f, or 7.13i. Here, indeed, we find an orthogonality relation between two solutions having *parallel* electric fields!

The net result of the power relations, Eqs. 7.13e, 7.13f, 7.13i, and 7.13j, is that in a lossless, homogeneous, linear medium with constant parameters the four possible linearly independent uniform plane waves that have a common (undirected) axis of propagation (e.g., the  $\pm z$ -axis) may always be, and have here been, chosen to be *mutually orthogonal*. That is, the total power (per unit area in this case) carried by the field when all the waves are simultaneously present is simply the vector sum of the powers that each would carry if it existed alone in space. There are no cross terms.

#### 7.1.4 Polarization

We have found that waves of Sets 1 and 2 *can* always be studied separately, not only in the light of normal superposition theory but also in connection with power. It is now appropriate to emphasize another characteristic of these waves which makes them particularly easy to treat separately: the space directions of  $\mathbf{E}_1$  (or  $\mathbf{E}_2$ ) and  $\mathbf{H}_1$  (or  $\mathbf{H}_2$ ) remain along fixed lines in any transverse plane at all times. Thus, as indicated by Eqs. 7.6 and 7.3,  $\mathbf{E}_1$  always lies along a line parallel to the  $x$ -axis. It may reverse direction along this line as time progresses, depending upon the behavior of  $f_+$  and  $f_-$ , but no other change of direction occurs. Similar comments apply to  $\mathbf{H}_1$ ,  $\mathbf{E}_2$ , and  $\mathbf{H}_2$ . To emphasize this behavior, these waves are referred to as being *linearly polarized*. In most of the recent electrical engineering literature, the direction of polarization is taken to be that of  $\mathbf{E}$ ; so we shall say that

the wave  $(E_1, H_1)$  is linearly polarized in the  $x$ -direction while  $(E_2, H_2)$  is linearly polarized in the  $y$ -direction. This situation is illustrated for the  $(+)$  waves by the sketches in Figs. 7.1a and 7.1c. A similar picture would apply for  $(-)$  waves. For both together, the linear polarization remains, but propagation direction loses meaning.

The most general uniform plane-wave propagating in a given direction is not linearly polarized. Indeed, Eqs. 7.13a, 7.8a, and 7.3a show that  $E_T^+$  has, in general, two space components in the transverse plane, and that at any given point in space these components may be quite different functions of the time. At one moment  $E_x^+$  might be large and  $E_y^+$  zero, whereas, at a later time,  $E_u^+$  might be large and  $E_x^+$  zero. Evidently the tip of the vector  $E_T^+$  traces some complicated path in the transverse plane, just as the spot on an oscilloscope screen executes an involved pattern when arbitrarily different voltage time functions are impressed upon the vertical and horizontal axes. An extreme case of such complicated behavior in electromagnetic waves is that of "unpolarized" light. Its two electric field components are statistically independent Gaussian random time functions, with equal rms amplitudes and zero average values. Its polarization is therefore "random," i.e.,  $E_T$  is at any instant as likely to be pointing in one direction as another in the transverse plane.<sup>1</sup> Therefore, in view of the wide latitude of the general case, it is comforting to know that for each direction of propagation we need consider only two independent solutions having mutually perpendicular *linear* polarizations.

### 7.1.5 Role of Uniform Plane Waves

Since the field of a uniform plane wave extends with constant strength over the infinite area of any transverse plane, the total power carried by such a wave is also infinite. Thus no physical source can possibly be expected to produce exactly such a wave. Nevertheless, we shall find later, from our study of radiation, that at large enough distances from any physical source the field in suitably defined *finite* regions of space approximates closely that of uniform plane waves propagating in appropriate directions. For this reason and others, a thorough understanding of these simple waves in space is fundamental to any study of electromagnetic energy transmission and radiation. There are, however, other simple solutions of Maxwell's equations which are even more important, and it is not our intention to exclude them by this statement.

<sup>1</sup> The reader interested in justifying this statement more carefully than is necessary for the purposes of the present discussion will find support in Prob. 7.6.

We have shown on physical grounds that one or more uniform plane waves propagating in any direction or directions in free space constitutes a solution of Maxwell's equations. If we imagine one such wave propagating in the  $+z$  direction, and regard this as an *incident* wave produced by some remote source, we may ask the question: "What happens when an object is placed in the path of this wave?" Unquestionably, the original wave alone will rarely satisfy the boundary conditions imposed by the object. The field in the space about the object will almost surely be modified. From our study of transmission lines, we have learned to interpret this modification as a "reflection" of some sort. In this case, however, the reflected field may or may not be another uniform plane wave. Its nature depends entirely upon the geometry and electrical character of the object.

A perfectly conducting metal sphere placed at  $z = 0$  may "scatter" the incident wave in all directions. The reflected field would then be more properly described as a scattered field, and it would not be a simple uniform plane wave.

On the other hand, we should not be surprised to find that a smooth, infinite, plane, perfectly conducting metal sheet placed normal to the direction of propagation will act like an optical mirror. It will simply throw the incident wave back upon itself. The reflected wave is then another uniform plane wave propagating in the opposite direction. If this mirror is not normal to the direction of propagation of the incident wave, optical experience suggests that the reflected field should be another uniform plane wave whose direction of propagation obeys the familiar law: angle of reflection equals angle of incidence.

When the object is a dielectric or a real metal rather than a perfect conductor, we expect to be concerned with refraction as well as reflection, although, again, the question of whether or not the reflected and refracted fields are simple uniform plane waves depends upon the shape and electrical character of the object.

To solve the more elaborate among the types of problems described above, uniform plane wave solutions are insufficient. In the sinusoidal steady state or frequency domain, however, it is not difficult to find some more general plane wave solutions to Maxwell's equations. These are called *nonuniform plane waves* in this book, although the nomenclature is not standard and perhaps not sufficiently descriptive. The important theoretical point about these solutions is that, with the uniform plane waves we have already found, *they suffice to solve any steady-state field problem comprising regions of different linear, homogeneous, isotropic, time-invariant materials*. Like the sinusoid (or exponential) in time, these plane waves form a set of building blocks

in space which may be combined by Fourier-integral methods to meet a wide selection of boundary conditions. Although we will not consider elaborate problems here, it is obviously important to study carefully the character of both uniform and nonuniform plane waves in the sinusoidal steady state, and to apply them to the solution of some simple examples.

Restriction to the sinusoidal steady state, of course, implies no loss of generality, in view of the normal Fourier-integral techniques for time functions.

## 7.2 Plane Waves in the Sinusoidal Steady State and Frequency Domain

As stated above, the nonuniform plane wave has significance only in the sinusoidal steady state or the frequency domain. The uniform plane wave, however, has significance both in the time domain, as discussed in the preceding section, and in the frequency domain. It is therefore advantageous to begin our study of plane waves in the frequency domain with the uniform plane wave. Our discussion of this subject is to be guided by the fact that we wish to go on into the more general case. The treatment may therefore appear to be less direct than the topic of uniform plane waves itself would require.

### 7.2.1 Uniform Plane Waves in the Frequency Domain

**7.2.1.1 FORM OF THE SOLUTION.** The formal similarity of Eqs. 7.2a, 7.2b, 7.3, and 7.4 to those of a lossless transmission line tells us at once that the complex steady-state solution for  $x$ -polarized uniform plane waves traveling in the  $\pm z$  directions is

$$(a) \quad E_x = E_{x0}^+ e^{-j\beta_0 z} + E_{x0}^- e^{j\beta_0 z} \quad (7.14)$$

$$(b) \quad H_y = \frac{1}{\eta} (E_{x0}^+ e^{-j\beta_0 z} - E_{x0}^- e^{j\beta_0 z})$$

where

$$\beta_0 = +\omega\sqrt{\epsilon\mu} \quad (7.15)$$

and  $E_{x0}^+$ ,  $E_{x0}^-$  are complex constants independent of  $(x, y, z)$ . For the (+) wave,  $E_x^+ (= \operatorname{Re}[E_{x0}^+ e^{j(\omega t - \beta_0 z)}])$  and  $H_y^+ (= \operatorname{Re}[H_{y0}^+ e^{j(\omega t - \beta_0 z)}] = \operatorname{Re}[(E_{x0}^+ / \eta) e^{j(\omega t - \beta_0 z)}])$  are in time phase and have the ratio  $\eta$  at every point in space, and at every instant. We may wish to interpret

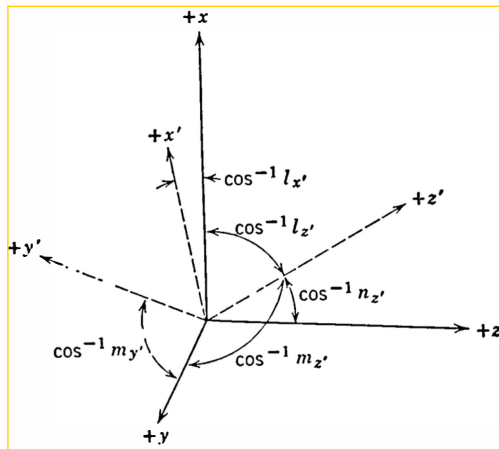


Fig. 7.2. Rotation of coordinate axes.

the (+) solution as an incident wave and the (−) one as a reflected wave. This interpretation certainly is valid under appropriate boundary conditions to which we will return in detail later. Now we prefer to examine the solution itself from another point of view.

Consider just the (+) wave in Eqs. 7.14 and 7.15, and suppose the axes  $(x, y, z)$  used to describe it there are not actually the ones we wish to use in our problem. Such a situation arises, for example, in describing simultaneously several uniform plane waves propagating in different space directions. Let us reserve  $(x, y, z)$  for the axes we really plan to use, and rewrite the (+) wave part of Eq. 7.14 with new variables  $(x', y', z')$  substituted for  $(x, y, z)$ . From the point of view of the  $(x, y, z)$  coordinates, the  $(x', y', z')$  axes are then a right-handed set of rotated axes having the same origin as  $(x, y, z)$ , Fig. 7.2, but with the  $+x'$ -axis chosen parallel to the (linearly polarized) electric field vector of the (+) wave of interest, and the  $+z'$ -axis chosen parallel to the direction of propagation. Therefore

$$(a) \quad \mathbf{E}^+ = a_x E_{x'0} e^{-j\beta_0 z'} \quad (7.16)$$

$$(b) \quad \mathbf{H}^+ = \frac{1}{\eta} a_y E_{x'0} e^{-j\beta_0 z'}$$

With reference to Fig. 7.2 again, let the (real) direction cosines of axis  $+z'$  with respect to axes  $(+x, +y, +z)$  respectively be  $(l_{z'}, m_{z'}, n_{z'})$ . Similarly, let  $(l_{x'}, m_{x'}, n_{x'})$  and  $(l_{y'}, m_{y'}, n_{y'})$  apply correspondingly to

axes  $+x'$  and  $+y'$  respectively. Then because the axes  $(x, y, z)$  are a rectangular set, we have for the  $+z'$ -axis direction cosines

$$l_{z'}^2 + m_{z'}^2 + n_{z'}^2 = 1 \quad (7.17)$$

Similar results for the  $+x'$  and  $+y'$  axes are obtained by simply replacing  $z'$  with  $x'$  or  $y'$ .

We wish now to describe the field (Eq. 7.16) in terms of the  $(x, y, z)$  coordinates and also the unit vectors  $\mathbf{a}_x, \mathbf{a}_y, \mathbf{a}_z$  along the corresponding axes, whereas it is presently described in the coordinates  $(x', y', z')$  and the unit vectors  $\mathbf{a}_{x'}, \mathbf{a}_{y'}, \mathbf{a}_{z'}$  along them.

To this end we note first that the position of any point in space is given by its vector displacement  $\mathbf{r}$  from the origin, and that this same vector is expressible in two ways, corresponding to the two sets of axes.

$$\mathbf{r} = \mathbf{a}_x x + \mathbf{a}_y y + \mathbf{a}_z z = \mathbf{a}_{x'} x' + \mathbf{a}_{y'} y' + \mathbf{a}_{z'} z' \quad (7.18)$$

Taking the dot product of both sides of Eq. 7.18 with  $\mathbf{a}_{z'}$ , and noting that axes  $(x', y', z')$  are a rectangular set, we find

$$z' = l_{z'} x + m_{z'} y + n_{z'} z \quad (7.19)$$

Therefore the phase factor  $\beta_0 z'$  in Eq. 7.16 becomes

$$\begin{aligned} \beta_0 z' &= (\beta_0 l_{z'}) x + (\beta_0 m_{z'}) y + (\beta_0 n_{z'}) z \\ &= \beta \cdot \mathbf{r} \end{aligned} \quad (7.20)$$

with

$$\begin{aligned} \beta &= \mathbf{a}_x (\beta_0 l_{z'}) + \mathbf{a}_y (\beta_0 m_{z'}) + \mathbf{a}_z (\beta_0 n_{z'}) \\ &= \mathbf{a}_x \beta_x + \mathbf{a}_y \beta_y + \mathbf{a}_z \beta_z \end{aligned} \quad (7.21a)$$

where

$$\beta_x = \beta_0 l_{z'} \quad \beta_y = \beta_0 m_{z'} \quad \beta_z = \beta_0 n_{z'} \quad (7.21b)$$

and

$$\beta \cdot \beta = |\beta|^2 = \beta_0^2 (l_{z'}^2 + m_{z'}^2 + n_{z'}^2) = \beta_x^2 + \beta_y^2 + \beta_z^2 = \beta_0^2 \quad (7.22)$$

The propagation vector  $\beta$  is in this case a *real* space vector, whose direction is that of the propagation of the wave and whose magnitude is the phase constant  $\beta_0 = \omega \sqrt{\epsilon \mu}$ .

Next, from the geometry of Fig. 7.2 we note that

$$\mathbf{a}_{x'} = \mathbf{a}_x l_{x'} + \mathbf{a}_y m_{x'} + \mathbf{a}_z n_{x'} \quad (7.23)$$

Consequently

$$\begin{aligned} \mathbf{a}_{x'} \mathbf{E}_{x'0}^+ &= \mathbf{a}_x l_{x'} \mathbf{E}_{x'0}^+ + \mathbf{a}_y m_{x'} \mathbf{E}_{x'0}^+ + \mathbf{a}_z n_{x'} \mathbf{E}_{x'0}^+ \\ &= \mathbf{E}_0^+ \end{aligned} \quad (7.24a)$$

where  $\mathbf{E}_0^+$  is a complex vector independent of  $(x, y, z)$ .

From Eqs. 7.24a and 7.21a we find

$$\beta \cdot \mathbf{E}_0^+ = \beta_0 \mathbf{E}_{x'0}^+ (l_{x'} l_{z'} + m_{x'} m_{z'} + n_{x'} n_{z'}) = 0 = \beta \cdot \mathbf{E}^+ \quad (7.24b)$$

since the  $[x']$ - and  $[z']$ -axes are perpendicular. The meaning of Eq. 7.24b is that the instantaneous electric field  $\mathbf{E}^+(t)$  is at all times perpendicular to the direction of propagation; but this conclusion is less obvious from Eq. 7.24b than it may appear offhand. In general, the vanishing of the dot product of two *complex* vectors does *not* imply any simple perpendicular condition in *real* space. In Eq. 7.24b, however,  $\beta$  is a *real* vector, so  $\beta \cdot \mathbf{E}^+ = 0$  only occurs if  $\beta \cdot \text{Re } \mathbf{E}^+ = 0$  and  $\beta \cdot \text{Im } \mathbf{E}^+ = 0$ . Since  $\text{Re } \mathbf{E}^+$  and  $\text{Im } \mathbf{E}^+$  determine the plane in which  $\mathbf{E}^+(t)$  lies at all times (Sec. 1.2.2.1),  $\beta$  is indeed perpendicular to this plane and, therefore, to  $\mathbf{E}^+(t)$ . Of course, this perpendicular relation was true of the original field (Eq. 7.16), and the use of new axes  $(x', y', z')$  could hardly be expected to alter it. Nevertheless, the point about interpreting Eq. 7.24b is important for our later work.

In connection with the magnetic field (Eq. 7.16b), we note that  $(x', y', z')$  is a right-handed set of rectangular axes like  $(x, y, z)$ . Therefore

$$\begin{aligned} a_{y'} \mathbf{E}_{x'0}^+ &= (\mathbf{a}_{z'} \times \mathbf{a}_{x'}) \mathbf{E}_{x'0}^+ = \mathbf{a}_{z'} \times (\mathbf{a}_{x'} \mathbf{E}_{x'0}^+) \\ &= \mathbf{a}_{z'} \times \mathbf{E}_0^+ = (a_x l_{z'} + a_y m_{z'} + a_z n_{z'}) \times \mathbf{E}_0^+ \\ &= \frac{\beta}{\beta_0} \times \mathbf{E}_0^+ \end{aligned} \quad (7.25)$$

where we have also used Eqs. 7.24a and 7.21a.

In summary, the solution (Eq. 7.16) in the  $(x, y, z)$  axis system becomes:

$$\begin{aligned} (a) \quad \mathbf{E}^+ &= \mathbf{E}_0^+ e^{-j\beta \cdot r} = \mathbf{E}_0^+ e^{-j\beta_x x} e^{-j\beta_y y} e^{-j\beta_z z} \\ (b) \quad \mathbf{H}^+ &= \frac{\beta \times \mathbf{E}^+}{\omega \mu} \end{aligned} \quad (7.26)$$

The fact that  $\beta$  is real allows us to interpret Eqs. 7.24b and 7.26b as showing the mutual perpendicularity of  $\beta$ ,  $\mathbf{H}^+(t)$ , and  $\mathbf{E}^+(t)$ , by the same kind of argument which followed Eq. 7.24b.

Observe from Eq. 7.24a that  $\mathbf{E}_0^+$  in Eq. 7.26 has three space components in the  $(x, y, z)$  system. They all have the same time-phase angle in the present case because  $[l_{x'}, m_{x'}, n_{x'}]$  are real numbers. Hence, as we expect, rotation of the coordinates has not altered the linear polarization of the wave (Eq. 7.16). It is worth remarking here, however, that we may also consider the second type of polarization in the

$(x', y', z')$  system, for which the complex steady-state solution comes from Eq. 7.8 in the form  $\mathbf{E}_2^+ = \mathbf{a}_{y'} \mathbf{E}_{y'0}^+ e^{-j\beta_0 z'}$ . If we combine the two fields to make  $\mathbf{E}_3^+ = (\mathbf{a}_x \mathbf{E}_{x'0}^+ + \mathbf{a}_{y'} \mathbf{E}_{y'0}^+) e^{-j\beta_0 z'}$ , the result in the  $(x, y, z)$  system is again of the form  $\mathbf{E}_3^+ = \mathbf{E}_{03}^+ e^{-j\beta_0 z}$ . This time, though,

$$\mathbf{E}_{03}^+ = \mathbf{a}_x (l_x \mathbf{E}_{x'0}^+ + l_y \mathbf{E}_{y'0}^+) + \mathbf{a}_y (m_x \mathbf{E}_{x'0}^+ + m_y \mathbf{E}_{y'0}^+) + \mathbf{a}_z (n_x \mathbf{E}_{x'0}^+ + n_y \mathbf{E}_{y'0}^+)$$

where the three space components do *not*, in general, have the same time phase. The point is: Eq. 7.26 is valid whether or not the uniform plane wave in question is linearly polarized. Consequently, the mutual perpendicularity of  $\beta$ ,  $\mathbf{H}^+(t)$ , and  $\mathbf{E}^+(t)$  remains true regardless of the type of polarization involved.

**7.2.1.2 PHASE, WAVE LENGTH, AND PHASE VELOCITY.** From Eq. 7.26, we learn that the time phase of the electric (or magnetic) field varies with position only as  $\beta \cdot \mathbf{r}$ . With reference to Fig. 7.3a, a *surface of constant phase* is therefore one for which

(a)

$$\beta \cdot \mathbf{r} = \text{const} = \beta_0 r \cos \psi$$

or

(7.27)

(b)

$$r \cos \psi = \text{const}$$

where  $r = |\mathbf{r}|$ . Equation 7.27b restricts  $\mathbf{r}$  to those points in space where its projection along the direction of  $\beta$  is a constant. The tip of  $\mathbf{r}$  must therefore lie in a plane perpendicular to  $\beta$ . Such planes, normal to the propagation direction, are the *planes of constant phase*. For the uniform plane wave, they are also *planes of constant magnitude* since  $\mathbf{E}_0^+$  does not vary with position. The electric and magnetic fields lie in these planes (Eqs. 7.24b and 7.26b).

The direction normal to the planes of constant phase is the one in

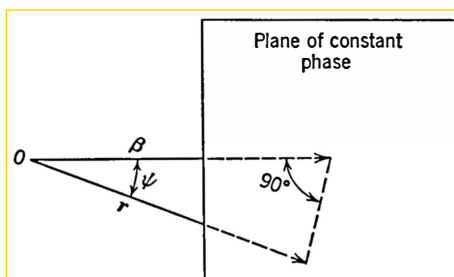


**Fig. 7.3a.** Equiphasic surface for a plane wave.

which the phase  $\varphi$  of the field changes most rapidly with position. To see this, we write with reference to Eqs. 7.26a, 7.27, and Fig. 7.3a,

$$\varphi = \beta \cdot r + \text{const} \quad (7.28)$$

$$\left( \frac{\partial \varphi}{\partial r} \right)_{\psi=\text{const}} = \beta_0 \cos \psi \quad (7.29)$$

$$\left( \frac{\partial \varphi}{\partial r} \right)_{\substack{\max \\ \text{vs } \psi}} = +\beta_0 \quad \text{for } \psi = 0, \text{ or } \mathbf{r} \parallel \beta \quad (7.30)$$

Hence another description of the propagation vector  $\beta$  of a uniform plane wave in a lossless medium is a vector whose direction is that of the maximum rate-of-change of phase with position, and whose magnitude  $\beta_0$  equals that maximum rate of change. In other words, by definition of the gradient operator,

$$\nabla \varphi = \beta = \mathbf{a}_x \beta_x + \mathbf{a}_y \beta_y + \mathbf{a}_z \beta_z \quad \text{for a uniform plane wave} \quad (7.31)$$

The meaning of the component phase constants  $\beta_x$ ,  $\beta_y$ , and  $\beta_z$  is the space-rate-of-change of phase as measured along the respective axes. According to Eqs. 7.21a and 7.28,

so

$$\begin{aligned} \varphi &= \beta_x x + \beta_y y + \beta_z z + \text{const} \\ \beta_x &= \mathbf{a}_x \cdot \nabla \varphi = \frac{\partial \varphi}{\partial x} \\ \beta_y &= \mathbf{a}_y \cdot \nabla \varphi = \frac{\partial \varphi}{\partial y} \\ \beta_z &= \mathbf{a}_z \cdot \nabla \varphi = \frac{\partial \varphi}{\partial z} \end{aligned} \quad (7.32a)$$

Observe that since the direction cosines  $[l, m, n]$  cannot exceed 1 in magnitude (also in view of Eq. 7.22),

$$|\beta_{x,y,z}| \leq \beta_0 \quad (7.32b)$$

Instead of considering the space-rate-of-change of phase along various directions, we can consider the distances between successive equiphasc surfaces on which the field phase differs by exactly  $2\pi$ . These distances will be *apparent wave lengths* because the phase shift is linearly proportional to distance in any direction. Measured along the propagation direction (Fig. 7.3b), the distance  $[\lambda]$ , in which the phase changes by  $2\pi$ , is the conventional wave length. Measured along any

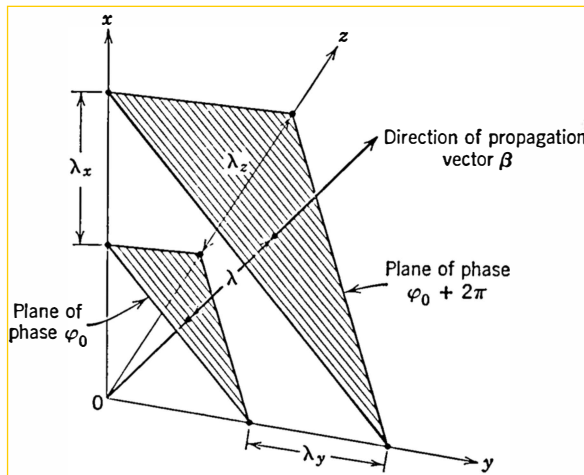


Fig. 7.3b. Various wave-length concepts for a plane wave.

other direction, the distances between the same two planes will be *greater* than  $\lambda$ , as shown in Fig. 7.3b, because the space-rate-of-change of phase along such a direction is *less* than it is along the propagation direction. Thus

$$\begin{aligned}\lambda &\equiv \frac{2\pi}{\beta} \\ \lambda_x &\equiv \frac{2\pi}{|\beta_x|} \geq \lambda \\ \lambda_y &\equiv \frac{2\pi}{|\beta_y|} \geq \lambda \\ \lambda_z &\equiv \frac{2\pi}{|\beta_z|} \geq \lambda\end{aligned}\tag{7.33}$$

and, in view of Eqs. 7.22 and 7.33,

$$\frac{1}{\lambda_x^2} + \frac{1}{\lambda_y^2} + \frac{1}{\lambda_z^2} = \frac{1}{\lambda^2}\tag{7.34}$$

Similarly, since in the time domain (for the sinusoidal steady state) a particular phase front (plane) moves uniformly with time at speed  $v = 1/\sqrt{\epsilon\mu} = \omega/\beta_0$  along the propagation direction, its intercept along any other direction also moves uniformly with time. As is shown in

Fig. 7.30, however, the apparent speed measured along any of the coordinate axes will be *greater* than that along  $\beta$ . In the time of one cycle ( $1/f$ ), a phase front moves a distance along  $x$  of  $2\pi/|\beta_x| = \lambda_x$ , because the total phase of the field involves  $\omega t - \beta_{xx}$ . Analogous comments apply for the other directions  $y$ , and  $z$ . Thus the various *apparent phase velocities* are  $v_x = f\lambda_x$ , etc.; or

$$\begin{aligned} v_x &\equiv \frac{\omega}{\beta_x} = \left( \frac{1}{l_z' \sqrt{\epsilon\mu}} \right) \geq v \\ v_y &\equiv \frac{\omega}{\beta_y} = \left( \frac{1}{m_z' \sqrt{\epsilon\mu}} \right) \geq v \\ v_z &\equiv \frac{\omega}{\beta_z} = \left( \frac{1}{n_z' \sqrt{\epsilon\mu}} \right) \geq v \end{aligned} \quad (7.35)$$

and in view of Eqs. 7.22, again

$$\frac{1}{v_x^2} + \frac{1}{v_y^2} + \frac{1}{v_z^2} = \frac{1}{v^2} = \epsilon\mu \quad (7.36)$$

There is a familiar analogy to the fact that the apparent wave length and phase velocity along any direction but that of the wave propagation *exceed* the same quantities along the propagation direction. Visualize water waves striking a beach obliquely. The distance between successive crests, for example, is large along the beach, especially if the waves are only slightly off normal incidence. Also to keep up with a given crest, one has to run much faster along the beach than the waves progress in their own normal direction.

In view of the manner of obtaining the field expressions (Eqs. 7.26) and the auxiliary relations (Eqs. 7.22 and 7.24b) by coordinate rotation from Eqs. 7.16, there is no doubt that in the  $(x, y, z)$  axes they constitute a solution to Maxwell's (vector) equations. The entire space dependence of this solution is a *simple exponential*, i.e., the exponent is *linear* in the variables  $(x, y, z)$ . There remains the question of whether or not we have found the *only* such simple exponential solution to Maxwell's equations in the sinusoidal steady state.

## 7.2.2 Nonuniform Plane Waves \*

**7.2.2.1 CHARACTER OF THE SOLUTION.\*** The most general exponential expressions for the complex fields, with exponent linear in

the variables  $(x, y, z)$ , are of the form

$$(a) \quad \mathbf{E} = \mathbf{E}_0 e^{-\tilde{\gamma}_x x} e^{-\tilde{\gamma}_y y} e^{-\tilde{\gamma}_z z} = \mathbf{E}_0 e^{-\tilde{\gamma} \cdot \mathbf{r}} \\ (b) \quad \mathbf{H} = \mathbf{H}_0 e^{-\tilde{\gamma}_x x} e^{-\tilde{\gamma}_y y} e^{-\tilde{\gamma}_z z} = \mathbf{H}_0 e^{-\tilde{\gamma} \cdot \mathbf{r}} \quad (7.37)$$

where  $\mathbf{E}_0$  and  $\mathbf{H}_0$  are constant complex vectors, independent of  $(x, y, z)$ , and the various  $\tilde{\gamma}$ 's are *complex numbers*

$$\begin{aligned} \tilde{\gamma}_x &= \alpha_x + j\beta_x \\ \tilde{\gamma}_y &= \alpha_y + j\beta_y \\ \tilde{\gamma}_z &= \alpha_z + j\beta_z \end{aligned} \quad (7.38a)$$

The propagation vector  $\tilde{\gamma}$  is then a *complex vector*

$$\begin{aligned} \tilde{\gamma} &= a_x \tilde{\gamma}_x + a_y \tilde{\gamma}_y + a_z \tilde{\gamma}_z = (a_x \alpha_x + a_y \alpha_y + a_z \alpha_z) + j(a_x \beta_x \\ &\quad + a_y \beta_y + a_z \beta_z) \\ &= \boldsymbol{\alpha} + j\boldsymbol{\beta} \end{aligned} \quad (7.38b)$$

$\boldsymbol{\alpha}$  and  $\boldsymbol{\beta}$  being *real space vectors*. We shall call  $\boldsymbol{\alpha}$  the *attenuation vector* and  $\boldsymbol{\beta}$  the *phase vector*. With  $\tilde{\gamma}$  complex, the field (Eq. 7.37) is by definition a *nonuniform plane wave*.

We know already that if  $\boldsymbol{\alpha} = 0$  the field of Eq. 7.37 can be a solution to Maxwell's equations, provided  $\mathbf{E}_0$ ,  $\mathbf{H}_0$ , and  $\boldsymbol{\beta}$  satisfy some auxiliary conditions. If they do, the resulting solution is interpretable as a *uniform* plane wave traveling in some arbitrary direction in space. If  $\boldsymbol{\alpha} \neq 0$ , however, we must determine whether or not Eq. 7.37 can be a solution to the equations

$$(a) \quad \nabla \times \mathbf{E} = -j\omega\mu\mathbf{H} \\ (b) \quad \nabla \times \mathbf{H} = j\omega\epsilon\mathbf{E} \quad (7.39)$$

and, if so, how to interpret this solution.

The first question above can be answered by substituting Eqs. 7.37 into Eqs. 7.39. Expansion of the curl term in Eq. 7.39a yields

$$\begin{aligned} \nabla \times \mathbf{E} &= \nabla \times (\mathbf{E}_0 e^{-\tilde{\gamma} \cdot \mathbf{r}}) = -\mathbf{E}_0 \times \nabla e^{-\tilde{\gamma} \cdot \mathbf{r}} + e^{-\tilde{\gamma} \cdot \mathbf{r}} \nabla \times \mathbf{E}_0 \\ &= \mathbf{E}_0 \times [e^{-\tilde{\gamma} \cdot \mathbf{r}} \nabla (\tilde{\gamma} \cdot \mathbf{r})] = (\mathbf{E}_0 \times \tilde{\gamma}) e^{-\tilde{\gamma} \cdot \mathbf{r}} \end{aligned}$$

because, since  $\mathbf{E}_0$  is independent of  $(x, y, z)$ ,  $\nabla \times \mathbf{E}_0 \equiv 0$ . A similar calculation is made of  $\nabla \times (\mathbf{H}_0 e^{-\tilde{\gamma} \cdot \mathbf{r}})$ . Substitution of these results, with Eqs. 7.37, into Eq. 7.39 yields the final conditions:

$$(a) \quad \tilde{\gamma} \times \mathbf{E}_0 = j\omega\mu\mathbf{H}_0 \\ (b) \quad \tilde{\gamma} \times \mathbf{H}_0 = -j\omega\epsilon\mathbf{E}_0 \quad (7.40)$$

It is clear that, if the exponential factors in  $\mathbf{E}$  and  $\mathbf{H}$  had been chosen unequal in Eq. 7.37, they would have been forced to equality at this point for any solution to be possible. Equations 7.40 result in any case.

Now dot-premultiplying Eqs. 7.40a and 7.40b by  $\bar{\gamma}$  and noting that

$$\bar{\gamma} \cdot (\bar{\gamma} \times \mathbf{E}_0) = (\bar{\gamma} \times \bar{\gamma}) \cdot \mathbf{E}_0 = 0 = \bar{\gamma} \cdot (\bar{\gamma} \times \mathbf{H}_0) = (\bar{\gamma} \times \bar{\gamma}) \cdot \mathbf{H}_0$$

because

$$\bar{\gamma} \times \bar{\gamma} = 0$$

we find

$$\begin{aligned} (a) \quad & \bar{\gamma} \cdot \mathbf{E}_0 = 0 \\ (b) \quad & \bar{\gamma} \cdot \mathbf{H}_0 = 0 \end{aligned} \tag{7.41}$$

Since  $\bar{\gamma}$ ,  $\mathbf{E}_0$ , and  $\mathbf{H}_0$  are complex vectors in general, Eqs. 7.40 and 7.41 do not imply any obvious conditions of perpendicularity in space.

To eliminate  $\mathbf{H}_0$  from Eqs. 7.40, cross-premultiply Eq. 7.40a by  $(\bar{\gamma}/j\omega\mu)$  and add Eqs. 7.40a and 7.40b. There results

$$\bar{\gamma} \times (\bar{\gamma} \times \mathbf{E}_0) = \omega^2 \epsilon \mu \mathbf{E}_0 = \beta_0^2 \mathbf{E}_0$$

or

$$\bar{\gamma}(\bar{\gamma} \cdot \mathbf{E}_0) - (\bar{\gamma} \cdot \bar{\gamma}) \mathbf{E}_0 = \beta_0^2 \mathbf{E}_0$$

In view of Eq. 7.41a and our wish to have  $\mathbf{E}_0 \neq 0$  (i.e., to find a non-trivial solution), we must require

$$\bar{\gamma} \cdot \bar{\gamma} = -\beta_0^2 \tag{7.42}$$

Because  $\bar{\gamma}$  may be complex, Eq. 7.42 is really two scalar equations. Using Eq. 7.38, we find

$$(\alpha \cdot \alpha - \beta \cdot \beta) + j2\alpha \cdot \beta = -\beta_0^2$$

or since  $\alpha$ ,  $\beta$ , and  $\beta_0^2$  are real,

$$\begin{aligned} (a) \quad & \beta \cdot \beta - \alpha \cdot \alpha = \beta_0^2 \\ (b) \quad & \alpha \cdot \beta = 0 \end{aligned} \tag{7.43}$$

**7.2.2 PHASE DELAY AND ATTENUATION.\*** To understand Eq. 7.45, we must recall that the space dependence of  $\mathbf{E}$  and  $\mathbf{H}$  is contained completely in the exponential factor

$$e^{-\bar{\gamma} \cdot \mathbf{r}} = e^{-\alpha \cdot \mathbf{r}} e^{-j\beta \cdot \mathbf{r}} \tag{7.44}$$

The first factor  $e^{-\alpha \cdot \mathbf{r}}$  is always real, whereas the second factor  $e^{-j\beta \cdot \mathbf{r}}$  always has unit magnitude. The phase of the second factor varies with

position as  $\beta \cdot r$ . Therefore a *surface of constant phase* is defined by the relation

$$\beta \cdot r = \beta r \cos \psi = \text{const} \quad (7.45)$$

with  $\beta = |\beta|$ . This equation pertains to a *plane normal to*  $|\beta|$  as illustrated in Fig. 7.3a.

The amplitude of the field, on the other hand, varies as  $e^{-\alpha \cdot r}$ . Accordingly, a *surface of constant amplitude* is defined by the relation

$$\alpha \cdot r = \alpha r \cos \psi = \text{const} \quad (7.46)$$

in which, by analogy with Eq. 7.45 and Fig. 7.3a,  $\psi$  is the angle between  $r$  and  $\alpha$ , and  $\alpha = |\alpha|$ . Again, a plane is described by Eq. 7.46. *This plane is normal to*  $|\alpha|$ .

The point of Eq. 7.43b is that the *real* vectors  $\alpha$  and  $\beta$  are perpendicular in space (if  $\alpha, \beta \neq 0$ ). Moreover, as long as the frequency is not zero ( $\omega \neq 0$ ),  $\beta_0 > 0$ , and Eq. 7.43a guarantees  $\beta \neq 0$ . Specifically,

$$\beta^2 = \beta_0^2 + \alpha^2 \geq \beta_0^2 \quad > 0 \text{ for } \omega \neq 0 \quad (7.47)$$

Therefore, if  $\alpha \neq 0$ , the field of a nonuniform plane wave (Eq. 7.37) has planes of constant amplitude (normal to  $|\alpha|$ ) and planes of constant phase (normal to  $|\beta|$ ) that are mutually perpendicular.

The most rapid space-rate-of-change of amplitude occurs in the direction of  $|\alpha|$  (Eq. 7.43), which is perpendicular to  $|\beta|$  and therefore parallel to the planes of constant phase. This field is still a *plane wave*,

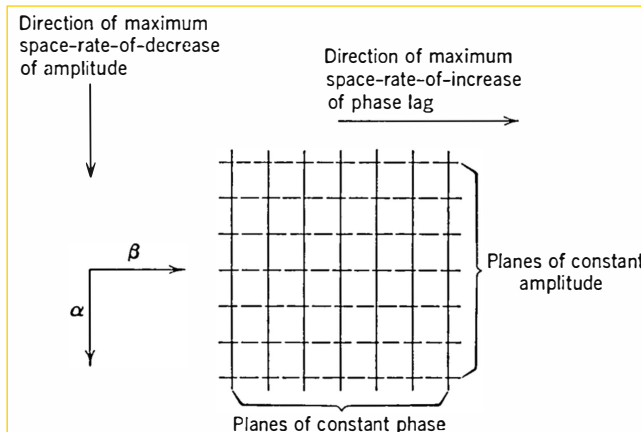


**Fig. 7.4.** Significant features of the space variation of  $e^{-\tilde{\gamma} \cdot r} = e^{-\alpha \cdot r} e^{-\beta \cdot r}$  for non-uniform plane waves without losses. Note that  $\alpha \cdot \beta = 0$ , and that there is no variation at all in the direction normal to the page.

because its equiphasic surfaces are planes; but it is not a uniform plane wave, because the field strength varies with position over the equiphasic planes. Similarly, the phase of the field varies most rapidly over the planes of constant amplitude.

There is evidently no variation of the field in the direction normal to both  $\alpha$  and  $\beta$  because this direction is characterized by the lines of intersection of planes of constant amplitude with planes of constant phase.

All the foregoing important features of space variation are illustrated in Fig. 7.4.

**7.2.2.3 TE AND TM PLANE WAVES.\*** We have found that at any nonzero frequency,  $\alpha \neq 0$  is acceptable to Maxwell's equations as long as  $\beta$  obeys Eqs. 7.43. The somewhat puzzling question of how an "attenuation" can take place in a lossless medium will be answered only after we study the details of the field vectors themselves. To do this conveniently, choose a  $+z$ -axis along  $\beta$  and a  $+y$ -axis along  $\alpha$  (always possible, since  $\alpha \cdot \beta = 0$ ). The  $+x$ -axis must then be along  $\alpha \times \beta$ . Consequently, as illustrated in Fig. 7.5,

$$\bar{v} \equiv \alpha + j\beta = a_y \alpha + a_z j\beta \quad \alpha, \beta > 0 \quad (7.48)$$

Then Eq. 7.41a becomes

$$\alpha E_{y0} + j\beta E_{z0} = 0 \quad (7.49)$$

Surprisingly enough, Eq. 7.49 does not restrict  $E_{z0}$  in any way. It is therefore certainly possible to choose as the electric field one with only

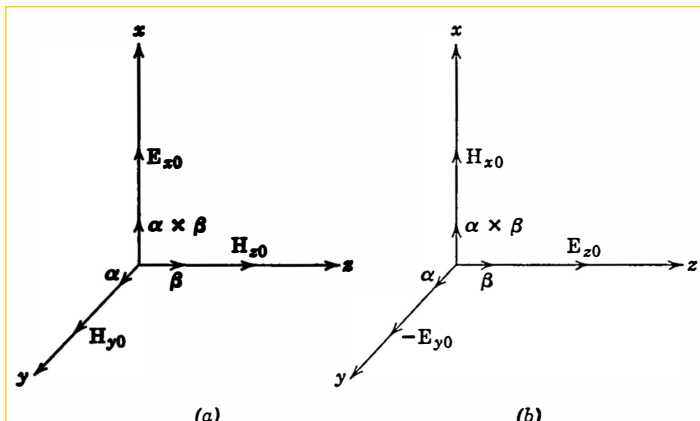


Fig. 7.5. Choice of axes and illustration of field components for (a) TE and (b) TM plane waves in a lossless medium.

a single component, in the  $x$ -direction, and this electric field automatically satisfies Eq. 7.49. Such a field is at all times parallel to  $\alpha \times \beta$ . It is linearly polarized along the direction in which there is no space variation of the solution. One solution of Eq. 7.49 or Eq. 7.41a is accordingly

$$\mathbf{E}_0 = a_x E_{x0} \quad (7.50)$$

The magnetic field corresponding to the choice (Eq. 7.50) for the electric field is given by Eqs. 7.40a and 7.48:

$$\mathbf{H}_0 = \frac{\bar{\gamma} \times \mathbf{E}_0}{j\omega\mu} = a_y \left( \frac{\beta}{\omega\mu} \right) E_{x0} - a_z \left( \frac{\alpha}{j\omega\mu} \right) E_{x0} \quad (7.51)$$

This magnetic field automatically satisfies Eq. 7.41b, as follows.

$$\bar{\gamma} \cdot \mathbf{H}_0 = \frac{\bar{\gamma} \cdot (\bar{\gamma} \times \mathbf{E}_0)}{j\omega\mu} = \frac{(\bar{\gamma} \times \bar{\gamma}) \cdot \mathbf{E}_0}{j\omega\mu} = 0$$

We have in Eqs. 7.50 and 7.51 a solution to Eqs. 7.39, because restrictions of Eqs. 7.41, 7.40a, and 7.43b are already met. Exercise of care to choose  $\alpha$  and  $\beta$  in accordance with Eq. 7.43a (or Eq. 7.47) will then guarantee consistency of Eq. 7.40b. The magnetic field defined by Eq. 7.51 is elliptically polarized in the plane  $(y, z)$  of  $\alpha$  and  $\beta$ , thereby remaining at all times perpendicular to the electric field described by Eq. 7.50. Since the electric field has no components in the plane of  $\alpha$  and  $\beta$ , in which all space variation takes place, this entire wave solution may be called a *Transverse Electric (TE)* plane wave. The important space relations are shown in Fig. 7.5a.

A similar (in fact dual) argument may now be applied, starting from Eq. 7.41b instead of Eq. 7.41a. One solution to the former is

$$\mathbf{H}_0 = a_x H_{x0} \quad (7.52)$$

with corresponding electric field given by Eqs. 7.40b and 7.48

$$\mathbf{E}_0 = \frac{\mathbf{H}_0 \times \bar{\gamma}}{j\omega\epsilon} = -a_y \left( \frac{\beta}{\omega\epsilon} \right) H_{x0} + a_z \left( \frac{\alpha}{j\omega\epsilon} \right) H_{x0} \quad (7.53)$$

This electric field automatically satisfies Eq. 7.41a.

Characterized by a magnetic field which is linearly polarized in the direction of no space variation,  $\alpha \times \beta$ , and an electric field elliptically polarized in the plane of  $\alpha$  and  $\beta$ , the solutions in Eqs. 7.52 and 7.53 may be called a *Transverse Magnetic (TM)* plane wave. The relevant illustration is Fig. 7.5b.

It is convenient to describe the foregoing TE and TM solutions in a form which does not depend upon the particular set of  $(x, y, z)$  axes chosen in Eqs. 7.48 through 7.53. As Fig. 7.5 shows, the fields can be described completely by axes along  $\alpha$ ,  $\beta$  and  $\alpha \times \beta$ , which happen to form a right-handed rectangular system. Using unit vectors  $a_\alpha, a_\beta$  and  $a_{\alpha \times \beta}$  along these directions respectively, and corresponding subscripts  $E_\alpha, H_{\alpha \times \beta}$ , etc., for the field components, we may summarize our results in the following way:

TE WAVE ( $\bar{\gamma} = \alpha + j\beta; \alpha \cdot \beta = 0; \beta^2 - \alpha^2 = \beta_0^2 = \omega^2 \epsilon \mu$ )

$$(a) \quad \mathbf{E} = a_{\alpha \times \beta} E_{\alpha \times \beta, 0} e^{-\bar{\gamma} \cdot r} = a_{\alpha \times \beta} E_{\alpha \times \beta, 0} e^{-\alpha \cdot r} e^{-j\beta \cdot r}$$

$$(b) \quad \mathbf{H} = \frac{\bar{\gamma} \times \mathbf{E}}{j\omega\mu} = \left[ a_\alpha \left( \frac{\beta}{\omega\mu} \right) - a_\beta \left( \frac{\alpha}{j\omega\mu} \right) \right] E_{\alpha \times \beta, 0} e^{-\alpha \cdot r} e^{-j\beta \cdot r} \quad (7.54)$$

TM WAVE ( $\bar{\gamma} = \alpha + j\beta; \alpha \cdot \beta = 0; \beta^2 - \alpha^2 = \beta_0^2 = \omega^2 \epsilon \mu$ )

$$(a) \quad \mathbf{H} = a_{\alpha \times \beta} H_{\alpha \times \beta, 0} e^{-\bar{\gamma} \cdot r} = a_{\alpha \times \beta} H_{\alpha \times \beta, 0} e^{-\alpha \cdot r} e^{-j\beta \cdot r}$$

$$(b) \quad \mathbf{E} = \frac{\mathbf{H} \times \bar{\gamma}}{j\omega\epsilon} = \left[ -a_\alpha \left( \frac{\beta}{\omega\epsilon} \right) + a_\beta \left( \frac{\alpha}{j\omega\epsilon} \right) \right] H_{\alpha \times \beta, 0} e^{-\alpha \cdot r} e^{-j\beta \cdot r} \quad (7.55)$$

We have unquestionably determined two linearly independent plane-wave solutions to Eqs. 7.39 of the form of Eq. 7.37. Are there any more solutions of this form? In what sense there are not may be seen by considering an arbitrary linear combination of a TE and a TM solution having the same  $\bar{\gamma}$ . The combined field meets all the conditions imposed by Eqs. 7.41 and 7.40, provided that  $\bar{\gamma}$  obeys Eq. 7.42. Moreover, Fig. 7.5 shows that the combined field has three space components of both  $\mathbf{E}$  and  $\mathbf{H}$ , neither of which is necessarily linearly polarized. A linear combination of a TE and a TM plane wave is the most general simple exponential solution possible for a given value of  $\bar{\gamma}$  consistent with Eq. 7.42.

Obviously, however, even at a fixed frequency (fixed value of  $\beta_0$ ), one may choose many different values of  $\bar{\gamma}$  consistent with Eqs. 7.42 or 7.43. For example, note that conditions of Eqs. 7.43a (or 7.47) and 7.43b allow independent choice of the algebraic sign of  $\alpha$  and  $\beta$ , given a value of  $|\alpha|$  or  $|\beta|$ , and given a frequency  $\omega$  (i.e., given a value of  $\beta_0$ ). Of course, the relative phases of the field components will vary with the various possible choices, as shown by Eqs. 7.51 and 7.53 (or 7.54 and 7.55). These facts simply express the idea that, as with uniform plane waves, a traveling TE or TM plane wave oriented in any direc-

tion in space is a valid solution of Maxwell's equations as long as  $E_0$ ,  $H_0$ , and  $\bar{v}$  bear the correct mutual relationships. Needless to say, sums of TE and/or TM plane waves in various space orientations are also solutions to the field equations.

#### 7.2.2.4 POWER CONSIDERATIONS AND WAVE IMPEDANCES.\* Examination of the complex power for the nonuniform plane waves discussed above will help to explain the "attenuation."

For example, we have noted that the electric field of the TE wave (Eq. 7.54) is linearly polarized in the direction normal to both  $\alpha$  and  $\beta$ , but the magnetic field is elliptically polarized in the plane of  $\alpha$  and  $\beta$ . Since  $E_{\alpha \times \beta,0}$  and  $H_{\beta,0}$  are in time phase, the component of the complex Poynting vector along  $\beta$  is *entirely real*. However  $E_{\alpha \times \beta,0}$  and  $H_{\beta,0}$  are  $90^\circ$  out of time phase, so the component of the complex Poynting vector along  $\alpha$  is *entirely reactive*. In other words: *only real (time-average) power flows in the direction  $\beta$  (normal to the constant-phase planes and parallel to the constant-amplitude planes), whereas only reactive power flows in the direction  $\alpha$  (normal to the constant-amplitude planes and parallel to the constant-phase planes)*. The "attenuation" therefore does not act to decrease with distance any space component of the time-average power and, consequently, causes no difficulty with conservation of energy in the lossless medium. Similar comments apply to the TM plane wave (Eq. 7.55). These power relationships are illustrated in Fig. 7.6 for both wave types.

Actually the idea of a decreasing field strength in a lossless situation is quite familiar. Imagine a ladder network of inductors only, driven from one end. Both the voltage and the current will decrease with distance away from the drive terminals; but since the whole network is reactive, no real power enters it from the source, and no power loss is implied by the decreasing voltage and current levels. We have simply a lossless "voltage (or current) divider."

The only new idea in the nonuniform plane wave field is the possibility of having real unattenuated power flow in one direction, analogous to a traveling wave on a lossless transmission line in that direction, and, at the same time, having a lossless voltage divider action in another (perpendicular) direction. This however is just the kind of difference we might expect to be brought about by considering problems in more than one space dimension.

Indeed, it is often convenient to define in terms of field components impedances that describe the nature of the complex-power components in various space directions. Thus, in general, field components  $+E_x$  and  $+H_y$  (or  $+E_y$  and  $-H_x$ ) enter into the  $+z$ -component of the complex Poynting vector  $S_z$ , while  $+E_x$  and  $-H_z$  (or  $+E_z$  and  $+H_x$ )

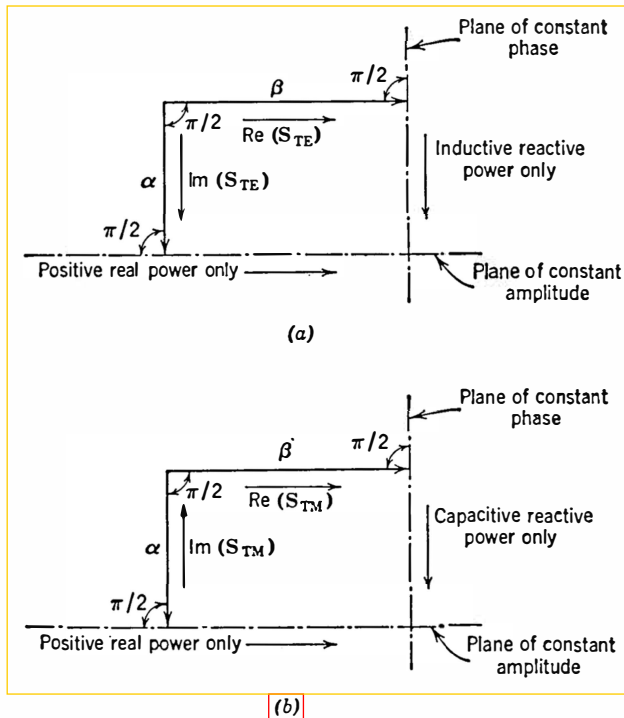


**Fig. 7.6.** Analysis of the complex Poynting vector for nonuniform plane waves in a lossless medium. (a) TE plane wave; (b) TM plane wave.

are the pertinent components for  $S_y$ . The relevant *wave impedances* may be introduced as follows, using  $S_z$  as example:

$$S_z = \frac{1}{2} E_x H_y^* - \frac{1}{2} E_y H_x^* = \frac{1}{2} \left( \frac{E_x}{H_y} \right) |H_y|^2 + \frac{1}{2} \left( \frac{-E_y}{H_x} \right) |H_x|^2 \quad (7.56a)$$

Letting

$$Z_z^{(x,y)} \equiv \frac{E_x}{H_y} \quad (7.56b)$$

and

$$Z_z^{(y,x)} \equiv -\frac{E_y}{H_x} \quad (7.56c)$$

we have

$$S_z = \frac{1}{2} |H_y|^2 Z_z^{(x,y)} + \frac{1}{2} |H_x|^2 Z_z^{(y,x)} \quad (7.56d)$$

Evidently the real and imaginary parts of the wave impedances give the correct algebraic sign of the real and reactive power associated with the pertinent field components. In many cases, one of the field com-

ponents responsible for power in a given direction is absent so that the distinction between the two wave impedances  $[Z_z^{(x,y)}]$  and  $[Z_z^{(y,x)}]$ , for example] for that direction need not be made. In such cases the super-script will simply be omitted, it being understood from the context which field components must be involved.

Applying the foregoing ideas to the TE and TM plane waves of Eqs. 7.54 and 7.55, we may define the following wave impedances:

TE	TM	
(a) $Z_\beta \equiv \frac{E_{\alpha \times \beta,0}}{H_{\alpha 0}} = \frac{\omega \mu}{\beta}$	(c) $Z_\beta \equiv \frac{-E_{\alpha 0}}{H_{\alpha \times \beta,0}} = \frac{\beta}{\omega \epsilon}$	(7.57)
(b) $Z_\alpha \equiv \frac{E_{\alpha \times \beta,0}}{-H_{\beta 0}} = \frac{j\omega \mu}{\alpha}$	(d) $Z_\alpha \equiv \frac{E_{\beta 0}}{H_{\alpha \times \beta,0}} = \frac{\alpha}{j\omega \epsilon}$	

Observe that, if  $\beta > 0$ ,  $Z_\beta$  is positive real, indicating again that only time-average power flows in the  $\beta$  direction. If  $\alpha > 0$ ,  $Z_\alpha$  is *inductive* for the TE wave, indicating that reactive power only flows in the  $\alpha$  direction and that *the TE field stores more time-average magnetic than electric energy per unit volume*. On the other hand,  $Z_\alpha$  is *capacitive* for the TM wave, which means that *the TM field stores more time-average electric than magnetic energy per unit volume*. These facts are also included in Fig. 7.6.

The most general lossless plane wave with a given  $\vec{y}$  is, as we have already mentioned, a linear combination of a TE and a TM plane wave with respect to the direction of the vectors  $\beta$  and  $\alpha$ . It is not difficult to see in Fig. 7.5 that *the field components missing from these waves make them orthogonal with respect to complex power in the  $\beta$  and  $\alpha$  directions*. That is, the complex power in these directions when both waves are present together is the sum of the complex powers which would be carried in these directions by each one separately. Unfortunately, however, this orthogonality does *not hold* for complex power in the direction normal to  $\alpha$  and  $\beta$  (i.e., the direction of  $\alpha \times \beta$ ). For either wave alone  $S_{\alpha \times \beta} \equiv 0$ , but, when both are present together, Eqs. 7.54 and 7.55 show that

$$S_{\alpha \times \beta} = \frac{1}{2} (E_\alpha H_\beta^* - E_\beta H_\alpha^*) = \frac{j\alpha\beta}{\beta_0^2} H_{\alpha \times \beta,0} E_{\alpha \times \beta,0} e^{-2\alpha \cdot r}$$

This is not in general zero, but depends upon  $E_{\alpha \times \beta,0}$  and  $H_{\alpha \times \beta,0}$  which we have seen are *independent* as far as Maxwell's equations are concerned. Their presence and relative magnitude and phase will therefore be determined completely by boundary conditions.

### 7.2.3 Relationships between Uniform and Nonuniform Plane Waves \*

The results of our work in Secs. 7.2.1 and 7.2.2 may be summarized as follows: The field

$$(a) \quad \mathbf{E} = \mathbf{E}_0 e^{-\tilde{\gamma} \cdot \mathbf{r}} = \mathbf{E}_0 e^{-\tilde{\gamma}_x x} e^{-\tilde{\gamma}_y y} e^{-\tilde{\gamma}_z z} \quad (7.58)$$

$$(b) \quad \mathbf{H} = \mathbf{H}_0 e^{-\tilde{\gamma} \cdot \mathbf{r}} = \frac{\tilde{\gamma} \times \mathbf{E}_0}{j\omega\mu} e^{-\tilde{\gamma} \cdot \mathbf{r}} = \frac{\tilde{\gamma} \times \mathbf{E}}{j\omega\mu}$$

is a sinusoidal steady-state solution to Maxwell's equations without loss if and only if the conditions

$$(a) \quad \tilde{\gamma}_x^2 + \tilde{\gamma}_y^2 + \tilde{\gamma}_z^2 = -\beta_0^2 (= -\omega^2 \epsilon \mu)$$

and

$$(b) \quad \left\{ \begin{array}{l} \text{or } \tilde{\gamma}_x E_{x0} + \tilde{\gamma}_y E_{y0} + \tilde{\gamma}_z E_{z0} = 0 \\ \tilde{\gamma}_x H_{x0} + \tilde{\gamma}_y H_{y0} + \tilde{\gamma}_z H_{z0} = 0 \end{array} \right. \quad (7.59)$$

are satisfied. Note that any two of  $\tilde{\gamma}_x, \tilde{\gamma}_y, \tilde{\gamma}_z$  are completely arbitrary complex numbers, with the third fixed (except for algebraic sign) by Eq. 7.59a. Similarly, any two of  $E_{x0}, E_{y0}, E_{z0}$  (or  $H_{x0}, H_{y0}, H_{z0}$ ) are also completely arbitrary complex numbers, with the third fixed by Eq. 7.59b. Equation 7.58b then determines the remaining complex vector  $\mathbf{H}_0$  (or  $\mathbf{E}_0$ ).

The following special cases have arisen:

1. If  $\tilde{\gamma} = j\beta$  (i.e.,  $\alpha = 0$ ), the solution is a uniform plane wave, which is one form of the TEM wave with respect to  $\beta$ .
2. If  $\alpha \neq 0$  and  $\mathbf{E}_0 = A\mathbf{E}_0$ , where  $A$  is any complex number and  $\mathbf{E}_0$  any real vector, the solution has a linearly polarized electric field and is a TE wave with respect to  $\beta$  and  $\alpha$ .
3. If  $\alpha \neq 0$  and  $\mathbf{H}_0 = B\mathbf{H}_0$ , where  $B$  is any complex number and  $\mathbf{H}_0$  any real vector, the solution has a linearly polarized magnetic field and is a TM wave with respect to  $\beta$  and  $\alpha$ .
4. If  $\alpha = 0$ , together with either  $\mathbf{E}_0 = A\mathbf{E}_0$  or  $\mathbf{H}_0 = B\mathbf{H}_0$ , then the solution is a uniform plane wave with linearly polarized electric and magnetic fields.

We see from the summary that the condition of Eq. 7.59a is of great importance. It was met automatically in the case of the uniform plane wave ( $\alpha = 0$ ) by the well-known geometric condition (Eq. 7.17) on the direction cosines  $(l_{z'}, m_{z'}, n_{z'})$  of the propagation direction with respect to the  $(x, y, z)$  axes. What, if any, are the geometric consequences of Eq. 7.59a when  $\alpha \neq 0$ ?

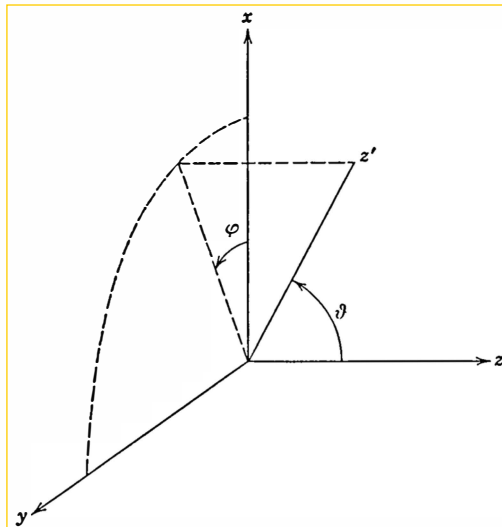


Fig. 7.7. Polar angles for location of a new axis.

With reference to Fig. 7.7, let  $+z'$  be an axis along  $\beta$  for a uniform plane wave. Instead of locating  $+z'$  by its direction cosines, use the polar angles  $\vartheta$  and  $\varphi$  shown. Then the direction cosines of  $+z'$  are:

$$\begin{aligned} l_{z'} &= \sin \vartheta \cos \varphi \\ m_{z'} &= \sin \vartheta \sin \varphi \\ n_{z'} &= \cos \vartheta \end{aligned} \quad 0 \leq \vartheta \leq \pi \quad 0 \leq \varphi < 2\pi \quad (7.60)$$

It is obvious that  $|l_{z'}|^2 + |m_{z'}|^2 + |n_{z'}|^2 \equiv 1$  automatically when expressed thus in terms of  $\vartheta$  and  $\varphi$ .

The exponential factor in the fields therefore becomes

$$e^{-j\vec{\gamma} \cdot \vec{r}} = e^{-j\beta \cdot \vec{r}} = e^{-(j\beta_0 \sin \vartheta \cos \varphi)x - (j\beta_0 \sin \vartheta \sin \varphi)y - (j\beta_0 \cos \vartheta)z} \quad (7.61)$$

so that we may write

- |     |   |
|-----|---|
| (a) | $\bar{\gamma}_x = j\beta_0 \sin \vartheta \cos \varphi$ |
| (b) | $\bar{\gamma}_y = j\beta_0 \sin \vartheta \sin \varphi$ |
| (c) | $\bar{\gamma}_z = j\beta_0 \cos \vartheta$              |
- (7.62)

with the consequence that, identically,

$$\bar{\gamma}_x^2 + \bar{\gamma}_y^2 + \bar{\gamma}_z^2 \equiv -\beta_0^2 \quad (7.59a)$$

The important point now is the fact that

$$\sin^2 \bar{\vartheta} \cos^2 \bar{\varphi} + \sin^2 \bar{\vartheta} \sin^2 \bar{\varphi} + \cos^2 \bar{\vartheta} \equiv 1 \quad (7.63)$$

when  $\bar{\vartheta}$  and  $\bar{\varphi}$  are any arbitrary complex numbers!

In other words, if we allow the notion of *complex polar angles*  $\bar{\vartheta}$  and  $\bar{\varphi}$  for the direction of propagation of a *uniform plane wave*, the corresponding solution becomes a *nonuniform plane wave* with complex  $\bar{\gamma}_x, \bar{\gamma}_y, \bar{\gamma}_z$  defined by Eq. 7.62 and satisfying the condition of Eq. 7.59a identically.

An illustrative example of the complex angles is furnished by the case treated in Sec. 7.2.2.3, where

$$\bar{\gamma} = a_y \alpha + a_z j \beta \quad (\alpha, \beta > 0) \quad (7.48)$$

and

$$\beta^2 = \beta_0^2 + \alpha^2 > \beta_0^2 \quad (7.47)$$

In this case it is easiest to start with Eq. 7.62a because  $\bar{\gamma}_x = 0$ . In other cases, Eq. 7.62c might be simpler because it contains only one angle.

Thus in the present example

$$\bar{\gamma}_x = 0 = \sin \bar{\vartheta} \cos \bar{\varphi}$$

so either  $\sin \bar{\vartheta} = 0$  or  $\cos \bar{\varphi} = 0$ , or both. But  $\bar{\gamma}_y \neq 0$ , so Eq. 7.62b shows that  $\sin \bar{\vartheta} \neq 0$ . Hence we must choose  $\cos \bar{\varphi} = 0$ . Since, however,  $\bar{\varphi}$  is a complex angle  $\varphi_R + j\varphi_I$ , we must set

$$\cos \bar{\varphi} = \cos(\varphi_R + j\varphi_I) = \cos \varphi_R \cosh \varphi_I - j \sin \varphi_R \sinh \varphi_I = 0$$

Because  $\cosh \varphi_I \geq 1$ , this implies in sequence

- |     |   |                           |
|-----|---|---------------------------|
| (a) | $\varphi_R = \frac{\pi}{2}$ (or $\frac{3\pi}{2}$ )    | $0 \leq \varphi_R < 2\pi$ |
| (b) | $\sin \varphi_R = +1$ (or $-1$ )                      |                           |
| (c) | $\varphi_I = 0$                                       |                           |
| (d) | $\sin \bar{\varphi} = \sin \varphi_R = +1$ (or $-1$ ) |                           |
- (7.64)

Now with reference to  $\bar{\gamma}_y$  in Eq. 7.62b, we need to know that

$$\sin \bar{\vartheta} = \sin(\vartheta_R + j\vartheta_I) = \sin \vartheta_R \cosh \vartheta_I + j \cos \vartheta_R \sinh \vartheta_I$$

It follows from this result, with the use of Eqs. 7.48, 7.62b, and the condition of Eq. 7.64d on  $\sin \bar{\varphi}$ , that

$$\alpha = (+j \sin \vartheta_R \cosh \vartheta_I - \cos \vartheta_R \sinh \vartheta_I)$$

Therefore, since  $\alpha$  is positive real and  $\cosh \vartheta_I \geq 1$ , we have in sequence that

- (a)  $\sin \vartheta_R \cosh \vartheta_I = 0$
- (b)  $\vartheta_R = 0$  [or  $\pi$ ]  $0 \leq \vartheta_R < 2\pi$
- (c)  $\cos \vartheta_R = 1$  [or  $-1$ ] (7.65)
- (d)  $\alpha = {}^+_{(-)} \beta_0 {}^+_{(-)} \sinh \vartheta_I > 0$

where we have used the curved  $(-)$  and square  $[+]$  marks in Eq. 7.65d to identify the algebraic sign alternatives from Eqs. 7.64d and 7.65c respectively.

To eliminate some of the various choices of algebraic sign and quadrant of angle remaining, we must look at Eq. 7.62c, when  $\bar{\gamma}_z = j\beta$ , as required by Eq. 7.48. We find

$$\beta = \beta_0(\cos \vartheta_R \cosh \vartheta_I - j \sin \vartheta_R \sinh \vartheta_I) = \beta_0 \cos \vartheta_R \cosh \vartheta_I > 0$$

in view of Eq. 7.65b.

Again, since  $\cosh \vartheta_I \geq 1$ ,  $\cos \vartheta_R > 0$ . This means

$$\vartheta_R = 0 \text{ (not } \pi\text{)}$$

in Eq. 7.65b, which removes completely the [ ] alternatives in Eqs. 7.65d. Accordingly, using the first choice in Eq. 7.65c, we have

$$\cosh \vartheta_I = \frac{\beta}{\beta_0} > 1$$

which leaves the algebraic sign of  $\vartheta_I$  still in doubt.

We are left with a choice of two solutions. Either

$$\varphi_R = \frac{\pi}{2} \quad \text{from Eq. 7.64a}$$

and

$$\sinh \vartheta_I = - \frac{\alpha}{\beta_0} \quad \text{from Eq. 7.65d}$$

or

$$\varphi_R = \frac{3\pi}{2} \quad \text{from Eq. 7.64a}$$

and

$$\sinh \vartheta_I = + \frac{\alpha}{\beta_0} \quad \text{from Eq. 7.65d}$$

The existence of these two possibilities has no particular physical significance. They are simply consequences of the multiple-valued

properties of the inverse trigonometric functions. A *uniform* plane wave at either set of complex angles

and

$$\bar{\vartheta} = -j \sinh^{-1} \left( \frac{\alpha}{\beta_0} \right)$$

or

$$\bar{\varphi} = \frac{\pi}{2}$$

and

$$\bar{\vartheta} = +j \sinh^{-1} \left( \frac{\alpha}{\beta_0} \right)$$

$$\bar{\varphi} = \frac{3\pi}{2}$$

represents physically the *same nonuniform* plane wave. We can choose either solution arbitrarily. Needless to say, the polarization of the uniform plane wave sets the TE, TM, or combined TE-TM character of the resulting wave.

Our understanding of the plane-wave solutions we have found will be weak unless we apply them to some situations involving boundaries. The principal purpose of the following sections of this chapter is therefore to discuss some problems in which it only takes a small number—one, two, three, etc.—of plane waves to meet the boundary conditions. We shall find many useful similarities between these problems and those encountered in transmission lines, but there are also important differences. The differences arise from both the three-dimensional variation of the fields, and their three-dimensional vector character. The examples chosen do illustrate significant physical phenomena in optics and radio transmission, but they are equally important as part of a background of understood cases upon which to develop a physical intuition suitable for dealing with harder field problems.

### 7.3 Normal Incidence of a Uniform Plane Wave

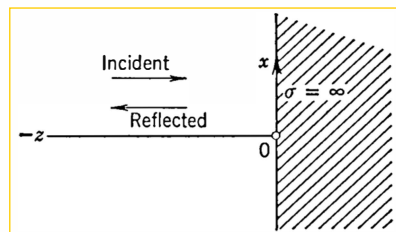
We suggested in connection with Eqs. 7.14 and 7.15, that we could interpret the (+) solution for a uniform plane wave as an incident wave and the (−) one as a reflected wave. We also suggested in Sec. 7.1.5, however, that such an interpretation would be meaningful only if the boundary conditions in *all space* could be met by Eq. 7.14. Specifically, we must have a physical situation in three-dimensional space for which the boundary conditions require only *x*-polarized uniform plane waves propagating in the ±*z* directions.

Now the boundary conditions for the complex fields involve only components of  $\mathbf{E}$  and  $\mathbf{H}$  tangential to interfaces between different media (Eqs. 1.22 and 1.25). If we take the incident wave (specified by some remote source) as an  $x$ -polarized uniform plane wave propagating in the  $+z$  direction, its electric and magnetic fields lie in planes normal to the  $z$  axis and extend uniformly throughout these planes. Thus a plane boundary or interface between different media which also extends uniformly in some plane normal to the  $z$ -axis should require only similar field components in the reflected wave.

### 7.3.1 Normal Incidence on a Perfect Conductor

For a first example, consider the situation in Fig. 7.8. A perfectly conducting metal wall occupies the entire  $x, y$  plane, and the incident

**Fig. 7.8.** Normal incidence of uniform plane wave on a perfect conductor. The  $+y$ -axis points out of the paper.



uniform plane wave (from a source at  $z = -\infty$ ) has the specified form

$$\mathbf{E}_i = a_x E_{x0}^+ e^{-j\beta_0 z} \quad (7.66)$$

in which  $E_{x0}^+$  is a given constant. In accordance with Eqs. 7.14, the corresponding magnetic field is

$$\mathbf{H}_i = a_y \frac{E_{x0}^+}{\eta} e^{-j\beta_0 z} \quad (7.67)$$

and the reflected field will be denoted by

$$(a) \quad \mathbf{E}_r = a_x E_{x0}^- e^{j\beta_0 z} \quad (7.68)$$

$$(b) \quad \mathbf{H}_r = -a_y \frac{E_{x0}^-}{\eta} e^{j\beta_0 z}$$

The boundary condition on the metal wall requires the total tangential electric field to vanish when  $z = 0$  for all  $x$  and  $y$ . Therefore

$$E_{x0}^+ + E_{x0}^- = 0 \quad (7.69)$$

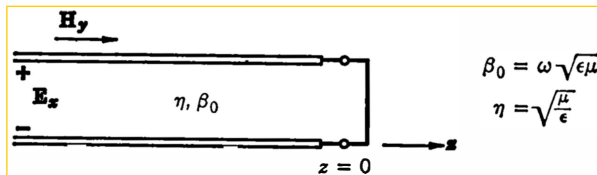


**Fig. 7.9.** Lossless transmission line analog for Fig. 7.8 with  $[x]$ -polarized uniform plane waves.

and the total field becomes

$$(a) \quad \mathbf{E} = \mathbf{E}_i + \mathbf{E}_r = -a_x 2j \mathbf{E}_{x0}^+ \sin \beta_0 z \quad (7.70)$$

$$(b) \quad \mathbf{H} = \mathbf{H}_i + \mathbf{H}_r = a_y \frac{2\mathbf{E}_{x0}^+}{\eta} \cos \beta_0 z$$

We see that, besides being perpendicular in space,  $\mathbf{E}$  [=  $\text{Re}(\mathbf{E}e^{j\omega t})$ ] and  $\mathbf{H}$  [=  $\text{Re}(\mathbf{H}e^{j\omega t})$ ] are  $90^\circ$  out of phase with respect to both their time and space variations. Indeed,  $\mathbf{E}$  and  $\mathbf{H}$  have relative phases and space variations exactly like the voltage and current respectively on a short-circuited lossless transmission line. As a matter of fact, if we simply remember that  $\mathbf{E}$  lies along the  $[x]$ -axis and  $\mathbf{H}$  lies along the  $[y]$ -axis, the solution (Eq. 7.70) is otherwise identical with that of the transmission line in Fig. 7.9. Note that the “characteristic wave impedance”

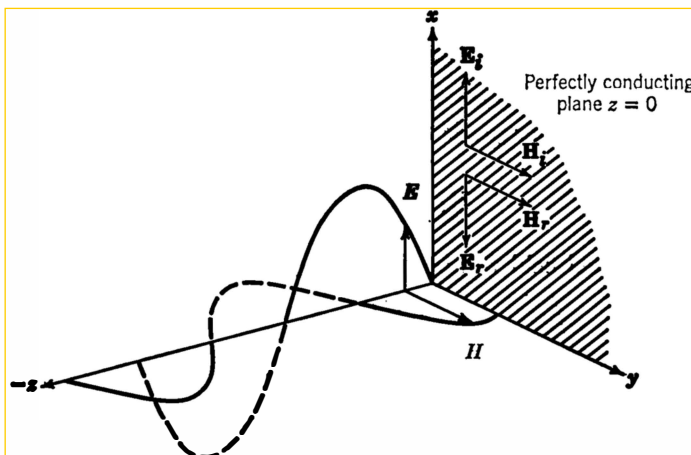


**Fig. 7.10.** Standing-wave pattern in front of a perfect conductor illuminated by a normally incident,  $[+x]$ -polarized uniform plane wave.

$\eta$  serves as characteristic impedance of the line in this case. In Fig. 7.10 we show space plots of  $\mathbf{E}$  and  $\mathbf{H}$  at a moment when neither one has its maximum magnitude. The relation between this figure and Fig. 3.6 should be studied carefully.

A little thought will convince us that, had we started with a  $y$ -polarized incident wave, the reflected wave would also have been  $y$ -polarized, and the standing-wave pattern of Fig. 7.10 would merely have been rotated about the  $+z$ -axis clockwise by  $90^\circ$  in space. Moreover, the equivalent transmission line of Fig. 7.9 would have remained the same, except that  $E_y$  would have replaced  $E_z$ , and  $-H_z$  would have replaced  $H_y$  (see Eqs. 7.2 and compare Eqs. 7.3 and 7.8).

If the incident uniform plane wave had electric field components along both the  $x$  and the  $y$  directions, we would simply treat each component (with its associated magnetic field according to Eqs. 7.5a and 7.9a) separately, and superpose the separate solutions after completing them independently.

### 7.3.2 Normal Incidence on a Lossless Dielectric

Our second example of a plane boundary normal to the direction of propagation of the incident wave involves two lossless dielectrics, as appear in Fig. 7.11. The incident wave is given in medium 1 as an  $x$ -polarized uniform plane wave:

$$(a) \quad \mathbf{E}_i = a_x E_{x1} e^{-j\beta_0 z} \quad (7.71)$$

$$(b) \quad \mathbf{H}_i = \frac{1}{\eta_1} \mathbf{a}_z \times \mathbf{E}_i$$

We must, in this case, allow for a wave transmitted into medium 2 as well as for a reflected wave in medium 1. We shall assume, however, that no  $(-)$  wave occurs in medium 2. Some discussion is in order to indicate that the absence of a  $(-)$  wave is in fact an assumption. There is a temptation to try to summarize it simply by pointing out that medium 2 extends infinitely far to the right, and by suggesting that no wave has time to come back from such a distance. These statements, however, do not explain the absence of a  $(-)$  wave in a lossless medium in the sinusoidal steady state. The steady-state idea itself supposes that we have, in fact, waited long enough for all initial transients to disappear, even if that takes infinite time! For example, if there were a perfectly conducting plane at  $z = z_0 > 0$ , our previous work shows that there would certainly be a  $(-)$  wave in medium 2, no matter how large  $z_0$  might be. If there is to be no  $(-)$  wave, the im-

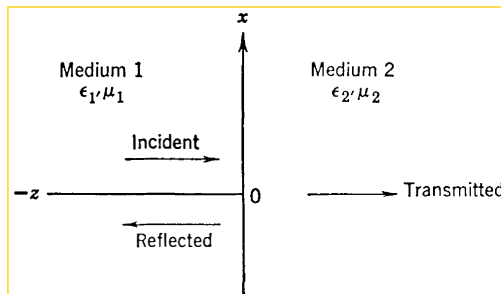


**Fig. 7.11.** Normal incidence of uniform plane wave on a lossless dielectric.

portant point is not how far medium 2 extends but rather that there cannot be (for example) a metal plane at the *end* of it, even if the end is at  $z = +\infty$ . The honest way to state our present assumption is *as a boundary condition on the solution when  $z \rightarrow +\infty$* . Specifically, we are arbitrarily looking for a solution which behaves like a right-going wave  $e^{-j\beta_{02}z}$  as  $z \rightarrow +\infty$ .

The immediate question is then whether such a solution can be found. If it can, the ensuing question of what real physical situations might correspond to it is quite another matter. Dealing with this one requires physical judgements, the successful making of which involves more than we can profitably discuss at this point in our argument.

Returning, then, to the solution itself, we take the form of the reflected wave in medium 1 to be

$$(a) \quad \mathbf{E}_r = a_x \mathbf{E}_{x1} e^{-j\beta_{01}z} \quad (7.72)$$

$$(b) \quad \mathbf{H}_r = -\frac{1}{\eta_1} \mathbf{a}_z \times \mathbf{E}_r$$

and the form of the transmitted wave in medium 2 to be

$$(a) \quad \mathbf{E}_t = a_x \mathbf{E}_{x2} e^{-j\beta_{02}z} \quad (7.73)$$

$$(b) \quad \mathbf{H}_t = \frac{1}{\eta_2} \mathbf{a}_z \times \mathbf{E}_t$$

The boundary conditions at the interface  $z = 0$  require both  $\mathbf{E}_{\text{tang}}$  and  $\mathbf{H}_{\text{tang}}$  to be continuous:

$$(a) \quad \mathbf{E}_i + \mathbf{E}_r = \mathbf{E}_t \quad \text{at } z = 0 \quad (7.74)$$

$$(b) \quad \mathbf{H}_i + \mathbf{H}_r = \mathbf{H}_t \quad \text{at } z = 0$$

Using Eqs. 7.71, 7.72, and 7.73 in Eq. 7.74, we have

$$(a) \quad E_{x1}^+ + E_{x1}^- = E_{x2}^+ \quad (7.75)$$

$$(b) \quad \frac{1}{\eta_1} (E_{x1}^+ - E_{x1}^-) = \frac{1}{\eta_2} E_{x2}^+$$

Multiplication of Eq. 7.75b by  $\eta_2$ , and subtraction from Eq. 7.75a yields

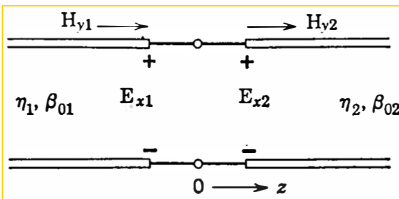
$$\frac{E_{x1}^-}{E_{x1}^+} \equiv \bar{\Gamma}_R = \frac{(\eta_2/\eta_1) - 1}{(\eta_2/\eta_1) + 1} \quad (7.76a)$$

which, in turn, upon substitution back into Eq. 7.75a also gives

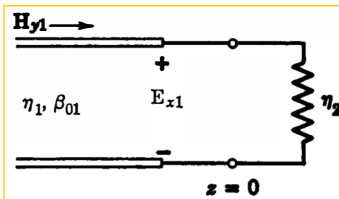
$$\frac{E_{x2}^+}{E_{x1}^+} \equiv T = \frac{2(\eta_2/\eta_1)}{(\eta_2/\eta_1) + 1} \quad (7.76b)$$

The use of the symbol  $\bar{\Gamma}_R$  in Eq. 7.76a stems from its clear analogy with the reflection coefficient of the load on a transmission line. In this case, the reflection coefficient  $\bar{\Gamma}_R$  is the ratio at the interface of the complex reflected electric field to the complex incident electric field. Indeed, both Eqs. 7.76a and 7.76b (or Eqs. 7.75) follow from the equivalent transmission-line system, shown in Fig. 7.12, in which the incident “voltage”  $E_{x1}^+$  is regarded as given. We can see this clearly by first replacing the second transmission line in Fig. 7.12 according to the modified form of Thévenin’s theorem proved for the time domain in Chapter 4. This step yields Fig. 7.13, from which Eq. 7.76a becomes apparent.

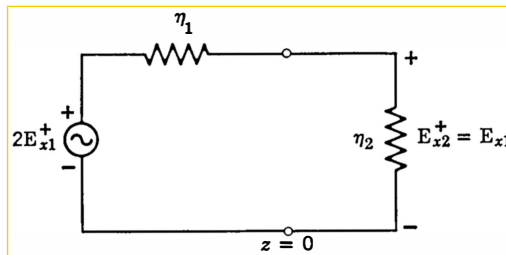
Next, we also replace line 1 in Fig. 7.13 by its Thévenin equivalent on the same basis, remembering that  $E_{x1}^+$  (the incident wave) is given. There results Fig. 7.14, exhibiting clearly Eq. 7.76b. The symbol T in this equation is called the *transmission coefficient*, defined as the



**Fig. 7.12.** Lossless transmission line analogy for Fig. 7.11.



**Fig. 7.13.** An equivalent circuit for Fig. 7.12 from the point of view of line 1.

Fig. 7.14. Complete equivalent circuit of Fig. 7.12 at  $z = 0$ .

ratio at the interface of the complex transmitted electric field to the complex incident electric field.

It follows from Eqs. 7.75a and the definitions of  $\bar{\Gamma}_R$  and  $T$  in Eqs. 7.76a and 7.76b, that

$$1 + \bar{\Gamma}_R = T \quad (7.77)$$

Also we note that the time-average power per unit area carried in the  $+z$  direction in medium 1 is

$$\langle S_{z1} \rangle = \frac{|E_{x1}^+|^2 - |E_{x1}^-|^2}{2\eta_1} = \frac{|E_{x1}^+|^2}{2} \eta_1 (1 - |\bar{\Gamma}_R|^2)$$

and that carried in the  $+z$  direction in medium 2 is

$$\langle S_{z2} \rangle = \frac{|E_{x2}^+|^2}{2\eta_2}$$

Since the interface is lossless, these should be equal

$$\left(\frac{\eta_1}{\eta_2}\right) |T|^2 = 1 - |\bar{\Gamma}_R|^2 \quad (7.78)$$

and direct substitution of Eqs. 7.76a and 7.76b into Eq. 7.78 shows that the latter is indeed correct. The transmitted power is equal to the incident power minus the reflected power.

In view of Eqs. 7.14 and 7.76a it is clear that a generalized reflection coefficient can be defined for situations involving uniform plane waves at normal incidence upon plane boundaries. By analogy with transmission lines, we write

$$\begin{aligned} \bar{\Gamma}(z) &\equiv \frac{E_x^-(z)}{E_x^+(z)} = \frac{E_{x0}^- e^{j\beta_0 z}}{E_{x0}^+ e^{-j\beta_0 z}} \\ &= \bar{\Gamma}(0) e^{j2\beta_0 z} \end{aligned} \quad (7.79)$$

We then *define* a normalized impedance  $Z_n(z)$  by the relation

$$Z_n(z) \equiv \frac{1 + \bar{\Gamma}(z)}{1 - \bar{\Gamma}(z)} \quad (7.80)$$

But by Eqs. 7.79 and 7.14 we can re-express  $Z_n(z)$  of Eq. 7.80 in the form

$$Z_n(z) = \frac{E_{x0}^+ e^{-j\beta_0 z} + E_{x0}^- e^{j\beta_0 z}}{E_{x0}^+ e^{-j\beta_0 z} - E_{x0}^- e^{j\beta_0 z}} = \frac{E_x}{\eta H_y} \quad (7.81)$$

It is often convenient, but by no means necessary, to regard  $\eta$  as a "characteristic impedance," in which case the unnormalized impedance  $Z(z)$  becomes equal to what we have previously called the wave impedance looking in the  $+z$  direction:

$$Z(z) = Z_z \equiv \frac{E_x}{H_y} \text{ ohms} \quad (7.82)$$

It is on this basis, in fact, that we have made the transmission-line representations in Figs. 7.9 and 7.12.

In any case, simply on the strength of Eqs. 7.79, 7.80, and 7.81, the entire set of procedures for transmission lines becomes applicable to these uniform plane-wave problems. In particular, the Smith chart (and others) can be used to great advantage instead of dealing directly with the boundary conditions at interfaces. The next section illustrates the techniques.

### 7.3.3 Normal Incidence on Multiple Dielectrics

Consider the problem of a sheet of dielectric of thickness  $l$ , upon one side ( $z = -l$ ) of which is incident normally from  $z = -\infty$  an  $x$ -polarized uniform plane wave (Fig. 7.15). Our interest might be in the percentage of the incident power which is reflected for various values of  $l$ , given the frequency and the dielectric constant  $\epsilon_2 > \epsilon_0$ .

A straightforward attack on the problem would require consideration of the five waves shown, and then a matching of tangential electric and magnetic fields at the two interfaces  $z = 0$  and  $z = -l$  to determine the amplitudes of the four unknown waves. Since, however, the wave propagation *within* each medium obeys transmission-line equations, and since the boundary conditions of continuity of tangential electric and magnetic fields are exactly like the continuity conditions of voltage and current at a line termination, the problem may be reduced to that shown in Fig. 7.16.

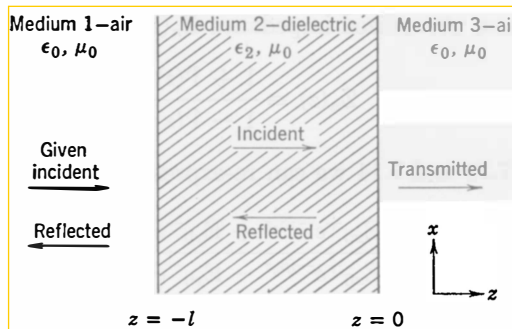


Fig. 7.15. A multiple-interface problem.

We wish to find the magnitude of the reflection coefficient on line 1, which requires that we determine the impedance  $Z$  normalized on the characteristic impedance  $\eta_0$ . For definiteness, let  $\epsilon_2 = 4\epsilon_0$ , and suppose that the frequency is such that the wave length  $\lambda_0$  in air is 3 cm. The wave length in the dielectric medium (line 2) is then  $\lambda_2 = \frac{1}{2} \times 3 = 1.5$  cm.

We see at once that, if  $l = \frac{1}{2}\lambda_2 = 0.75$  cm (or any integer multiple thereof), line 2 becomes a half-wave line and  $Z = \eta_0$ . Then line 1 is matched, and there is no reflection at all. There will, however, be reflections for other values of  $l$ .

From the point of view of line 2, the normalized load impedance at  $z = 0$  is  $\eta_0/\eta_2 = \sqrt{\epsilon_2/\epsilon_0} = 2$ , shown at point  $A$  in Fig. 7.17. As  $l$  is increased from zero, the Smith chart shows that  $Z/\eta_2$  becomes smallest in magnitude and real at point  $B$ , when  $l = \frac{1}{4}\lambda_2 = 0.375$  cm. Its smallest value is 0.5. From the point of view of line 1, the normalized

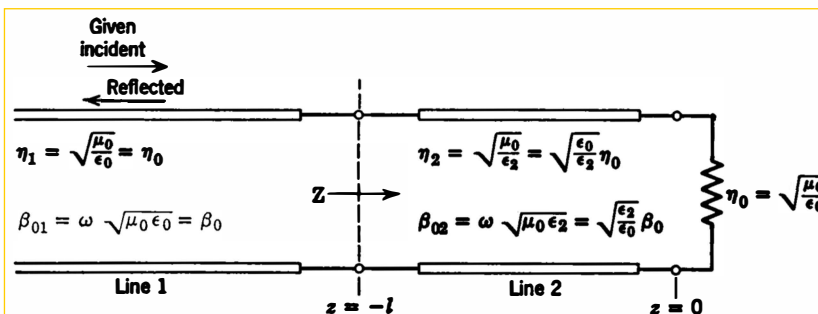
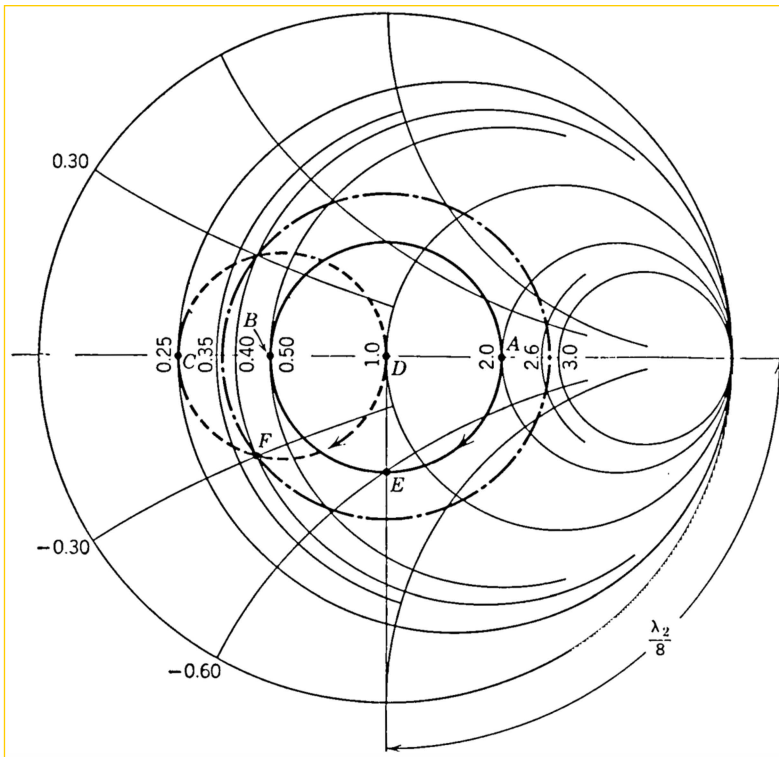


Fig. 7.16. Transmission-line equivalent of Fig. 7.15.



**Fig. 7.17.** Smith chart for the example of Figs. 7.15 and 7.16

load impedance is  $Z/\eta_0 = (Z/\eta_2)(\eta_2/\eta_0) = \frac{1}{2}(Z/\eta_2)$ , which traces the dashed circle on the chart passing through the real axis at normalized resistance values 0.25 and 1.0 when  $l = \frac{1}{4}\lambda_2$  and  $l = 0$  (points C and D) respectively.<sup>1</sup> The largest reflection coefficient on line 1 thus occurs when  $l = \frac{1}{4}\lambda_2$  and has the value

$$|\bar{\Gamma}|_{\max} = \frac{1 - 0.25}{1 + 0.25} = \frac{3}{5} = 0.6$$

Thus the maximum percentage reflected power is  $|\bar{\Gamma}|_{\max}^2 = 9/25 = 0.36$ , or 36%, when  $l = 0.375$  cm (or an odd multiple thereof).

For the case  $l = \frac{1}{8}\lambda_2 = 0.1875$  cm, the Smith chart shows  $Z/\eta_2 = 0.8 - j0.6$  at point E. Normalized on  $\eta_0$  to refer to line 1, this be-

<sup>1</sup> That the dashed locus must be a circle follows from Sec. 3.5, Eq. 3.79 ff., and the reference cited there.

## 344 ELECTROMAGNETIC ENERGY TRANSMISSION AND RADIATION

comes  $0.4 - j0.3$  (point  $F$ ), which lies on the dash-dot circle of constant  $|\Gamma|$  passing through normalized resistance values 0.36 and 2.78. Thus the standing-wave ratio on line 1 is  $s = 2.78$ , and  $|\Gamma| = \frac{s-1}{s+1} = 1.78/3.78 = 0.471$ . This corresponds to  $(0.471)^2$  or 22.2% reflected power.

Needless to say, since the dielectric is lossless, the power transmitted into medium 3 (Fig. 7.15) is equal to the difference between the incident and reflected powers in medium 1. Expressed as a percentage of the incident power, that transmitted in our numerical example is 100% for  $l = 0$  (or  $l = \lambda_2/2$ ), 77.8% for  $l = \lambda_2/8$ , and a minimum of 64% for  $l = \lambda_2/4$ .

Perhaps it is worth while to see the analytical treatment of the problem of Fig. 7.15 (or the equivalent in Fig. 7.16), if only to appreciate the simplification available from the previous Smith-chart solution. Thus, for medium 2 at  $z = 0$ , we have

$$\Gamma_{R2} = \frac{\eta_0 - \eta_2}{\eta_0 + \eta_2}$$

since  $\Gamma_{R2}$  is real here. At  $z = -l$ , however,

$$\bar{\Gamma}_2(-l) = \Gamma_{R2} e^{-j2\beta_{02}l}$$

The corresponding normalized impedance in medium 2 at  $z = -l$  is

$$\frac{Z}{\eta_2} = \frac{1 + \bar{\Gamma}_2(-l)}{1 - \bar{\Gamma}_2(-l)} = \frac{1 + \Gamma_{R2} e^{-j2\beta_{02}l}}{1 - \Gamma_{R2} e^{-j2\beta_{02}l}}$$

But the wave impedance  $Z$  in ohms must look the same at  $z = -l$ , whether we consider ourselves to be just in medium 1 or just in medium 2. This is, in fact, a direct result of the boundary condition requiring tangential  $E$  and tangential  $H$  to be separately continuous across the interface. In the transmission-line analogy (Fig. 7.16), the continuity of  $Z$  follows likewise from the separate continuity of voltage and current. Thus the normalized load impedance seen by medium 1 at  $z = -l$  is

$$\frac{Z}{\eta_0} = \frac{\eta_2}{\eta_0} \left( \frac{Z}{\eta_2} \right) = \frac{\eta_2}{\eta_0} \left( \frac{1 + \Gamma_{R2} e^{-j2\beta_{02}l}}{1 - \Gamma_{R2} e^{-j2\beta_{02}l}} \right)$$

leading to a load reflection coefficient in medium 1 at  $z = -l$  of

$$\Gamma_{R1} = \frac{(Z/\eta_0) - 1}{(Z/\eta_0) + 1} = \Gamma_{R2} \left( \frac{e^{j2\beta_{02}l} - 1}{e^{j2\beta_{02}l} + 1} \right)$$

where a considerable amount of algebra has been omitted which the reader is urged to reproduce on a separate sheet.

Now we are interested in  $|\bar{\Gamma}_{R1}|^2$ , which can be found most easily from sketches showing the geometry of the complex numbers in the numerator and denominator of  $\bar{\Gamma}_{R1}$ . We find

$$|\bar{\Gamma}_{R1}|^2 = \frac{4\Gamma_{R2}^2 \sin^2 \beta_{02}l}{(1 - \Gamma_{R2}^2)^2 + 4\Gamma_{R2}^2 \sin^2 \beta_{02}l}$$

Evidently  $|\bar{\Gamma}_{R1}| = 0$  if  $\beta_{02}l = 0, \pi, 2\pi, \dots$  i.e., the medium thickness  $l$  is an integer multiple of  $\lambda_2/2$ . Also it is clear that the whole fraction is largest (as a function of  $l$ ) when  $\sin^2 \beta_{02}l$  is largest, i.e., when  $2\beta_{02}l = \pi, 3\pi, 5\pi, \dots$ , or  $l = \lambda_2/4, 3\lambda_2/4, 5\lambda_2/4$ , etc. Under this condition the (maximum) value of  $|\bar{\Gamma}_{R1}|$  is

$$|\bar{\Gamma}_{R1}|_{\max} = \frac{2|\Gamma_{R2}|}{1 + |\Gamma_{R2}|^2}$$

In our numerical example, where  $\eta_0/\eta_2 = 2$ , we have  $\Gamma_{R2} = (2 - 1)/(2 + 1) = \frac{1}{3}$ . Hence  $|\bar{\Gamma}_{R1}|_{\max} = \frac{2}{3}/(1 + \frac{1}{9}) = \frac{3}{5}$ , as found previously from the Smith-chart solution.

If the polarization of the incident wave were along the  $y$ -axis, our previous work would remain essentially unchanged. In fact, the simplest procedure would be to relabel the axes so that  $y$  became  $x$  and  $-x$  became  $y$ . Since the boundary conditions are not affected physically by the direction of the electric field in the  $x, y$  plane, the formal solution of the problem then remains completely unchanged.

In the sinusoidal steady state at frequency  $\omega$ , the comments about polarization made in Sec. 7.1.4 and Sec. 1.3.2 mean that the most general incident wave might simply have an  $E_{x0}^+$  and an  $E_{y0}^+$  of different magnitudes and phases. Thus we would make (and later superpose) two solutions to our problem, the difference between these solutions being only a  $+90^\circ$  rotation about the  $+z$ -axis and a magnitude and phase difference corresponding to those of  $E_{x0}^+$  and  $E_{y0}^+$ .

An interesting practical example of transmission-line thinking applied to plane-wave problems is that of "coated optics." If, in Fig. 7.15, medium 3 were glass rather than air—representing a lens or show window—and medium 1 were still air, one might ask for a coating (medium 2) which would match  $\eta_3$  to  $\eta_0$  and thereby eliminate objectionable reflections from the front surface. One solution would be a quarter-wave coating acting as a matching transformer whose characteristic wave impedance  $\eta_2$  would have to satisfy the relation  $\eta_2 = \sqrt{\eta_0 \eta_3}$ . Such materials exist for visible-light wave lengths, and are

used on some optical-instrument lenses. It is important to note that the thickness must be a quarter of a wave length as measured *in the coating material itself*, not of the wave length in glass or air. Moreover, the matching behavior of the coating is exact only at the single frequency for which the film is a quarter wave thick, and when the light waves strike it at normal incidence.

Before leaving the topic of uniform plane waves at normal incidence in lossless media, we should mention that the rather complete analogy of these problems to those of lossless transmission lines applies in the time domain, for transients, as well as in the frequency domain for sinusoidal steady state. This is evident either directly from Eqs. 7.3, 7.4, and 7.8 or from a Fourier point of view applied to our results for the steady state. As long as the characteristic impedance  $\eta = \sqrt{\mu/\epsilon}$  and phase velocity  $v_p = 1/\sqrt{\epsilon\mu}$  are independent of frequency, the steady-state idea of independent (+) and (-) waves propagating with corresponding time delays proportional to distance, and with voltage-to-current ratios  $\eta$  and  $-\eta$  respectively, carries over directly into the time domain. Only the question of rotating polarizations is slightly new; but since such situations can always be resolved into two separate linear polarizations, the difficulty amounts merely to solving twice as many of the same old problems.

Transmission-line analogies are present, but more subtle, in our next topics, which begin with oblique incidence upon plane boundaries and conclude with some examples of guided waves.

## 7.4 Oblique Incidence of a Uniform Plane Wave

### 7.4.1 Geometry of Oblique Incidence

We already know that a uniform plane wave propagating in any space direction is a solution to Maxwell's equations, and that it can always be decomposed into two linearly polarized components with mutually perpendicular electric (and magnetic) fields. These facts have not really helped us greatly in our consideration of normal incidence, for two reasons:

1. The direction of propagation of the incident wave could always be chosen as the  $z$ -axis, and the normal to the plane boundary would coincide with it (as would the direction of propagation of the reflected and transmitted waves).
2. The polarization of the incident wave could not only be considered linear but also its orientation needed little attention because of the

uniform electrical structure and symmetrical orientation of the boundary with respect to the  $z$ -axis.

When we come to oblique incidence, however, the questions of direction of propagation and polarization are by no means trivial physically. Therefore we must acknowledge them in our analysis.

The geometry for a uniform plane wave at oblique incidence upon a uniform plane boundary is shown in Fig. 7.18. The unit vector  $n_1$ , normal to the boundary, and the propagation vector  $\beta_{0i}$  of the incident wave define what is called the *plane of incidence*. The *angle of incidence*  $\vartheta_i$  is measured in this plane as the acute angle between  $-\beta_{0i}$  and  $n_1$ . A unit vector  $n_2$ , normal to the plane of incidence, is also parallel to the boundary plane.

Now the electric and magnetic field vectors of the incident wave must lie in planes perpendicular to its propagation vector  $\beta_{0i}$ . There is only one direction in space which is parallel to these planes and also parallel to the boundary plane. This direction is defined by the unit vector  $n_2$ , normal to both  $n_1$  and  $\beta_{0i}$ . We shall make the  $+x$ -axis parallel to  $n_2$ . For the  $+z$ -axis we shall choose the line normal to the boundary plane, i.e., that defined by  $-n_1$ . The  $y$ -axis is finally determined by the line perpendicular to  $n_2$  and  $n_1$  in such a sense that it forms a right-handed coordinate system with the  $+z$ - and  $+x$ -axes. The  $+y$ -axis is therefore in the direction  $(-n_1) \times n_2$  parallel to both the boundary plane and the plane of incidence.

It should now be clear that the electric and magnetic fields of the incident wave, which are mutually perpendicular and lie in a plane normal to its direction of propagation, cannot *both* also be parallel (tangential) to the boundary. Thus, the simplest polarizations we can

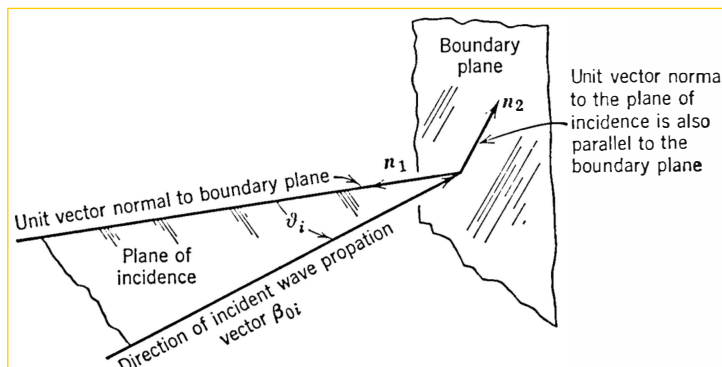
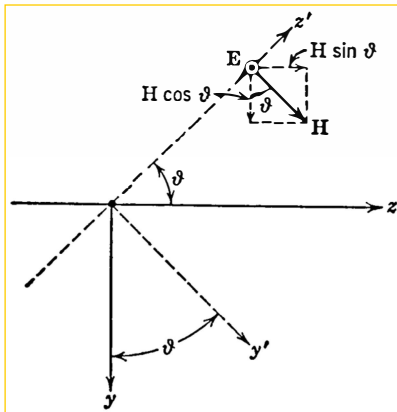


Fig. 7.18. Geometry of oblique incidence.



**Fig. 7.19.** Rotation of coordinates for a uniform plane wave.

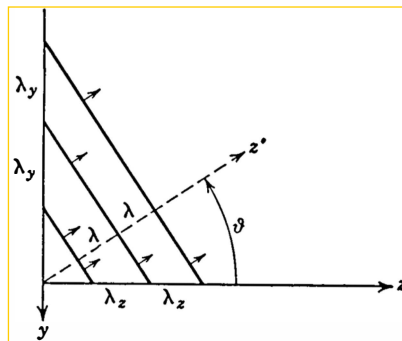
have, from the point of view of meeting boundary conditions on tangential field components, are those for which either  $\mathbf{E}_i$  or  $\mathbf{H}_i$  is linearly polarized along the  $[x]$ -axis ( $n_2$ ). Then either  $\mathbf{E}_i$  or  $\mathbf{H}_i$  (but not both) becomes parallel to the boundary plane. Since  $\mathbf{E}_i$  and  $\mathbf{H}_i$  are always mutually perpendicular in a linearly polarized uniform plane wave, these two cases, in fact, also represent two mutually perpendicular electric-field polarizations of the incident wave. Therefore, if for every  $\vartheta_i$  we treat these two cases, we shall be able to handle all possibilities through subsequent use of superposition.

Our choice of the  $z$ -axis normal to the boundary surface means that it neither coincides with the direction of propagation of the incident wave nor, in general, with that of the reflected or transmitted waves. This leaves us with the task of expressing analytically the field of a uniform plane wave in a rotated coordinate system, a problem which we have discussed previously in connection with Figs. 7.2 and 7.7.

In the present case, consider the wave propagating along the  $[+z']$  direction in Fig. 7.19, and take the polarization (direction of  $\mathbf{E}$ ) to be linear and along the  $[+x]$ -axis, which points out of the paper. The complex vector  $\mathbf{E}$  will then also be along the  $[+x]$ -axis, and the magnetic field will be along the  $[+y']$  axis, as shown. In the  $(x, y', z')$  coordinates, which are the familiar ones, we have

$$\begin{aligned}
 (a) \quad & \mathbf{E} = a_x \mathbf{E} e^{-j\beta_0 z'} \\
 (b) \quad & \mathbf{H} = a_y \mathbf{H} e^{-j\beta_0 z'} \\
 (c) \quad & \mathbf{H} = \frac{\mathbf{E}}{\eta}
 \end{aligned} \tag{7.83}$$

**Fig. 7.20.** A uniform plane wave moving along the  $[+z']$  direction.



For the new coordinates  $(x, y, z)$  of Fig. 7.19, the  $x$ -axis has remained unchanged, but the others have been rotated by the angle  $\vartheta$  defined on the sketch. Therefore, to express unit vector  $\mathbf{a}_{y'}$  in terms of unit vectors  $\mathbf{a}_y$  and  $\mathbf{a}_z$ , we have from the geometry

$$\mathbf{a}_{y'} = \mathbf{a}_y \cos \vartheta + \mathbf{a}_z \sin \vartheta \quad (7.84)$$

Comparing Fig. 7.19 with Fig. 7.2 in regard to  $z'$ , we note that in Fig. 7.19

$$l_{z'} = 0 \quad m_{z'} = -\sin \vartheta \quad n_{z'} = \cos \vartheta \quad (7.85a)$$

so that from Eq. 7.19 there follows the relation

$$z' = z \cos \vartheta - y \sin \vartheta \quad (7.85b)$$

Consequently Eqs. 7.83 become

- |     |  |
|-----|--|
| (a) | $\mathbf{E} = \mathbf{a}_x \mathbf{E} e^{j\beta_0 y \sin \vartheta} e^{-j\beta_0 z \cos \vartheta}$  |
| (b) | $\mathbf{H} = (\mathbf{a}_y \mathbf{H} \cos \vartheta + \mathbf{a}_z \mathbf{H} \sin \vartheta) e^{j\beta_0 y \sin \vartheta} e^{-j\beta_0 z \cos \vartheta} \quad (7.86)$ |
| (c) | $\mathbf{H} = \frac{\mathbf{E}}{\eta}$   |

which should be compared with Eqs. 7.26 and 7.32a. Observe particularly the relationship between the vector components of  $\mathbf{H}$  in Eq. 7.86b and the corresponding geometric representation of them in Fig. 7.19. Obviously this part of  $\mathbf{H}$  could be written by *inspection* from the figure. The same is true of the exponential factors in Eqs. 7.86a and 7.86b. A special case of Fig. 7.3b for the present situation is shown in Fig. 7.20. The corresponding form of Eqs. 7.33 through 7.36 may be written in view of either Eqs. 7.85a or, preferably, of the geometry of Fig. 7.20 directly:

$$(a) \lambda_y \equiv \frac{\lambda}{\sin \vartheta} = \frac{2\pi}{\beta_0 \sin \vartheta} \equiv \frac{2\pi}{|\beta_y|} \quad (7.87)$$

$$(b) \lambda_z \equiv \frac{\lambda}{\cos \vartheta} = \frac{2\pi}{\beta_0 \cos \vartheta} \equiv \frac{2\pi}{|\beta_z|}$$

$$(a) |\beta_y| = \beta_0 \sin \vartheta \quad (7.88)$$

$$(b) |\beta_z| = \beta_0 \cos \vartheta$$

$$(a) v_y \equiv \frac{\omega}{|\beta_y|} = \frac{\omega}{\beta_0 \sin \vartheta} = \frac{v}{\sin \vartheta} \quad (7.89)$$

$$(b) v_z \equiv \frac{\omega}{|\beta_z|} = \frac{\omega}{\beta_0 \cos \vartheta} = \frac{v}{\cos \vartheta}$$

and because  $\sin^2 \vartheta + \cos^2 \vartheta = 1$

$$(a) \beta_z^2 + \beta_y^2 = \beta_0^2$$

$$(b) \frac{1}{\lambda_z^2} + \frac{1}{\lambda_y^2} = \frac{1}{\lambda^2} \quad (7.90)$$

$$(c) \frac{1}{v_z^2} + \frac{1}{v_y^2} = \frac{1}{v^2}$$

It should be emphasized in connection with Fig. 7.20 that when the actual wave moves in the arrow directions as time goes on, the phase fronts advance along  $+z'$ ,  $+z$ , and  $-y$ . This accounts for the different signs of the exponents containing  $z$  and  $y$  in Eqs. 7.86.

If the plane wave had the alternate linear polarization (i.e., **II** parallel to the boundary) but still propagated in the  $+z'$  direction, it could have **E** along  $+y'$  and **II** along  $-x$ :

$$(a) \mathbf{E} = a_y \mathbf{E} e^{-j\beta_0 z'} \quad (7.91)$$

$$(b) \mathbf{II} = -a_x \mathbf{II} e^{-j\beta_0 z'} \quad (7.91)$$

$$(c) \mathbf{II} = \frac{\mathbf{E}}{\eta}$$

In the  $(x, y, z)$  coordinates, Eqs. 7.91 become

$$(a) \mathbf{E} = (a_y \mathbf{E} \cos \vartheta + a_z \mathbf{E} \sin \vartheta) e^{j|\beta_y| y} e^{-j\beta_z z} \quad (7.92)$$

$$(b) \mathbf{II} = -a_x \mathbf{II} e^{j|\beta_y| y} e^{-j\beta_z z} \quad (7.92)$$

$$(c) \mathbf{II} = \frac{\mathbf{E}}{\eta}$$

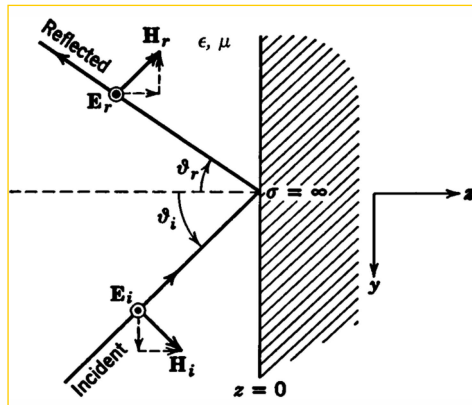
It is extremely desirable to learn to write equations like Eqs. 7.86 and 7.92 directly from pictures of the  $\mathbf{E}$  and  $\mathbf{H}$  vectors (in the manner of Fig. 7.19) and of the phase fronts (in the manner of Fig. 7.20). Such pictures are surprisingly helpful in resolving ambiguities of algebraic sign connected with the field components and the propagation exponents along the coordinate axes. A thorough mastery of these matters now will remove the major difficulties from the forthcoming discussions.

We are now in a position to examine reflection and refraction of uniform plane waves at oblique incidence upon the interface between lossless media.

#### 7.4.2 Oblique Incidence upon a Perfect Conductor

First we may consider the perfectly conducting metal mirror at  $z = 0$  in Fig. 7.21, upon which is incident an  $x$ -polarized wave from a direc-

**Fig. 7.21.** Oblique incidence upon a perfect conductor with polarization parallel to the boundary.



tion  $\vartheta_i$  with the normal. Since no field exists within the metal, we have only to deal with a possible reflected wave. Moreover, inasmuch as the incident wave has its electric field parallel to the conducting plane, and the boundary condition requires the total electric field parallel to that plane at  $z = 0$  to vanish, it is clear that the reflected wave will have the same polarization as the incident wave. Hence the direction of propagation of the reflected wave will lie in the plane of incidence, as shown in Fig. 7.21, at some angle  $\vartheta_r$  with respect to the boundary normal.

The incident wave is given as

$$(a) \quad \mathbf{E}_i = \mathbf{a}_x E_i e^{j\beta_0 y \sin \vartheta_i} e^{-j\beta_0 z \cos \vartheta_i}$$

$$(b) \quad \mathbf{H}_i = (\mathbf{a}_y \frac{E_i}{\eta} \cos \vartheta_i + \mathbf{a}_z \frac{E_i}{\eta} \sin \vartheta_i) e^{j\beta_0 y \sin \vartheta_i} e^{-j\beta_0 z \cos \vartheta_i}$$
(7.93)

and the reflected wave is of the form

$$(a) \quad \mathbf{E}_r = \mathbf{a}_x E_r e^{j\beta_0 y \sin \vartheta_r} e^{j\beta_0 z \cos \vartheta_r}$$

$$(b) \quad \mathbf{H}_r = \left( -\mathbf{a}_y \frac{E_r}{\eta} \cos \vartheta_r + \mathbf{a}_z \frac{E_r}{\eta} \sin \vartheta_r \right) e^{j\beta_0 y \sin \vartheta_r} e^{j\beta_0 z \cos \vartheta_r}$$
(7.94)

At  $z = 0$ , for all  $y$  (and  $x$ ), we require  $\mathbf{E}_i + \mathbf{E}_r = 0$ ; i.e.,

$$\mathbf{E}_i e^{j\beta_0 y \sin \vartheta_i} = -\mathbf{E}_r e^{j\beta_0 y \sin \vartheta_r}$$
(7.95)

so

$$(a) \quad \vartheta_r = \vartheta_i (\equiv \vartheta)$$

$$(b) \quad -\mathbf{E}_r = \mathbf{E}_i (\equiv \mathbf{E})$$
(7.96)

Equation 7.96a is the familiar optical law that the angles of incidence and reflection are equal. From Eq. 7.96b we see that all the incident power is reflected.

The total field for  $z \leq 0$  is given by the sum of the incident and reflected waves under conditions of Eq. 7.96.

$$(a) \quad \mathbf{E} = -\mathbf{a}_x 2j E e^{j\beta_0 y \sin \vartheta} \sin(\beta_0 z \cos \vartheta)$$

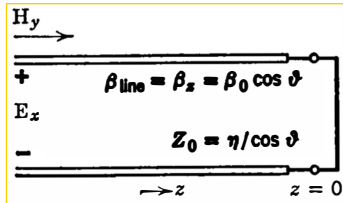
$$(b) \quad \mathbf{H} = \frac{2\mathbf{E}}{\eta} [\mathbf{a}_y \cos \vartheta \cos(\beta_0 z \cos \vartheta) - \mathbf{a}_z j \sin \vartheta \sin(\beta_0 z \cos \vartheta)] e^{j\beta_0 y \sin \vartheta}$$
(7.97)

We observe that  $\mathbf{E}_x$  and  $\mathbf{H}_y$  are  $90^\circ$  out of time phase. This is to be expected on the basis that the  $[z]$  component of the complex Poynting vector is  $\frac{1}{2} \mathbf{E}_x \mathbf{H}_y^*$ , which cannot have a real part because no average power is absorbed by the mirror. It is also noteworthy that  $\mathbf{E}_x = 0$  whenever  $\beta_0 z \cos \vartheta = -m\pi$ ,  $m = 0, 1, 2, \dots$ , or

$$z = \frac{-m\lambda}{2 \cos \vartheta} = -\frac{m\lambda_z}{2} \quad m = 0, 1, 2, \dots$$

The electric field has nodal planes parallel to the mirror at multiples of  $\frac{1}{2}\lambda_z$  from it. Observed along  $[z]$ , all the field components have standing-wave character; but  $\mathbf{E}_x$  and  $\mathbf{H}_z$  have nodes at the same planes, while

**Fig. 7.22.** Transmission line analogy for the  $z$  dependence and the  $x$  and  $y$  field components in Fig. 7.21.



the nodes of  $\Pi_y$  are displaced  $\frac{1}{4}\lambda_z$  from those of  $E_x$  and  $\Pi_z$ . The  $y$  variation of all the field components, on the other hand, has traveling-wave character with effective wave length  $\lambda_y$  and propagation in the  $-y$  direction. This fact checks with the  $y$  component of the complex Poynting vector  $(-\frac{1}{2}E_x\Pi_z^*)$ , which is real and negative, indicating average power flowing in the  $-y$  direction.

It is therefore convenient to think of the whole field as a pure standing wave extending along  $-z$ , which, however, also "slides" bodily along  $-y$ . Indeed, we note that the field components parallel to the mirror are

$$(a) E_x = \left[ -2jE \sin\left(\frac{2\pi z}{\lambda_z}\right) \right] e^{j(2\pi y/\lambda_y)} \quad (7.98)$$

$$(b) \Pi_y = \left[ \frac{2E}{(\eta/\cos \vartheta)} \cos\left(\frac{2\pi z}{\lambda_z}\right) \right] e^{j(2\pi y/\lambda_y)}$$

which, examined along  $z$  at fixed  $y$ , look exactly like the voltage and current standing waves on the transmission line of Fig. 7.22. Of course, we see from Eqs. 7.93 and 7.94 that this line shows only *some* of the features of the actual problem inasmuch as it omits all information relating to the traveling-wave nature of the  $y$  dependence, and to the corresponding magnetic field component  $\Pi_z$ . Nevertheless, such partial equivalence is often useful. It is however most important to remember that both the characteristic impedance of the line and its phase constant involve the angle of incidence. It is not hard to see why this is so, if we look back at just the incident wave in Fig. 7.21. Whereas  $(|E_i|/|\Pi_i|) = \eta$ ,<sup>1</sup> our transmission line deals only with  $|E_{xi}|/|\Pi_{yi}|$ , i.e., only with the  $+z$ -directed wave impedance  $Z_z$ . For the case at hand,  $|E_{xi}| = |E_i|$ , but  $|\Pi_{yi}| = |\Pi_i| \cos \vartheta$ . Hence the appropriate line impedance is  $\eta/\cos \vartheta$ . Similarly, the appearance of  $\beta_z = \beta_0 \cos \vartheta$  is evident from Fig. 7.20, where the wave length observed along  $z$  is seen to be greater than  $\lambda$  by the factor  $1/\cos \vartheta$ .

<sup>1</sup>  $\|A\| \equiv \sqrt{A \cdot A^*} = \sqrt{|A_x|^2 + |A_y|^2 + |A_z|^2} = \sqrt{|A_r|^2 + |A_i|^2}$ . Hence for a linearly polarized vector  $A = \text{Re}(Ae^{j\omega t})$ ,  $\|A\| = |A|_{\max}$ .

If these ideas are understood, it will be clear that a revision of Fig. 7.21 for the alternate polarization in which  $\mathbf{H}_i$  is parallel to the mirror requires that in Fig. 7.22 we exchange  $E_y$  for  $E_x$ ;  $-H_x$  for  $H_y$ ;  $\eta \cos \vartheta$  for  $Z_0$  instead of  $\eta/\cos \vartheta$ ; and  $\beta_{\text{line}} = \beta_0 \cos \vartheta$ , as before. The reader is urged not only to check these relationships carefully but also to write out completely all the field components and boundary conditions for this polarization in the manner of Eqs. 7.93 through 7.98.

It is significant to realize in this connection that the familiar law of reflection [7.96a] comes directly from the form of the exponential factors in Eqs. 7.93 and 7.94 and, therefore, is not influenced by the polarization. Indeed, it is really quite obvious from Fig. 7.20 that, since the boundary condition on the fields has to be satisfied for *all* values of  $y$ , a necessary (but not sufficient) condition is that all the waves concerned in the problem have the same phase constant (or wave length or phase velocity) *when measured along the boundary* (in the manner of Eqs. 7.87, 7.88, and 7.89). Only in this way can the various waves "keep in step" along the interface, so that the remainder of the boundary conditions can be met at more than just a single point on it.

#### 7.4.3 Oblique Incidence upon an Interface between Lossless Dielectrics

**7.4.3.1 POLARIZATION PARALLEL TO THE BOUNDARY.** The next example for consideration involves incidence of a uniform plane wave upon the interface between lossless dielectrics (Fig. 7.23). The incident wave is  $x$ -polarized (parallel to the boundary) as shown, and is given analytically by Eq. 7.93. Again, it is clear that the reflected and transmitted (refracted) waves are also  $x$ -polarized, so that all propagation directions lie in the plane of incidence, as indicated by the figure.

If we are to have any hope of establishing the necessary continuity of tangential  $\mathbf{E}$  and  $\mathbf{H}$  across the boundary plane  $z = 0$  (for *all*  $y$ ), the phase velocities of the three waves *as measured along the y axis* must be the same in magnitude *and* sense. Thus, from the figure [which, for convenience, shows  $\lambda$  rather than  $v = (\omega\lambda)/(2\pi)$ ],

$$(a) \quad \frac{v_1}{\sin \vartheta_i} = \frac{v_1}{\sin \vartheta_r} \quad (7.99)$$

$$(b) \quad \frac{v_1}{\sin \vartheta_i} = \frac{v_2}{\sin \vartheta_2}$$

or

(a)

$$\vartheta_r = \vartheta_i \equiv \vartheta_1$$

(b)

$$\sin \vartheta_2 = \left( \frac{v_2}{v_1} \right) \sin \vartheta_1 = \sqrt{\frac{\epsilon_1 \mu_1}{\epsilon_2 \mu_2}} \sin \vartheta_1 \quad (7.100)$$

Equation 7.100a is again the law of reflection and Eq. 7.100b is the equally well-known optical result called Snell's law of refraction. They arise here from that part of the boundary conditions which merely de-

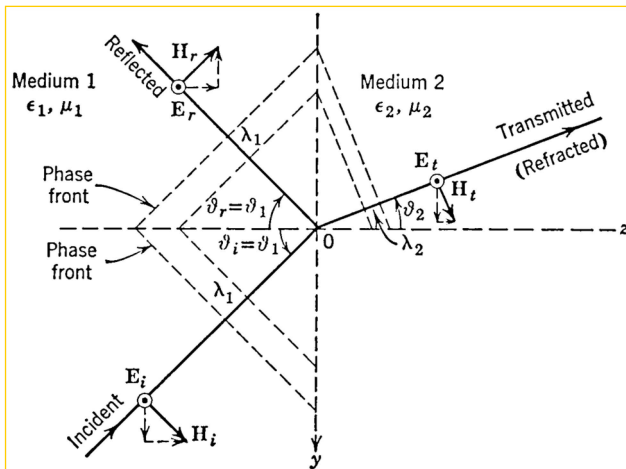


**Fig. 7.23.** Oblique incidence on an interface between lossless dielectrics with polarization parallel to interface.

mands that the three waves be "in step" along the interface; thus these laws do not depend upon the polarization.

The remainder of the required conditions, however, will involve the specific continuity of  $E_x$  and  $H_y$  across the boundary  $z = 0$ ; but, since Eq. 7.100 already guarantees the common phase velocity of the three waves along  $y$ , it will be sufficient to apply the field continuity condition at any single point. We choose  $y = 0$ ; so

(a)

$$E_{xi} + E_{xr} = E_{xt} \quad (7.101)$$

(b)

$$H_{yi} + H_{yr} = H_{yt}$$

But from Fig. 7.23, and the fact that the complete electric and mag-

netic fields of a uniform traveling plane wave have the ratio  $\eta$ . Eqs. 7.101 may be recast to read

$$\left. \begin{array}{l} (a) \quad E_{xi} + E_{xr} = E_{xt} \\ (b) \quad \frac{E_{xi} - E_{xr}}{(\eta_1/\cos \vartheta_1)} = \frac{E_{xt}}{(\eta_2/\cos \vartheta_2)} \end{array} \right\} \quad \text{E parallel to boundary} \quad (7.102)$$

Eliminating first  $E_{xt}$  and then  $E_{xr}$ , we find from Eq. 7.102

$$\left. \begin{array}{l} (a) \quad \frac{E_{xr}}{E_{xi}} \equiv \Gamma_R = \frac{Z_2 - Z_1}{Z_2 + Z_1} \\ (b) \quad \frac{E_{xt}}{E_{xi}} \equiv T = \frac{2Z_2}{Z_2 + Z_1} \end{array} \right\} \quad (7.103)$$

where

$$\left. \begin{array}{l} (a) \quad Z_1 = \frac{\eta_1}{\cos \vartheta_1} = \frac{E_{xi}}{H_{yi}} = -\frac{E_{xr}}{H_{yr}} \\ (b) \quad Z_2 = \frac{\eta_2}{\cos \vartheta_2} = \frac{E_{xt}}{H_{yt}} \end{array} \right\} \quad \text{E parallel to boundary} \quad (7.104)$$

The similarity of Eqs. 7.103 to those of a transmission-line junction is evident. The fact that the characteristic impedances  $Z_1$  and  $Z_2$  are wave impedances and, therefore, involve the angles of incidence and refraction (Eq. 7.104) is very important. The reason for their appearance has been discussed in connection with Fig. 7.22. If we wish to draw an analogous transmission-line system to represent the  $z$  dependence of all the waves, as we did in Fig. 7.22, the propagation constants also must contain these angles, because they will refer to phases only along the  $z$ -axis. In Fig. 7.24, we show the line system for this case. As in Fig. 7.22, it is vital to understand that Fig. 7.24 contains no information about either  $H_z$  or the  $y$  dependence of any of the fields in the actual problem.

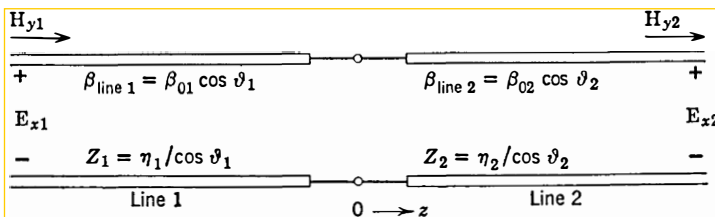


**Fig. 7.24.** Transmission line analogy for the  $z$  dependence and the  $x$  and  $y$  field components in Fig. 7.23.

It is equally significant that Snell's law (Eq. 7.100) relates  $\vartheta_1$  and  $\vartheta_2$ ; thus a knowledge of either angle is sufficient to determine the parameters of both lines in Fig. 7.24, assuming, of course, that we know  $\epsilon$  and  $\mu$  in both media of the physical problem.

In spite of the fact that some information about the actual physical problem (Fig. 7.23) is absent from the transmission-line system of Fig. 7.24, the latter contains the most involved aspects of the situation, and it does so in a form for which the Smith chart is applicable. With just a single interface, the advantages of the transmission-line representation are hardly evident. Equations 7.103 are really all we need in that case. If there are several interfaces, however, the problem of determining  $\bar{\Gamma}$  at the first one involves considerations like those we encountered in Fig. 7.15, for which the Smith chart is a great help. In fact, the only added complication in the oblique case is the need to apply Snell's law at each interface to find the directions of the refracted waves in each medium. If this is done at the start of the problem, the parameters of the transmission line for each medium are determined in the manner of Fig. 7.24. From here on, the rest of the work follows exactly the usual transmission-line pattern.

There is one point about the flow of power in the case of oblique incidence which deserves special comment. In Fig. 7.23, all the waves have components of the Poynting vector along  $-y$ . There is no reason why these components of the power flow should obey the relation that the "incident" power minus that "reflected" equals that "transmitted," for they are all in the same direction—parallel to the boundary. On the other hand, all the waves also have components of the Poynting vector along  $+z$ . It is clear in this case that none of the power flowing normal to the boundary in medium 2 can have originated anywhere but as  $+z$ -directed power in medium 1. Hence, for these normal components, we would expect the aforementioned power relation. In particular, the  $+z$ -directed incident power is

$$\frac{1}{2} E_{xi} H_{yi}^* = \frac{|E_{xi}|^2 \cos \vartheta_1}{2\eta_1} = \frac{|E_{xi}|^2}{2Z_1}$$

Similarly, the  $+z$ -directed reflected power is

$$-\frac{1}{2} E_{xr} H_{yr}^* = \frac{-|E_{xr}|^2}{2Z_1}$$

and that transmitted is

$$\frac{1}{2} E_{xt} H_{yt}^* = \frac{|E_{xt}|^2}{2Z_1}$$

The “conservation” relation for  $+z$ -directed power therefore reads

$$|E_{xi}|^2 - |E_{xr}|^2 = \frac{Z_1}{Z_2} |E_{xt}|^2$$

or, by definition of  $\bar{\Gamma}_R$  and  $|T|$ ,

$$1 - |\bar{\Gamma}_R|^2 = \frac{Z_1}{Z_2} |T|^2 \quad E \text{ parallel to boundary} \quad (7.105)$$

This is also the conclusion we would reach from Fig. 7.24. Substitution of Eqs. 7.103 into 7.105 shows that the latter is indeed true.

It is also true that the ratio of *total* power per unit area in the reflected wave  $((|E_{xr}|^2)/(2\eta_1))$  to that in the incident wave  $((|E_{xi}|^2)/(2\eta_1))$  is just  $|\bar{\Gamma}_R|^2$ ; but the ratio of the *total* power per unit area in the transmitted wave  $((|E_{xt}|^2)/(2\eta_2))$  to that in the incident wave is  $(\eta_2/\eta_1)|T|^2$ , which by Eq. 7.105 is obviously *not* equal to  $1 - |\bar{\Gamma}_R|^2$ . The explanation for this result is the one suggested above: While the *normal* components of the power flow must obey the familiar relation between incident, reflected, and transmitted powers, the *parallel* components need not—and, in general, do not—behave similarly. Hence the *total* power-flow-per-unit-area vectors need not—and, in general, do not—obey the familiar “conservation” relation!

**7.4.3.2 POLARIZATION IN THE PLANE OF INCIDENCE.** The alternate polarization for the problem of Fig. 7.23 places  $\mathbf{H}$  parallel to the boundary and  $\mathbf{E}$  in the plane of incidence. As mentioned previously, Eqs.

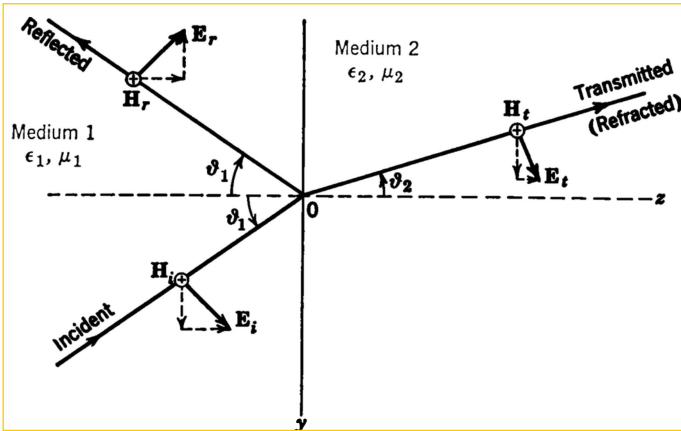


**Fig. 7.25a.** Oblique incidence on interface between lossless dielectrics with polarization in the plane of incidence.

7.99 and 7.100, relating the propagation constants along  $y$  and  $z$ , are unchanged. Therefore the directions of propagation of all the waves remain unaltered. On this basis the situation is as shown in Fig. 7.25a.

At the point  $(z = 0, y = 0)$ , the remaining boundary conditions require

$$\begin{array}{ll} \text{(a)} & E_{yi} + E_{yr} = E_{yt} \\ \text{(b)} & H_{xi} + H_{xr} = H_{xt} \end{array} \quad \text{II parallel to boundary} \quad (7.106)$$

In this case, however,

$$\begin{aligned} H_{xi} &= -\left(\frac{E_{yi}}{\cos \vartheta_1}\right) \frac{1}{\eta_1} \\ H_{xr} &= +\left(\frac{E_{yr}}{\cos \vartheta_1}\right) \frac{1}{\eta_1} \\ H_{xt} &= -\left(\frac{E_{yt}}{\cos \vartheta_2}\right) \frac{1}{\eta_2} \end{aligned} \quad \text{II parallel to boundary}$$

So Eqs. 7.106 become

$$\begin{array}{ll} \text{(a)} & E_{yi} + E_{yr} = E_{yt} \\ \text{(b)} & \frac{E_{yi} - E_{yr}}{\eta_1 \cos \vartheta_1} = \frac{E_{yt}}{\eta_2 \cos \vartheta_2} \end{array} \quad \text{II parallel to boundary} \quad (7.107)$$

or

$$\begin{array}{ll} \text{(a)} & \frac{E_{yr}}{E_{yi}} \equiv \bar{\Gamma}_R' = \frac{Z_2' - Z_1'}{Z_2' + Z_1'} \\ \text{(b)} & \frac{E_{yt}}{E_{yi}} \equiv T' = \frac{2Z_2'}{Z_2' + Z_1'} \end{array} \quad (7.108)$$

where

$$\begin{array}{ll} \text{(a)} & Z_1' \equiv \eta_1 \cos \vartheta_1 = \frac{-E_{yi}}{H_{xi}} = \frac{E_{yr}}{H_{xr}} \\ \text{(b)} & Z_2' \equiv \eta_2 \cos \vartheta_1 = \frac{-E_{yt}}{H_{xt}} \end{array} \quad \text{II parallel to boundary} \quad (7.109)$$

Consequently, this time the propagation angles enter the impedances  $Z'$  differently from the way they entered the previous impedances  $Z$ . Compare Eqs. 7.108 and 7.103, on the one hand, and Eqs. 7.109 and 7.104 on the other. In other words: For the same media and angle of incidence, the angles of reflection and refraction are the same for both polarizations; so also are the propagation constants along  $y$  and  $z$ ; but the percentage power reflected (and transmitted) may be radically different in the two cases.

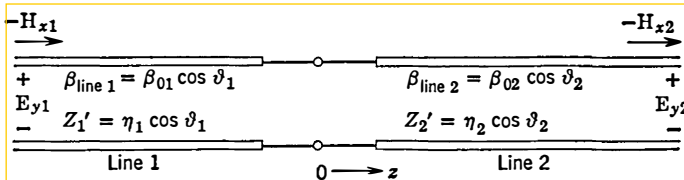


**Fig. 7.25b.** Transmission line analogy for the  $z$  dependence and the  $x$  and  $y$  field components in Fig. 7.25a.

Unlike any of the cases of normal incidence we have treated, or even of oblique incidence on a perfect conductor, a change of the polarization of the wave incident obliquely on an interface between two dielectrics does much more than merely produce a trivial corresponding change in the polarization of the reflected and transmitted waves. These matters are summarized by comparing the transmission-line analogy of Fig. 7.25a (which we show in Fig. 7.25b) with that of Fig. 7.23 (shown in Fig. 7.24).

An interesting example of the different effects produced by the two polarizations arises if we ask for what angle of incidence the reflected wave will vanish: i.e., all the normally directed incident power will be transmitted.

Taking first Fig. 7.24 ( $E$  parallel to the boundary), we note that the required condition is a “match” at  $z = 0$ :

$$Z_1 = Z_2$$

or

$$\eta_2 \cos \vartheta_{1p} = \eta_1 \cos \vartheta_{2p} \quad E \text{ parallel to boundary} \quad (7.110)$$

where  $\vartheta_{1p}$  and  $\vartheta_{2p}$  are the particular angles being sought. Squaring Eq. 7.110 yields

$$\eta_2^2(1 - \sin^2 \vartheta_{1p}) = \eta_1^2(1 - \sin^2 \vartheta_{2p})$$

which, in the light of Snell’s law (Eq. 7.100), becomes

$$\begin{aligned} \sin^2 \vartheta_{1p} &= \frac{\eta_1^2 - \eta_2^2}{\eta_1^2[(v_2/v_1)]^2 - \eta_2^2} \\ &= \frac{(\eta_1/\eta_2)^2 - 1}{[(\eta_1 v_2)/(\eta_2 v_1)]^2 - 1} \end{aligned}$$

or

$$\sin^2 \vartheta_{1p} = \frac{(\mu_1 \epsilon_2 / \mu_2 \epsilon_1) - 1}{(\mu_1 / \mu_2)^2 - 1} \quad E \text{ parallel to boundary} \quad (7.111a)$$

The angle  $\vartheta_{1p}$  is sometimes called *Brewster's angle*. As shown by Eq. 7.111a, a real solution for  $\vartheta_{1p}$  does not always exist for this polarization. One important situation for which there is no real solution to Eq. 7.111a is that in which  $\mu_1 = \mu_2$  but  $\epsilon_1 \neq \epsilon_2$ . This is the very common case of two nonmagnetic dielectrics, say, air and glass. On the other hand, for the very uncommon situation  $\epsilon_1 = \epsilon_2, \mu_1 \neq \mu_2$ , Eq. 7.111a becomes

$$\sin^2 \vartheta_{1p} = \frac{1}{(\mu_1/\mu_2) + 1}$$

or

$$\tan \vartheta_{1p} = \sqrt{\frac{\mu_2}{\mu_1}} \quad \text{E parallel to boundary and } \epsilon_1 = \epsilon_2 \quad (7.111b)$$

which always has a real solution  $\vartheta_{1p} < \pi/2$ .

In the second polarization, when  $\mathbf{H}$  is parallel to the boundary, Fig. 7.25b shows that a "match" occurs for

$$Z_1' = Z_2'$$

or

$$\eta_1 \cos \vartheta_{1p}' = \eta_2 \cos \vartheta_{2p}' \quad \mathbf{H} \text{ parallel to boundary} \quad (7.112)$$

Squaring Eq. 7.112 and using Snell's law as before yield

$$\sin^2 \vartheta_{1p}' = \frac{(\eta_2/\eta_1)^2 - 1}{(\eta_2 v_2/\eta_1 v_1)^2 - 1}$$

or

$$\sin^2 \vartheta_{1p}' = \frac{(\mu_2 \epsilon_1 / \mu_1 \epsilon_2) - 1}{(\epsilon_1 / \epsilon_2)^2 - 1} \quad \mathbf{H} \text{ parallel to boundary} \quad (7.113a)$$

Again, a real Brewster's angle  $\vartheta_{1p}'$  for this polarization does not always exist; but, as duality ideas suggest, there is now no solution in the uncommon case when  $\epsilon_1 = \epsilon_2, \mu_1 \neq \mu_2$ , while there is always a solution in the very common case  $\mu_1 = \mu_2, \epsilon_1 \neq \epsilon_2$ . In fact, under this latter condition, Eq. 7.113a becomes

$$\sin^2 \vartheta_{1p}' = \frac{1}{(\epsilon_1 / \epsilon_2) + 1}$$

or

$$\tan \vartheta_{1p}' = \sqrt{\frac{\epsilon_2}{\epsilon_1}} \quad \mathbf{H} \text{ parallel to boundary and } \mu_1 = \mu_2 \quad (7.113b)$$

which is the dual of Eq. 7.111b.

Advantage is taken of the circumstances described above to produce polarized light. As we have previously pointed out, ordinary light is not linearly polarized, but has instead (on a statistical basis) about equal amounts of each fundamental linear polarization. A slab of glass, oriented with respect to an incident beam of ordinary light so that the angle of incidence is  $\vartheta_{1p}$ , will not reflect any of the light polarized in the plane of incidence. The reflected wave will then be polarized entirely parallel to the boundary; but its intensity may be rather low because the relative dielectric constant of glass is not very large ( $\approx 4-5$ ). Use of many such slabs stacked together overcomes this difficulty, because at each interface a fixed small fraction of the parallel-polarized light is reflected, thereby removing it from the transmitted beam. Finally, the *transmitted* beam contains the light originally polarized in the plane of incidence, with very little contamination by the parallel-polarized part. The latter appears almost entirely in the net reflected wave; thus the pile of glass slabs effectively separates the unpolarized incident beam into two separate polarized ones. It is on account of this application that Brewster's angle is more commonly known as the *polarizing angle*.

**7.4.3.3 CRITICAL REFLECTION.\*** We have seen that Snell's law (Eq. 7.100b) does not depend upon the polarization. According to this law, whenever  $v_2 > v_1$ , there exist large angles of incidence  $\vartheta_1$  for which  $\sin \vartheta_2$  would have to exceed unity. In other words, if the incident wave is in a medium of slower light velocity (larger index of refraction) than that in which the transmitted wave propagates, Snell's law demands

$$\sin \vartheta_2 \geq 1$$

whenever

$$\sin \vartheta_1 \geq \frac{v_1}{v_2} = \sqrt{\frac{\epsilon_2 \mu_2}{\epsilon_1 \mu_1}} \quad (7.114)$$

or

$$\vartheta_1 \geq \vartheta_c \equiv \sin^{-1} \left( \frac{v_1}{v_2} \right) \quad (7.115)$$

The angle  $\vartheta_c$  is called the *critical angle*.

Let us examine first the situation of Fig. 7.23 (E parallel to the boundary) as  $\vartheta_1 \rightarrow \vartheta_c$  when  $v_2 > v_1$ . We note from the condition  $v_2 > v_1$  that in Snell's law  $\vartheta_2 > \vartheta_1$  for  $\vartheta_1 < \vartheta_c$ ; hence the direction of propagation of the transmitted wave in this case actually makes a larger angle with the  $+z$ -axis than does that of the incident wave. The refraction bends the wave *away* from the normal. When  $\vartheta_1 = \vartheta_c$ ,  $\sin \vartheta_2 = 1$  and  $\vartheta_2 = 90^\circ$ . The transmitted wave is then propagating

entirely parallel to the boundary, so we would expect that  $H_{yt} = 0$ . Since  $\cos 90^\circ = 0$ , Fig. 7.24 shows that  $Z_2 = \infty$  and that the incident and reflected electric fields must be equal (see also Eq. 7.103a). We have a condition of “total reflection” in which the power reflected back into medium 1 equals that incident in medium 1. The real power transmitted in a normal direction into medium 2 (i.e., along  $+z$ ) is zero, although there is a field in medium 2 representing a uniform plane wave traveling along the  $-y$ -axis. As such, this field does not vary with  $z$  at all.

What must happen physically if we now make  $\vartheta_1 > \vartheta_c$ ?

First, there must be *some* field in medium 2; for, if not, medium 2 would suddenly be acting just like a perfect conductor, merely because we happened to choose some special angles of incidence in medium 1. This is unreasonable. Besides, we should be reminded of the experimental fact in optics that, if a prism is causing an internal critical reflection, and another similar one is pressed closely against one of the sides at which the critical reflection is occurring, most of the light goes into the second prism instead of being critically reflected! There must have been some field just *outside* the original prism surface; otherwise, how could bringing up the second prism cause any change?

Granted that there is *some* field in medium 2, then, it must be such that no real (time-average) power flows in the  $+z$  direction as long as  $\vartheta_1 \geq \vartheta_c$ . This requirement stems from the well-known experimental fact in optics that “total reflection” occurs for *all* angles of incidence greater than the critical angle.

Thirdly, with reference to Fig. 7.23, there is still the problem of insuring that the incident, reflected, and transmitted waves stay “in step” along the  $y$  direction. For the reflected wave, this condition is easily met if  $\vartheta_r = \vartheta_i$  as usual. For the refracted wave, however, the present situation  $\vartheta_1 > \vartheta_c$  makes Snell’s law demand  $(v_1/\sin \vartheta_1) < v_2$ , or  $\beta_{01} \sin \vartheta_1 > \beta_{02}$ . But the wave in medium 2 must have an effective phase constant along  $y$  which equals  $\beta_{01} \sin \vartheta_1$ , and we see that this is *greater* than that ( $\beta_{02}$ ) of any possible *uniform plane wave* in medium 2!

Finally, since the incident wave is  $x$ -polarized, it should be possible to meet the boundary conditions with reflected and transmitted waves, both also  $x$ -polarized.

The conclusion is almost inescapable: The wave in medium 2 must be a *nonuniform plane wave*, arranged to *attenuate* in the  $+z$  direction (boundary condition at infinity), have a phase delay along  $-y$  with a phase constant  $\beta_2 = +\sqrt{\beta_{02}^2 + \alpha^2} > \beta_{02}$ , and to be TE with respect to the  $y$  (or  $z$ ) directions. A sketch of the conditions appears in Fig. 7.26.

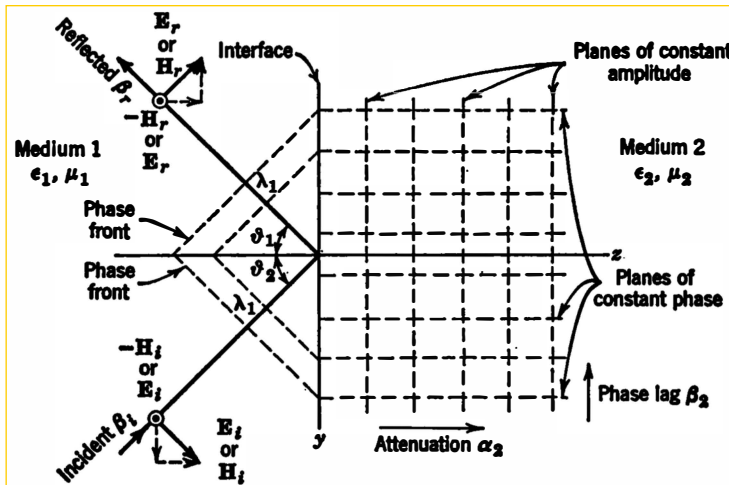


**Fig. 7.26.** Oblique incidence beyond the critical angle on an interface between lossless dielectrics ( $\epsilon_1\mu_1 > \epsilon_2\mu_2$ ). Drawn either for polarization in the plane of incidence, or parallel to the interface.

Analytically, referring to the foregoing discussion and to Eqs. 7.54, this field must be of the TE form:

- $\bar{\gamma}_2 = -a_y j \beta_2 + a_z \alpha_2 \quad \alpha_2, \beta_2 > 0 \quad \beta_2^2 - \alpha_2^2 = \beta_{02}^2$
- $E_t = a_x E_{xt} e^{j\beta_2 y} e^{-\alpha_2 z}$
- $\mathbf{H}_t = \frac{\bar{\gamma} \times \mathbf{E}_t}{j\omega\mu_2} = \left( \frac{a_y \alpha_2 + a_z j \beta_2}{j\omega\mu_2} \right) E_{xt} e^{j\beta_2 y} e^{-\alpha_2 z}$

The requirement of phase match along the boundary becomes

$$\beta_2 = \beta_{01} \sin \vartheta_1 \quad (7.117a)$$

and therefore on account of Eqs. 7.116a and 7.115

$$\alpha_2 = +\sqrt{\beta_{01}^2 \sin^2 \vartheta_1 - \beta_{02}^2} = +\beta_{01} \sqrt{\sin^2 \vartheta_1 - \sin^2 \vartheta_c} \quad (7.117b)$$

With regard to the remaining boundary conditions on the tangential fields, we may still apply Eqs. 7.101 and 7.102a. For Eq. 7.102b, however, matters are altered slightly because, whereas

$$\frac{E_{xi}}{H_{yi}} = -\frac{E_{xr}}{H_{yr}} = \frac{\eta_1}{\cos \vartheta_1} = Z_1 = \text{real}$$

as before, we now find from Eqs. 7.116b, 7.116c, 7.117b, and 7.115

$$\begin{aligned} Z_2 &= \frac{E_{zt}}{H_{yt}} = \frac{j\omega\mu_2}{\alpha_2} = \frac{j\omega\mu_2}{\beta_{01}\sqrt{\sin^2 \vartheta_1 - \sin^2 \vartheta_c}} \\ &= \frac{j\eta_2}{\sqrt{(\sin \vartheta_1/\sin \vartheta_c)^2 - 1}} = jX_2 \end{aligned} \quad (7.118)$$

which is positive imaginary (inductive) and independent of frequency. Consequently the form of Eqs. 7.103 remains unchanged, but the values in it are rather different:

$$\begin{aligned} (a) \quad \frac{E_{xr}}{E_{xi}} &= \Gamma_R = \frac{Z_2 - Z_1}{Z_2 + Z_1} = \frac{jX_2 - Z_1}{jX_2 + Z_1} = e^{i\psi} \\ (b) \quad \frac{E_{zt}}{E_{zi}} &= T = \frac{2Z_2}{Z_2 + Z_1} = \frac{2jX_2}{Z_1 + jX_2} \end{aligned} \quad (7.119)$$

where

$$\psi = 2 \tan^{-1} \left( \frac{Z_1}{X_2} \right) \quad 0 \leq \tan^{-1} \left( \frac{Z_1}{X_2} \right) \leq \frac{\pi}{2} \quad (7.120)$$

The boundary condition results just found are partially summarized in Fig. 7.27a, which represents them in the form of the equivalent transmission line appropriate to the  $z$ -axis features of the problem. Note that medium 2 presents a lossless (inductive) load to the line of medium

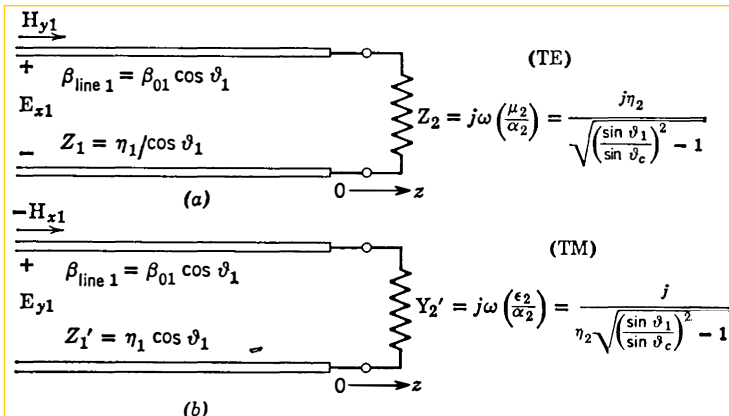


**Fig. 7.27.** Transmission-line analogies for  $z$  dependence and  $x$  and  $y$  field components in Fig. 7.26; (a) with polarization parallel to interface, and (b) with polarization in the plane of incidence.

1 in this case, which accounts properly for the absence of real power entering medium 2 in the  $z$  direction. This is, of course, checked by the fact that  $|\bar{\Gamma}_R| = 1$  in Eq. 7.119a. Again, one must not lose sight of the fact that traveling-wave propagation is taking place along the  $-y$  direction on *both* sides of the boundary, and that time-average power is flowing accordingly along  $-y$  in both media.

In the case of polarization in the plane of incidence, beyond critical angle (Figs. 7.25a and 7.26), the magnetic field will have only an  $x$  component. The transmitted nonuniform plane wave in medium 2 will be of the TM type (Eqs. 7.55),

$$\begin{aligned} \text{(a)} \quad & \bar{\gamma}_2 = -a_y j \beta_2 + a_z \alpha_2 \quad \alpha_2, \beta_2 > 0 \quad \beta_2^2 - \alpha_2^2 = \beta_{02}^2 \\ \text{(b)} \quad & \mathbf{H}_t = a_x \mathbf{H}_{xt} e^{j\beta_2 y} e^{-\alpha_2 z} \\ \text{(c)} \quad & \mathbf{E}_t = -\frac{\bar{\gamma} \times \mathbf{H}_t}{j\omega\epsilon_2} = \frac{-(a_y \alpha_2 + a_z j \beta_2)}{j\omega\epsilon_2} \mathbf{H}_{xt} e^{j\beta_2 y} e^{-\alpha_2 z} \end{aligned} \quad (7.121)$$

with Eqs. 7.117a and 7.117b remaining unchanged. Also as before

$$\frac{-E_{yi}}{H_{xi}} = \frac{E_{yr}}{H_{xr}} \equiv Z_1' = \eta_1 \cos \vartheta_1 = \text{real} \quad (7.109a)$$

but now

$$\frac{-E_{yt}}{H_{xt}} \equiv Z_2' = \frac{\alpha_2}{j\omega\epsilon_2} = -j\eta_2 \sqrt{\left(\frac{\sin \vartheta_1}{\sin \vartheta_c}\right)^2 - 1} = -jX_2' \quad (7.122)$$

which is negative imaginary (capacitive) and independent of frequency.

Thus

$$\begin{aligned} \text{(a)} \quad & \frac{E_{yr}}{E_{yi}} \equiv \bar{\Gamma}_{R'} = \frac{Z_2' - Z_1'}{Z_2' + Z_1'} = \frac{-Z_1' - jX_2'}{Z_1' - jX_2'} = e^{j\psi'} \\ \text{(b)} \quad & \frac{E_{yt}}{E_{yi}} \equiv T' = \frac{2Z_2'}{Z_2' + Z_1'} = \frac{-2jX_2'}{Z_1' - jX_2'} \end{aligned} \quad (7.123)$$

In this case, however, we must put

$$\psi' = -2 \tan^{-1} \left( \frac{Z_1'}{X_2'} \right) \quad 0 \leq \tan^{-1} \left( \frac{Z_1'}{X_2'} \right) \leq \frac{\pi}{2} \quad (7.124)$$

which should be compared carefully with Eq. 7.120, recognizing that by our definitions  $Z_1$ ,  $X_2$ ,  $Z_1'$ , and  $X_2'$  are all positive real numbers. Figure 7.27b summarizes the conditions leading to Eqs. 7.123 and 7.124.

We have now seen for the first time a physical situation giving rise to nonuniform plane waves. They occur here as the refracted wave "on

the other side of a reflection beyond critical angle," when the incident and reflected waves are both *uniform* plane waves! This being the case, however, one may wonder whether or not the burden of shifting the refracted wave from a uniform to a nonuniform plane wave, as the angle of incidence passes smoothly from zero to values beyond the critical angle  $\vartheta_c$ , must always be handled as a brand-new problem—completely independent of the solution for  $\vartheta_1 \leq \vartheta_c$ .

The answer is that the idea of a *complex angle of refraction*,  $\bar{\vartheta}_2 = \vartheta_{2R} + j\vartheta_{2I}$ , can be used to make the transition in an almost completely automatic manner. As an example, take the case of polarization parallel to the boundary (Fig. 7.23).

When  $\vartheta_1 < \vartheta_c$ , or, indeed, before we had any particular reason to expect a "critical angle" problem at all, we would have said that the transmitted wave must be given by a *uniform* plane wave expression similar to Eq. 7.86. Specifically,

$$(a) \quad \mathbf{E}_t = \mathbf{a}_x E_{xt} e^{-j\beta_{02}z \cos \vartheta_2} e^{+j\beta_{02}y \sin \vartheta_2}$$

$$(b) \quad \mathbf{H}_t = \frac{\mathbf{E}_{xt}}{\eta_2} (\mathbf{a}_y \cos \vartheta_2 + \mathbf{a}_z \sin \vartheta_2) e^{-j\beta_{02}z \cos \vartheta_2} e^{+j\beta_{02}y \sin \vartheta_2}$$

with Eqs. 7.100, 7.103, and 7.104 used to meet the boundary conditions.

When it came to evaluation of  $\bar{\vartheta}_2$ , however, we might discover that in Snell's law

$$\sin \vartheta_2 = \left( \frac{v_2}{v_1} \right) \sin \vartheta_1 = \text{real and } > 1$$

because  $v_2 > v_1$ , and  $\vartheta_1$  was rather large. In that case, let  $\bar{\vartheta}_2$  be complex, and find out what it must be to satisfy Snell's law anyway! Accordingly,

$$\sin \bar{\vartheta}_2 = \sin \vartheta_{2R} \cosh \vartheta_{2I} + j \cos \vartheta_{2R} \sinh \vartheta_{2I}$$

$$= \left( \frac{v_2}{v_1} \right) \sin \vartheta_1 = \text{real and } > 1$$

Therefore the only possibility is

$$\cos \vartheta_{2R} = 0 \quad \vartheta_{2R} = \frac{\pi}{2}$$

to make

$$\sin \bar{\vartheta}_2 = +\cosh \vartheta_{2I} = \left( \frac{v_2}{v_1} \right) \sin \vartheta_1 = \text{real and } > 1$$

This defines  $\vartheta_{2I}$ , except for algebraic sign;  $\vartheta_{2I} = \pm \cosh^{-1} [(v_2/v_1) \sin \vartheta_1]$ . Consequently,

$$\cos \bar{\vartheta}_2 = \cos \vartheta_{2R} \cosh \vartheta_{2I} - j \sin \vartheta_{2R} \sinh \vartheta_{2I} = -j \sinh \vartheta_{2I}$$

Employing the above values for  $\sin \bar{\vartheta}_2$  and  $\cos \bar{\vartheta}_2$  in the transmitted-field expressions, and using Snell's law,  $\beta_{02} \sin \bar{\vartheta}_2 = \beta_{01} \sin \vartheta_1$  in the exponents, we find

$$(a) \quad \mathbf{E}_t = a_x \mathbf{E}_{xt} e^{j\beta_{01}y \sin \vartheta_1} e^{-\beta_{02}z \sinh \vartheta_{2I}}$$

$$(b) \quad \mathbf{H}_t = \frac{\mathbf{E}_{xt}}{\eta_2} (-a_y j \sinh \vartheta_{2I} + a_z \cosh \vartheta_{2I}) e^{j\beta_{01}y \sin \vartheta_1} e^{-\beta_{02}z \sinh \vartheta_{2I}}$$

Now it is reasonable to assume that the solution we want must die out rather than become infinite as  $z \rightarrow +\infty$ ; at least this is the only boundary condition at infinity which is consistent with our previous assumptions about the incident wave being the only source in the problem. Thus we may write

$$(c) \quad \alpha_2 = \beta_{02} \sinh \vartheta_{2I} > 0 \quad \vartheta_{2I} > 0$$

$$(d) \quad \beta_2 = \beta_{01} \sin \vartheta_1 = \beta_{02} \cosh \vartheta_{2I}$$

so that

$$\frac{\cosh \vartheta_{2I}}{\eta_2} = \frac{\beta_2}{\beta_{02}\eta_2} = \frac{\beta_2}{\omega\mu_2}$$

and

$$\frac{-j \sinh \vartheta_{2I}}{\eta_2} = \frac{-j\alpha_2}{\beta_{02}\eta_2} = \frac{\alpha_2}{j\omega\mu_2}$$

We can therefore convert the last field expressions to

$$(a) \quad \mathbf{E}_t = a_x \mathbf{E}_{xt} e^{j\beta_{2I}y} e^{-\alpha_2 z}$$

$$(b) \quad \mathbf{H}_t = \left( \frac{a_y \alpha_2 + a_z j \beta_2}{j \omega \mu_2} \right) \mathbf{E}_{xt} e^{j\beta_{2I}y} e^{-\alpha_2 z}$$

$$(c) \quad \beta_2^2 - \alpha_2^2 = \beta_{02}^2$$

$$(d) \quad \beta_2 = \beta_{01} \sin \vartheta_1$$

which agrees precisely with Eqs. 7.116 and 7.117.

The straightforward use of a complex angle of refraction in Snell's law, plus the election of a choice regarding the behavior of the refracted solution at infinity, allows us to carry the refracted field solution continuously through from uniform to nonuniform plane waves as the incident angle  $\vartheta_1$  passes through the critical value  $\vartheta_d$ .

One of the roles of the nonuniform plane wave in a lossless medium may be summarized from the examples just treated. It arises when boundary conditions require an effective phase velocity (or wave length) in some space direction which is less than that provided at the

given frequency by the conventional “free space” phase velocity  $1/\sqrt{\epsilon\mu}$  [or wave length  $2\pi/(\omega\sqrt{\epsilon\mu})$ ] in the surrounding medium. Larger phase velocities (or wave lengths) in a given direction can be achieved with uniform plane waves at real oblique angles of propagation; smaller ones, however, require “uniform” plane waves at *complex* angles of propagation—which is to say, actually, *nonuniform* plane waves oriented to provide large space-rates-of-change of phase along the direction in question. The price of such small wave lengths (or rapid phase changes) along one direction, however, is complete attenuation in another (perpendicular) direction. Compressing phase velocity along one axis loses amplitude at right angles!

These matters are illustrated even more forcefully in the following examples of guided waves.

## 7.5 Guided Waves \*

In studying the oblique incidence of uniform plane waves upon plane boundaries, we have so far stressed primarily the behavior of the fields as regards the direction *normal* to the boundary. Examination of these problems from the point of view of the direction *parallel* to the boundary instead leads to the concept of guided waves. This approach is by no means the only one for introducing guided waves, but it does furnish one illuminating view of the problem.

### 7.5.1 Metallic (Rectangular) Wave Guides \*

Consider the problem of an  $x$ -polarized uniform plane wave at an oblique angle of incidence  $\vartheta$  upon a perfect conductor (Fig. 7.21). The total field is given in Eq. 7.97.

This field has the property that  $E_x = 0$ , not only on the plane  $z = 0$  but also on the planes

$$z_m = \frac{-m\lambda}{2 \cos \vartheta} = \frac{-m\lambda_z}{2} \quad m = 1, 2, \dots \quad (7.125)$$

Thus it will still be a solution both to Maxwell's equations and the boundary conditions if a second perfect conductor is inserted at the position  $z_m = -a$ , with

$$a = \frac{m\lambda}{2 \cos \vartheta} = \frac{m\lambda_z}{2} \quad m = 1, 2, \dots \quad (7.126)$$

Under these conditions, the tangential electric field ( $E_x$ ) vanishes

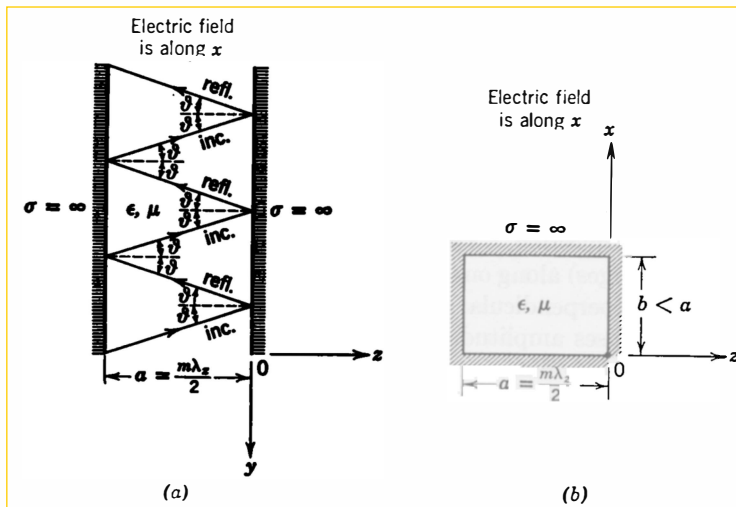


**Fig. 7.28.** Construction of a rectangular wave-guide solution from the obliquely incident and reflected waves for a metal plane  $z = 0$ . (a) Addition of side wall,  $z = -a = -(m\lambda_z/2)$ ; (b) addition of top and bottom walls,  $x = 0$  and  $x = b < a$ .

automatically on the surface of both conductors. Consequently, as shown schematically in Fig. 7.28a, the field

$$(a) \quad \mathbf{E} = [-a_x 2j E \sin(\beta_0 z \cos \vartheta)] e^{j\beta_0 y \sin \vartheta}$$

$$(b) \quad \mathbf{H} = \frac{2E}{\eta} [a_y \cos \vartheta \cos(\beta_0 z \cos \vartheta)$$

$$- a_z j \sin \vartheta \sin(\beta_0 z \cos \vartheta)] e^{j\beta_0 y \sin \vartheta}$$
(7.127)

is a solution in the space region  $(-a \leq z \leq 0; -\infty < y < +\infty)$ , provided Eq. 7.126 is met. Moreover, this solution constitutes a traveling wave in the  $-y$  direction, completely confined in the  $|z|$  direction. The "source" for it must now be regarded as located at  $y = +\infty$ .

Evidently, two more perfectly conducting planes might just as well be added to the system, one at  $x = 0$  and the other at  $x = b < a$ , as shown in Fig. 7.28b. Since these planes are perpendicular to the only component of the electric field ( $E_x$ ), they do not require any modification of the field solution to meet their boundary conditions.<sup>1</sup>

We now have a traveling wave along  $-y$ , completely confined in a hollow rectangular pipe defined by  $0 \leq x \leq b$  and  $-a \leq z \leq 0$  (Fig. 7.28b). The structure is serving as a *wave guide*. It is of interest, then,

<sup>1</sup> It is worth while to pause here and consider whether this whole scheme would work if one were to start with the magnetic instead of the electric field along  $x$ .

to ask how the propagation of this wave in the wave guide varies with frequency, assuming dimensions  $a$  and  $b$  are fixed. In view of Eq. 7.126,  $\vartheta$  now becomes merely a parameter, fixed by the value of  $a$  and the free-space (not vacuum) wave length  $\lambda$ . The latter is really just a measure of the frequency, given the values  $\epsilon$  and  $\mu$  of the medium which fills the guide, because by definition

$$\lambda \equiv \frac{2\pi}{\beta_0} = \frac{2\pi}{\omega\sqrt{\epsilon\mu}} \quad (7.128)$$

Thus we shall wish to eliminate  $\vartheta$  in some of our immediate discussion.

The important questions about this wave are: (1) How does the  $y$  variation depend on  $\omega$  (or  $\lambda$ )? (2) How does the flow of complex power along  $-y$  depend upon frequency? (3) How does the field distribution across the transverse dimensions  $(x, z)$  vary with frequency?

First, we define the *guide wave length*  $\lambda_g$  as the distance between equiphasе surfaces measured along the guide propagation axis ( $-y$  in this case). Previously we called this  $\lambda_y$ , so

$$\lambda_g \equiv \lambda_y = \frac{\lambda}{\sin \vartheta} \quad (7.129)$$

But in view of Eq. 7.120

$$\sin \vartheta = \sqrt{1 - \cos^2 \vartheta} = \sqrt{1 - \left(\frac{\lambda}{2a/m}\right)^2} \quad (7.130)$$

and Eq. 7.129 becomes

$$\lambda_g = \frac{\lambda}{\sqrt{1 - (\lambda/\lambda_{m,0})^2}} > \lambda \quad \text{for } \lambda \leq \lambda_{m,0} \quad (7.131)$$

where

$$\lambda_{m,0} \equiv \frac{2a}{m} \quad (7.132)$$

Then using Eqs. 7.126 and 7.129 to eliminate  $\vartheta$  from the field expressions (Eqs. 7.127), and defining

$$\beta_g \equiv |\beta_y| \equiv \frac{2\pi}{\lambda_g} = \beta_0 \sin \vartheta \quad (7.133)$$

we find

$$(a) \quad \mathbf{E} = - \left[ a_x 2jE \sin \left( \frac{m\pi z}{a} \right) \right] e^{j\beta_g y} \quad m = 1, 2, 3, \dots \quad (7.134)$$

$$(b) \quad \mathbf{H} = \frac{2E}{\eta} \left[ a_y \left( \frac{\lambda}{\lambda_{m,0}} \right) \cos \left( \frac{m\pi z}{a} \right) \right. \\ \left. - a_z j \left( \frac{\lambda}{\lambda_g} \right) \sin \left( \frac{m\pi z}{a} \right) \right] e^{j\beta_g y} \quad m = 1, 2, 3, \dots$$

It is clear from Eq. 7.134 that the behavior of the fields as a function of the transverse coordinates  $(x, z)$  does *not* depend upon frequency. There is actually no  $x$  dependence, and the  $z$  dependence is sinusoidal with dimension  $a$ , an integer number ( $m$ ) of half-periods. The wave is TE with respect to the guide ( $y$ ) axis, having an electric field linearly polarized in the transverse plane (along  $x$ ) and both a transverse ( $z$ ) component and a longitudinal ( $y$ ) component of magnetic field.

On account of their  $m$  half-period variations along the wide dimension  $a$ , and their zero variation along the narrow dimension  $b$ , these rectangular wave-guide field solutions are called  $\text{TE}_{m,0}$  waves or modes. They are different for different (arbitrary) integer choices of  $m$ , so we actually have an infinite set of solutions for a given guide size and a specified frequency. Nevertheless, the transverse variation of the fields depends *only* on  $m$ , and not on frequency, so we can easily identify one solution by its  $m$  value and then consider its behavior as a function of frequency. Each of the "modes"  $\text{TE}_{1,0}, \text{TE}_{2,0}, \dots, \text{TE}_{m,0}$  may be regarded as a separate rectangular wave-guide solution which varies in its own way with frequency.

To study the frequency variation of a  $\text{TE}_{m,0}$  mode, refer first to Eqs. 7.131 and 7.132. At very high frequencies,  $\lambda \rightarrow 0$  and  $\lambda_g \rightarrow \lambda \rightarrow 0$ . As the frequency is lowered, however,  $\lambda \rightarrow \lambda_{m,0}$  and  $\lambda_g \rightarrow \infty$ . When  $\lambda > \lambda_{m,0}$ , on the other hand,  $\lambda_g$  must become imaginary

$$\lambda_g = \frac{\pm j\lambda}{\sqrt{(\lambda/\lambda_{m,0})^2 - 1}} \quad \text{for } \lambda > \lambda_{m,0} \quad (7.135)$$

The meaning of Eq. 7.135 stems from Eq. 7.134, where

$$\begin{aligned} e^{j\beta_g y} &= e^{j(2\pi y/\lambda_g)} = e^{(\pm)([(2\pi/\lambda)(\sqrt{(\lambda/\lambda_{m,0})^2 - 1})]y)} \\ &= e^{(\pm)\alpha_g y} \quad \text{for } \lambda > \lambda_{m,0} \end{aligned} \quad (7.136)$$

shows pure attenuation along  $(\mp) y$ ! Actually we would choose the  $+$  sign in Eqs. 7.135 and 7.136, since we are discussing the problem for a source at  $y = +\infty$ . The solution should therefore vanish (rather than grow exponentially) as  $y \rightarrow -\infty$ , and grow (rather than vanish) at  $y = +\infty$ .

At long wave lengths (low frequencies), the *uniform* plane waves from which we originally constructed the wave guide solution have changed into *nonuniform* plane waves. This assertion is confirmed from Eqs. 7.126 and 7.132 by the fact that  $\cos \vartheta > 1$  when  $\lambda > \lambda_{m,0}$ , and  $\sin \vartheta$  is pure imaginary in Eq. 7.130. The angle  $\vartheta$  becomes complex,  $\vartheta = \pi + j\vartheta_I$  (or  $\bar{\vartheta} = -j\vartheta_I$ ). We expect no *real* (time-average) power flow down the guide under these conditions and, of course, we never ex-

pected any in directions normal to each of the four perfectly conducting walls. Let us check these features of the power flow by examining the wave impedances.

Observe from Eq. 7.134 that

$$(a) Z_{-y} \equiv \frac{E_x}{H_z} = \eta \left( \frac{\lambda_g}{\lambda} \right)$$

$$(b) Z_z \equiv \frac{E_x}{H_y} = -j\eta \left( \frac{\lambda_{m,0}}{\lambda} \right) \tan \left( \frac{m\pi z}{a} \right) \quad (7.137)$$

Accordingly, since  $Z_z$  is always pure imaginary, there is only reactive power flowing in the  $\pm z$  directions at all frequencies.  $Z_{-y}$ , however is positive real when  $\lambda < \lambda_{m,0}$  and becomes pure imaginary (inductive) when  $\lambda > \lambda_{m,0}$  ( $\lambda_g$  becomes positive imaginary). Real power does flow down the guide at high frequencies ( $\lambda < \lambda_{m,0}$ ), but only (inductive) reactive power flows at low frequencies ( $\lambda > \lambda_{m,0}$ ). Thus the wave guide acts like a *high-pass filter*, with a *cutoff frequency*  $\omega_{m,0}$  defined by

$$\omega_{m,0} = \frac{2\pi}{\lambda_{m,0}\sqrt{\epsilon\mu}} = \frac{\pi m}{a\sqrt{\epsilon\mu}} \quad (7.138)$$

The mechanism of propagation ( $\lambda < \lambda_{m,0}$ ) down the guide can be represented in terms of uniform plane waves by the familiar optical type of ray-tracing picture of a single unit-field-strength ray alternately reflected from each side wall, as in Fig. 7.28a, in which we focus attention only on the space between  $z = 0$  and  $z = -a$ ; or, more symmetrically, by considering two sets of multiply reflected rays, each of half field strength, shown in the similar picture Fig. 7.29a. Alternatively, if we mentally remove the side walls at  $z = 0$  and  $z = -a$ , the interference pattern in *all space* of just *two* rays, each of unit field strength, as shown in Fig. 7.29b, will produce tangential electric field nodal planes (dotted lines) where the walls used to be (and also at other such planes spaced  $\lambda/2$  from these).

In either view, regarding the dimension  $a$  and mode index  $m$  as fixed, we may use Eqs. 7.126 and 7.132 to determine  $\vartheta$  as a function of frequency for the  $m$ th mode field,

$$\cos \vartheta = \frac{\lambda}{\lambda_{m,0}} \quad (7.139)$$

As long as  $\lambda < \lambda_{m,0}$ ,  $a > m\lambda/2$  from Eq. 7.126, and, according to Eq. 7.129 or 7.131,  $\lambda_z > \lambda$ . This condition can always be met with a real angle  $\vartheta$ . At high frequencies ( $\lambda \rightarrow 0$ ),  $\vartheta \rightarrow \pi/2$ , and the two com-

ponent uniform plane waves are propagating in directions nearly parallel to the guide axis ( $y$ ). The wave-guide fields approach something very much like a uniform plane wave (though the side-wall boundary conditions prevent it from actually becoming one; see Eqs. 7.131, 7.133, 7.134, and 7.137 as  $\lambda \rightarrow 0$ ). When the frequency is lowered to  $\omega_{m,0}$  ( $\lambda = \lambda_{m,0}$ ),  $\vartheta = 0$ , and the two-component uniform plane waves are propagating directly across the transverse face of the guide, at normal incidence to the side walls. There is no  $y$  variation of the fields ( $\lambda_g = \infty$ ) and  $H_z = 0$ ; energy simply rattles back and forth between the side walls, making no progress down the guide at all. Under this condition,  $a = (m\lambda_{m,0})/2 = m(\lambda/2)$ , so the boundary conditions of Eq. 7.126 demand that  $\lambda_z$  equal the free-space wave length  $\lambda$  at this frequency ( $\omega_{m,0}$ ). Further lowering of the frequency will result in the requirement  $a < m\lambda/2$ , or  $\lambda_z < \lambda$ , for which the side walls force a compressed wave length condition along  $z$ . We expect, therefore, that the two component plane waves will become nonuniform and will produce attenuation along the guide axis ( $y$ ). This does in fact occur.

Among the  $TE_{m,0}$  waves that we have found, it is clear from Eq. 7.138 that, for a given guide dimension  $a$ , the  $TE_{1,0}$  ( $m = 1$ ) mode has the lowest cutoff frequency  $\omega_{1,0}$ :

$$\omega_{1,0} = \frac{\pi}{a\sqrt{\epsilon\mu}} \quad \lambda_{1,0} = 2a \quad (b < a) \quad (7.140)$$

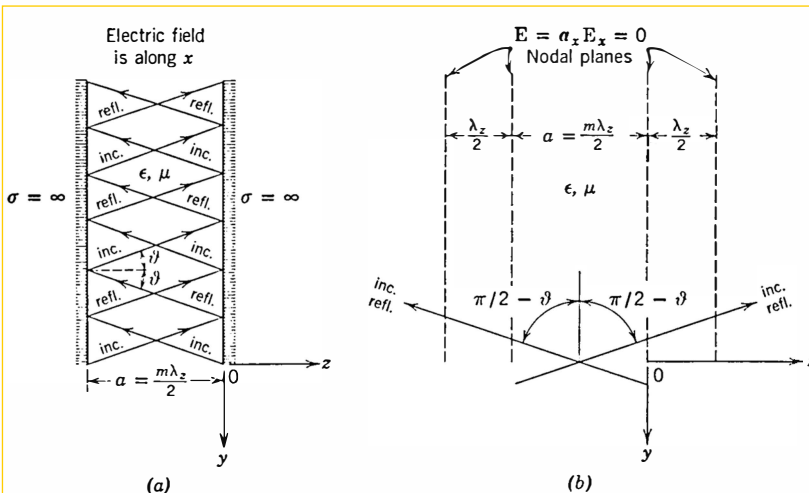


**Fig. 7.29.** Ray representations of  $TE_{m,0}$  propagation in a rectangular wave guide. Note that each ray in (a) represents half the field strength of each one in (b).

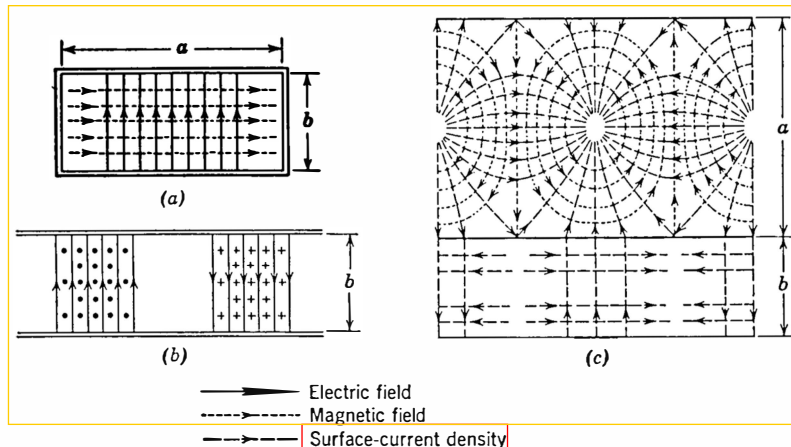


**Fig. 7.30.** Field lines for  $\text{TE}_{1,0}$  mode in rectangular wave guide. (a) Cross section; (b) longitudinal section, along center line; (c) views of top and side plates as seen from inside, showing surface-current densities and magnetic fields on inner surfaces.

The fields for the  $\text{TE}_{1,0}$  mode undergo only a single half-period variation across the guide from  $z = 0$  to  $z = -a$ . Some sketches of the field lines from Eq. 7.134 for this important mode (when  $\omega > \omega_{1,0}$ ) appear in Fig. 7.30. These field lines are actually contours to which the instantaneous fields  $\mathbf{E}$  and  $\mathbf{H}$  of a single traveling wave are tangent, at some arbitrary moment of time. The contours are spaced closely where the instantaneous field strength is great. In Fig. 7.30c we have also shown the wall currents, which clarify the connection between the strong magnetic field at the walls, and the strong electric field (displacement current) along the center regions of the interior.

It turns out, from an extended analysis of all possible rectangular wave-guide modes which behave exponentially ( $e^{iy_1}$ ) along the guide axis ( $-y$ )<sup>1</sup> that TE solutions exist with standing-wavelike field variations along either or both transverse axes ( $x$  and  $z$ ). These are called  $\text{TE}_{m,n}$  modes ( $m = 0, 1, 2, \dots$ ;  $n = 0, 1, 2, \dots$ ; but not  $m = n = 0$ ). This nomenclature for the rectangular guide is based on the convention that the first subscript ( $m$ ) refers to the number of half-period field variations along a path parallel to the wide dimension of the cross section, and the second subscript ( $n$ ) to the number of half-period field variations along a path parallel to the narrow dimension of the cross section. By convention also, the wide dimension is denoted by  $a$ , the narrow by

<sup>1</sup> The analysis involves the field produced by four plane waves instead of two. It is taken up in the Problems.

$b$  (Fig. 7.28b). The character of some of these modes, namely, the  $\text{TE}_{0,n}$  is obvious from our solutions here. These are identical in form to the  $\text{TE}_{m,0}$  modes, except that the whole field solution is turned  $90^\circ$  inside the guide so that the electric field is parallel to the long dimension ( $a$  or  $z$ ). Their cutoff frequencies will be given by Eq. 7.138 with  $n$  for  $m$  and  $b$  for  $a$ , but their numerical values will be different, even when  $n = m$ , because dimension  $b$  is less than  $a$ . There are also  $\text{TM}_{m,n}$  modes ( $m = 1, 2, \dots; n = 1, 2, \dots$ ) which necessarily have standing-wavelike field variations along both transverse axes. Among all the TE and TM solutions, the  $\text{TE}_{1,0}$  has the lowest cutoff frequency. This frequency  $\omega_{1,0}$ , given in Eq. 7.140, defines, in fact, the lowest frequency for which an infinitely long rectangular wave guide will propagate real power. For this reason, the  $\text{TE}_{1,0}$  is called the *dominant mode* of the wave guide.<sup>1</sup>

It develops that the mode with the next higher cutoff frequency is either the  $\text{TE}_{0,1}$  or the  $\text{TE}_{2,0}$ , depending upon the particular value of  $b/a < 1$ . It is then clear from Eq. 7.138 that if  $b \leq a/2$ ,  $\omega_{2,0} \leq \omega_{0,1}$  and the  $\text{TE}_{2,0}$  is the mode with the next higher cutoff frequency. Under these particular conditions, in the frequency range  $\omega_{1,0} \leq \omega \leq \omega_{2,0}$  ( $= 2\omega_{1,0}$ ) only the  $\text{TE}_{1,0}$  mode can propagate without attenuation along the guide axis. In fact, rectangular wave guides are normally designed with  $b \leq a/2$  in order to have this full-octave frequency range for single-mode transmission. At frequencies above  $2\omega_{1,0}$ , in a lossless structure, more than one mode may propagate without attenuation at the same time. This condition complicates considerably the use of the guide for transmission, and is avoided except in rather special circumstances.

A graphical representation of the multimode situation described above is shown in Fig. 7.31 in terms of the variation of  $\beta_g$  (or  $\alpha_g$ ) with frequency  $\omega$  for the various possible modes. Analytically, for the  $\text{TE}_{m,0}$  waves, we have from Eqs. 7.133, 7.131, and 7.138 (or 7.136 and 7.138),

$$(a) \quad \begin{aligned} \beta_g &= \frac{2\pi}{\lambda_g} = \frac{2\pi}{\lambda} \sqrt{1 - \left(\frac{\lambda}{\lambda_{m,0}}\right)^2} \\ &= \sqrt{\epsilon\mu} \sqrt{\omega^2 - \omega_{m,0}^2} \quad \omega \geq \omega_{m,0} \end{aligned} \quad (7.141)$$

$$(b) \quad \alpha_g = \sqrt{\epsilon\mu} \sqrt{\omega_{m,0}^2 - \omega^2} \quad \omega \leq \omega_{m,0}$$

<sup>1</sup>Sometimes, the nomenclature of wave-guide modes is chosen to emphasize which field *has* a longitudinal component rather than which one *does not* have such a component. In that case,  $\text{TE}_{m,n}$  modes are called  $\Pi_{m,n}$ , and  $\text{TM}_{m,n}$  modes are called  $E_{m,n}$ . In rectangular guide, then, the  $\Pi_{1,0}$  mode is dominant.

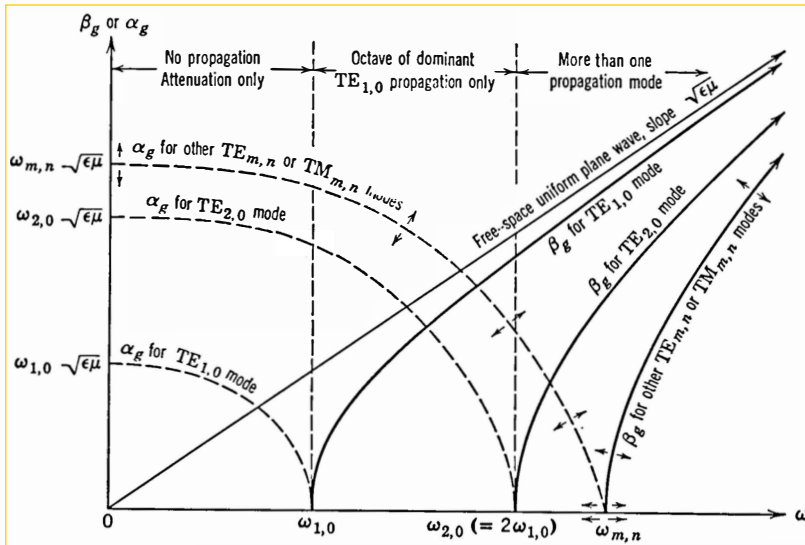


**Fig. 7.31.** Attenuation ( $\alpha_g$ ) and phase ( $\beta_g$ ) constants versus frequency  $\omega$  for modes in a lossless rectangular wave guide with narrow dimension not exceeding half the wide one. Note  $\beta_{g,m,n} < \omega\sqrt{\epsilon\mu}$  and  $\alpha_{g,m,n} < \omega_{m,n}\sqrt{\epsilon\mu}$ .

These relations contain some additional interesting information, also discernible in Fig. 7.31.

Above cutoff frequency, the phase velocity along the guide axis is greater than that of light in the medium filling the guide:

$$v_{\text{phase}} \equiv \frac{\omega}{\beta_g} = \frac{1}{\sqrt{\epsilon\mu}} \left[ \frac{1}{\sqrt{1 - (\omega_{m,0}/\omega)^2}} \right] \\ > \frac{1}{\sqrt{\epsilon\mu}} \quad \text{for } \omega \geq \omega_{m,0} \quad (7.142)$$

The fact that the phase velocity depends upon frequency makes the wave guide a *dispersive* (though lossless) transmission system. Because there is no attenuation under these conditions, however, the idea of group velocity has a valid meaning (see Chapter 5). For the case at hand,

$$v_{\text{group}} \equiv \left( \frac{\partial \beta_g}{\partial \omega} \right)^{-1} = \left( \frac{\omega \sqrt{\epsilon\mu}}{\sqrt{\omega^2 - \omega_{m,0}^2}} \right)^{-1} = \frac{1}{\epsilon\mu} \left( \frac{1}{v_{\text{phase}}} \right) = \frac{\sin \vartheta}{\sqrt{\epsilon\mu}}$$

or

$$v_{\text{group}} v_{\text{phase}} = \frac{1}{\epsilon\mu} = v_{\text{light}}^2 \quad (7.143)$$

This is to say, the free-space light velocity  $1/\sqrt{\epsilon\mu}$  is the geometric mean between the wave-guide group and phase velocities. Whereas the guide phase velocity always exceeds that of light in the medium filling the guide, the group velocity never does so. Indeed the group velocity is just the speed of light in the medium filling the guide, projected along the guide axis from the oblique angle of bounce.

We have just learned that electromagnetic waves can be guided along one axis by confining them from spreading in other directions with the aid of entirely opaque (metal) walls. The now relatively common phenomenon of extraordinary light transmission through solid lucite rods suggests that much less stringent transverse constraints will suffice to guide electromagnetic energy along a single solid. The analysis of some such situations follows.

### 7.5.2 Nonmetallic Wave Guides \*

The possibility of total reflection arises at the interface between different lossless dielectrics when incidence occurs on the side with the greater index of refraction. This suggests that a slab (or perhaps even a rod) of such material with a high index of refraction may be able to confine and guide electromagnetic waves by successive internal reflections at angles  $\theta_1$  beyond the critical angle. The idea is illustrated for a dielectric slab in Fig. 7.32a, to which the nonuniform plane-wave pattern of Fig. 7.26 presumably applies not only for  $z > 0$  but also for  $z < -a$  (with an appropriate exchange of "left" for "right").

Analytical determination of the conditions for guidance along the  $-y$  direction requires application of boundary conditions at both  $z = 0$  and  $z = -a$ . The TM case (magnetic field parallel to the boundaries) is to be treated here, Eqs. 7.121 being the relevant field expressions pertinent to that part of medium 2 in the region  $z > 0$ . In the part of medium 2 occupying  $z < -a$ , however,  $\alpha_2$  must be directed *left*, to make the solution vanish at  $z = -\infty$ . Otherwise the entire field could hardly be considered "confined" to the slab in the  $\pm z$  directions. Naturally Snell's law (Eq. 7.117a) applies at both boundaries.

The equivalent transmission line in Fig. 7.27b accounts for the  $z$ -axis features of the problem in regard to medium 1 and the boundary conditions at  $z = 0$ . The tangential field continuity conditions at  $z = -a$  are represented in the equivalent transmission line by terminating the line on the left ( $z = -a$ ) in the same impedance as on the right ( $z = 0$ ). This step appears in Fig. 7.32b, justified by the symmetry of the entire problem about the plane  $z = -\frac{1}{2}a$ .

According to Eqs. 7.123a and 7.124, we know the reflection coefficient

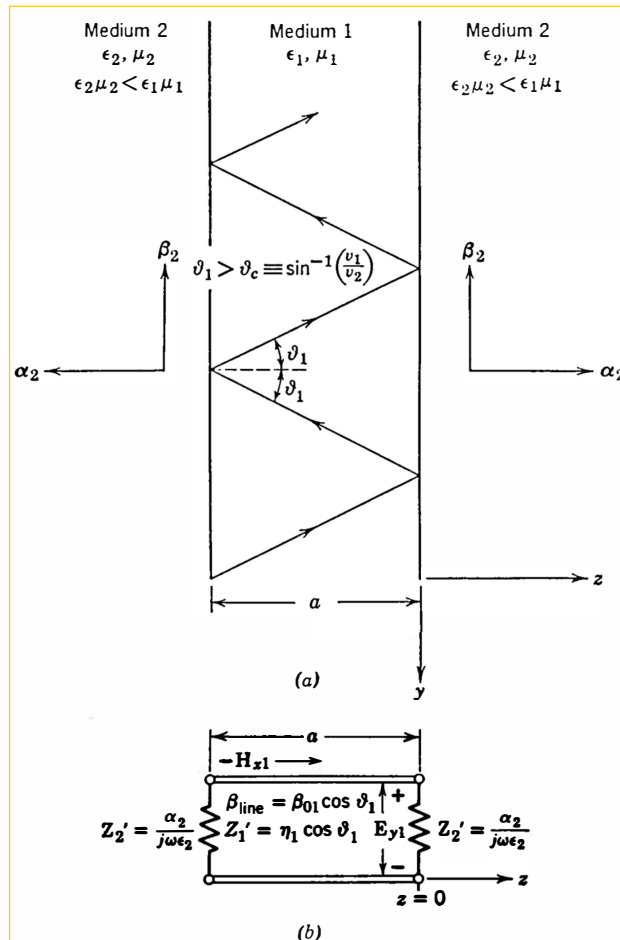


**Fig. 7.32.** Dielectric slab (medium 1) as a wave guide. (a) Mechanism of successive total internal reflection; (b) transmission-line representation with respect to  $z$ -axis; TM case,  $H$  parallel to boundaries.

$\Gamma_R'$  looking to the right at  $z = 0$ . The reflection coefficient looking to the right at  $z = -a$  is accordingly required by the transmission line for medium 1 to be

$$\Gamma'(-a) = \Gamma_R' e^{-j2\beta_z a} = e^{j(\psi' - 2\beta_z a)} \quad (7.144)$$

where we have written  $\beta_z \equiv \beta_{\text{line}} = \beta_0 \cos \vartheta_1$  for convenience.

On the other hand, looking to the left at  $z = -a$ , we must see the same load impedance  $Z_2'$  as appears in the calculation [7.123a] for  $\Gamma_R'$ .

Inasmuch as “looking to the right” and “looking to the left” at a given point on the line merely exchanges the roles of “incident” and “reflected” waves, the corresponding reflection coefficients are simply reciprocals of each other, as pointed out in Chapter 6 (Eq. 6.15). The presence of  $Z_2'$  at  $z = -a$  therefore requires

$$\bar{\Gamma}'(-a) = \frac{1}{\bar{\Gamma}_R'} \quad (7.145)$$

In view of Eqs. 7.144 and 7.145 then,

or

$$\begin{aligned} e^{j(\psi' - 2\beta_z a)} &= e^{-j\psi'} \\ e^{j2(\psi' - \beta_z a)} &= +1 \end{aligned} \quad (7.146a)$$

It follows that

$$\psi' - \beta_z a = k\pi \quad k = 0, \pm 1, \pm 2, \dots \quad (7.146b)$$

which, by Eq. 7.124, becomes

$$\frac{n\pi}{2} - \tan^{-1}\left(\frac{Z_1'}{X_2'}\right) = \frac{\beta_z a}{2} \quad n = +1, +2, \dots \quad (7.147a)$$

and

$$\frac{p\pi}{2} + \tan^{-1}\left(\frac{Z_1'}{X_2'}\right) = -\frac{\beta_z a}{2} \quad p = 0, +1, +2, \dots \quad (7.147b)$$

Use of  $n$  and  $p$  in Eqs. 7.147a and 7.147b is for the purpose of separating explicitly the cases for negative and positive values of  $k$  respectively in Eq. 7.146b. Inasmuch as  $\beta_z$  must be positive for Eq. 7.144 to be correct, however, only Eq. 7.147a is appropriate here (bear in mind that  $0 \leq \tan^{-1}(Z_1'/X_2') \leq \pi/2$  according to Eq. 7.124). Thus considering separately odd and even values of  $n$  in Eq. 7.147a, we find

$$\begin{aligned} (a) \quad \frac{X_2'}{Z_1'} &= +\tan \frac{\beta_z a}{2} \quad n = 1, 3, 5, \dots \\ (b) \quad \frac{X_2'}{Z_1'} &= -\cot \frac{\beta_z a}{2} \quad n = 2, 4, \dots \end{aligned} \quad (7.148)$$

In the interests of examining the “guide wave length”  $\lambda_g (\equiv \lambda_y)$  or the guide propagation constant  $\beta_g (\equiv \beta_2 = 2\pi/\lambda_g)$  as functions of frequency  $\omega$ , we shall write the function  $X_2'/Z_1'$  as follows from Eqs.

7.109a, 7.122, 7.121a, and the definition  $\beta_z = \beta_{01} \cos \vartheta_1$

$$\frac{X_2'}{Z_1'} = \frac{\alpha_2}{\omega \epsilon_2 \eta_1 \left( \frac{\beta_z}{\beta_{01}} \right)} = \frac{\sqrt{\beta_g^2 - \beta_{02}^2}}{\beta_z} \left( \frac{\epsilon_1}{\epsilon_2} \right) \quad (7.149)$$

But in medium 1

$$\beta_g^2 + \beta_z^2 = \beta_{01}^2 = \omega^2 \epsilon_1 \mu_1 \quad (7.150)$$

so Eq. 7.149 becomes, upon eliminating  $\beta_g^2$ ,

$$\frac{X_2'}{Z_1'} = \frac{\epsilon_1}{\epsilon_2} \sqrt{\left( \frac{\beta_{01}^2 - \beta_{02}^2}{\beta_z^2} \right) - 1} \quad (7.151)$$

Equation 7.151 expresses  $X_2'/Z_1'$  as a function of  $\beta_z$  [or  $(\beta_z a)/2$ ] for any given frequency  $\omega$  (which fixes  $\beta_{01} = \omega \sqrt{\epsilon_1 \mu_1}$  and  $\beta_{02} = \omega \sqrt{\epsilon_2 \mu_2}$ ). This allows a graphical solution of Eqs. 7.148a or 7.148b for the quantity  $(\beta_z a)/2$  at the frequency  $\omega$ . The graphical solution entails plotting both sides of Eqs. 7.148a and 7.148b against  $(\beta_z a)/2$  on the same abscissa to determine intersection points. Figures 7.33a and 7.33c respectively present these solutions ( $\circ$ ) for three different frequencies  $\omega_A < \omega_B < \omega_C$ , pertaining to the curves marked A, B and C respectively. Figure 7.33b shows the calculation of  $\beta_g$  from Eq. 7.150. This equation plots as a circle, relating  $\beta_g$  to  $\beta_z$ , having a radius directly proportional to  $\omega$ .

The important restriction from Eq. 7.151 that

$$0 \leq \beta_z \leq \sqrt{\beta_{01}^2 - \beta_{02}^2} = \omega \sqrt{\epsilon_1 \mu_1 - \epsilon_2 \mu_2} \quad (7.152)$$

should not be overlooked. It defines the points at which curves A, B and C strike the abscissa in Figs. 7.33a and 7.33c. Nor should its consequences from Eq. 7.150 be neglected:

$$\beta_{02} < \beta_g < \beta_{01} \quad (7.153)$$

The guide wave length always must lie between that of free-space uniform plane waves (or light) in medium 1 and in medium 2. Similarly, the guide phase velocity exceeds that of light in medium 1 (with the higher refractive index), but is less than the (greater) light velocity in medium 2.

Although no generally valid analytical relation for  $\beta_g(\omega)$  may be written in the present circumstances, a study of Eqs. 7.151, 7.148, 7.150, and Fig. 7.33 provides satisfying insight into the effect of frequency variation when the dimension  $a$  is fixed. At a high frequency  $\omega_C$ , the curve (Eq. 7.151) extends over a large range of  $\beta_z$ , because the

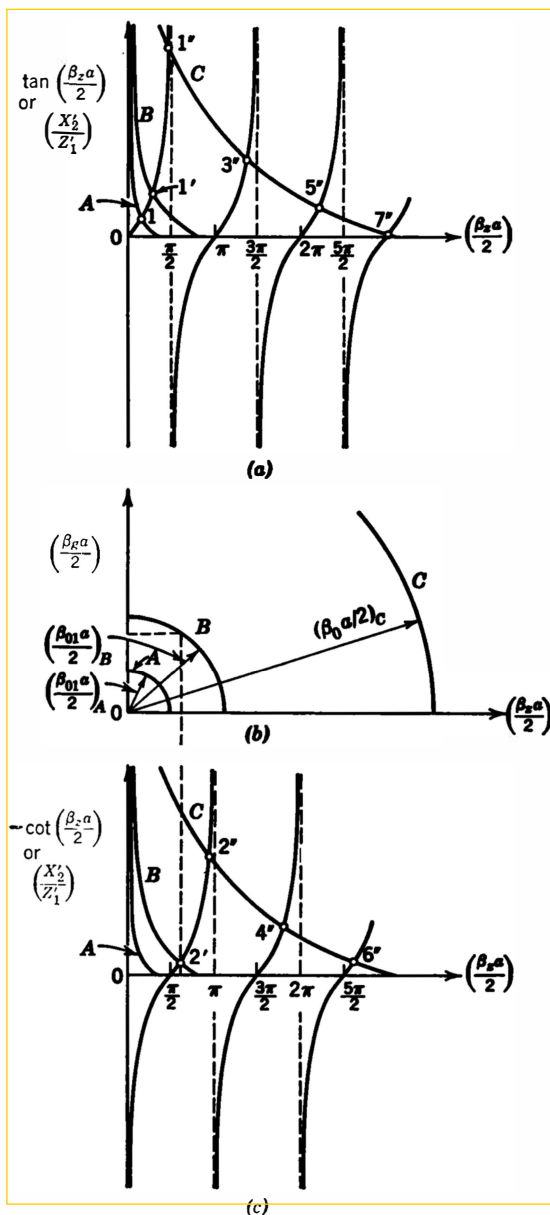


**Fig. 7.33.** Solution for TM-wave propagation constants for Fig. 7.32. (a), (b), and (c) represent Eqs. 7.148a and 7.151, Eq. 7.150, and Eqs. 7.148b and 7.151 respectively. Points marked (0) are solutions for  $\beta_z$ . Parts (a) and (b) also apply to TM waves, and (c) and (b) to TE waves, for Fig. 7.35.

upper bound (Eq. 7.152) increases directly with  $\omega$ . There are then many intersections (1'' through 7'') of the curves in Figs. 7.33a and 7.33c, which represent solutions to Eqs. 7.148. Evidently many of these TM waves can propagate together along the slab at high frequencies.

As frequency is lowered continuously, the various intersection points in Figs. 7.33a and 7.33c slide downward (see points 1'', 1', and 1, or 2'' and 2'), each on its own (positive) branch of the tan or  $-\cot$  function. Accordingly we can identify each such (positive) branch with a field solution or "mode" whose properties change continuously with frequency. At least this appears to be the case for any such branch until a frequency is reached for which the intersection arrives at the abscissa. (Refer to points 2'' and 2' on curves C and B in Fig. 7.33c, and then especially to curve A there.) Any additional lowering of the frequency suddenly leaves us with *no solution corresponding to this mode! The wave under consideration simply ceases to exist.*

In surprising contrast with our metal wave-guide solutions, the present ones do *not* go into an attenuating condition *below* cutoff, but rather reach a cutoff (or *critical*) condition and vanish forthwith from the scene.

The explanation for this behavior is found by computing the angle  $\vartheta_1$  in Fig. 7.32 at the *critical* frequency  $\omega_{\text{crit}}$  of any mode. At such frequency, the end point of validity of Eq. 7.151 falls at the base of a positive branch of the tan or  $-\cot$  function, as would occur for example at a frequency between  $\omega_A$  and  $\omega_B$  on branch 2''-2' in Fig. 7.33c. Then from Eq. 7.151

$$\beta_{z\text{crit}}^2 = \beta_{01\text{crit}}^2 - \beta_{02\text{crit}}^2 \quad (7.154)$$

and from Eq. 7.150

$$\beta_{g\text{crit}}^2 = \beta_{01\text{crit}}^2 - \beta_{z\text{crit}}^2 = \beta_{02\text{crit}}^2 \quad (7.155)$$

But in general

$$\beta_g = \beta_{01} \sin \vartheta_1$$

so

$$\sin(\vartheta_{1\text{crit}}) = \frac{\beta_{g\text{crit}}}{\beta_{01\text{crit}}} = \frac{\beta_{02\text{crit}}}{\beta_{01\text{crit}}} = \frac{v_1}{v_2} \quad (7.156)$$

This result shows that at the critical frequency, the internal reflections have just reached the critical angle. Any lower frequency will bring the incident angle below critical, and there will be no basis for confining the waves to the slab.

A calculation of the critical frequencies in terms of the geometry stems from recognizing that the intersection points on Figs. 7.33a and 7.33c fall at zeros of the tan or  $-\cot$  functions, in addition to being

end points of curves like A, B, or C. These zeros, in both figures, can be summarized by the statement

$$\begin{aligned} \beta_{zm\text{crit}} &= \frac{m\pi}{a} & m = 0, 1, 2, \dots \\ \text{or} \\ \lambda_{zm\text{crit}} &= \frac{2a}{m} & m = 0, 1, 2, \dots \end{aligned} \quad (7.157)$$

even values of  $m$  arising from Fig. 7.33a and odd values of  $m$  from Fig. 7.33c. With Eq. 7.154, Eq. 7.157 becomes

$$\omega_{merit} = \frac{m\pi}{a\sqrt{\epsilon_1\mu_1 - \epsilon_2\mu_2}} \quad m = 0, 1, 2, \dots \quad (7.158)$$

The existence of one TM solution which persist down to zero frequency is a remarkable feature of these results. It occurs in the case  $m = 0$  in Eq. 7.158, leading to  $\omega_{0\text{crit}} = 0$ . This solution corresponds to branch I'', I', I, in Fig. 7.33a. Thus very low frequency waves may, in principle, be guided by a dielectric sheet.

Before extrapolating this conclusion any further, however, attention is directed to the fact that for any TM mode at high frequencies

$$\beta_{gm} \xrightarrow[\omega \rightarrow \infty]{} \beta_{01} = \omega\sqrt{\epsilon_1\mu_1} \quad (7.159)$$

This follows from the feature of Figs. 7.33a and 7.33c that

$$\beta_{zm} \xrightarrow[\omega \rightarrow \infty]{} \frac{(m+1)\pi}{a} \quad m = 0, 1, 2, \dots \quad (7.160)$$

which remains finite, while in Eq. 7.150  $\beta_{01}$  (and hence  $\beta_g$ ) approaches infinity with  $\omega$ . At high frequencies, then, one expects most of the real longitudinal power flow to occur within the slab (medium 1), inasmuch as its phase velocity dominates the longitudinal propagation. A check upon this conclusion is supplied by the relation

$$\alpha_2 = \sqrt{\beta_g^2 - \beta_{02}^2} \xrightarrow[\omega \rightarrow \infty]{} \omega\sqrt{\epsilon_1\mu_1 - \epsilon_2\mu_2} \xrightarrow[\omega \rightarrow \infty]{} \infty \quad (7.161)$$

The penetration of the field into medium 2, outside the slab, becomes arbitrarily small at high frequencies as the transverse attenuation becomes indefinitely large.

On the other hand, Eqs. 7.161 and 7.155 show that

$$\begin{aligned} (a) \quad \beta_g &= \beta_{02} \\ (b) \quad \alpha_2 &= 0 \end{aligned} \quad \left. \right\} \quad \text{at } \omega = \omega_{\text{crit}} \quad (7.162)$$

The field extends uniformly to infinity outside the slab, in medium 2, at the critical frequency. An infinite amount of real longitudinal power is carried *outside* medium 1! Medium 2 dominates the longitudinal propagation constant [Eq. 7.162a]. The spread of the field outward from the slab increases as frequency drops toward the critical one, even if the critical frequency is zero. While the lowest TM mode can therefore *in principle* be excited at very low frequencies, the extension of the field far beyond the slab requires that any source supply large amounts of total power to do so. Just as is the case in any critical reflection (*at* the critical angle), the field in medium 2 at frequency  $\omega_{\text{crit}}$  becomes a *uniform plane wave* traveling along  $-y$ . When  $\omega_{\text{crit}} = 0$ , this behavior is approached, but never actually reached, as  $\omega \rightarrow \omega_{\text{crit}} = 0$ .

An examination of Fig. 7.32b shows the standing-wave character of the field distribution across the  $z$  dimension of the slab (in medium 1). The impedance  $Z_2'$  is a function of frequency (see Eqs. 7.161 and 7.162):

$$(a) \quad Z_2' \xrightarrow[\omega \rightarrow \infty]{} -j\eta_2 \sqrt{\left(\frac{v_2}{v_1}\right)^2 - 1}$$

$$(b) \quad Z_2' \xrightarrow[\omega = \omega_{\text{crit}}, \neq 0]{} 0 \quad (7.163)$$

Equation 7.163b makes clear the reason for the “half-wave” conditions (Eq. 7.157) at the critical frequency. It also clarifies the fact that  $E_{y2} = 0$ , which supports the previous contention that the field in medium 2 is a uniform plane wave traveling along  $-y$  at this frequency. Characteristically different from the modes in a metal wave guide, these modes *do* change their field distributions over the guide cross section as frequency is altered. Concentrated strongly within the slab at high frequencies, the field energy of a given mode spreads laterally into the surrounding space as the frequency is lowered until, finally, at the critical frequency, it has spread to infinity and no further guided wave of that mode can be supported at reduced frequencies.

Sketches of  $\beta_g(\omega)$  for the various TM modes discussed can be made essentially by visualizing carefully Fig. 7.33 and noting Eqs. 7.153, 7.159, 7.160, and 7.162a. In this connection it helps, however, to consider analytically the slope  $(d\beta_g/d\omega) = v_{\text{group}}^{-1}$ , implicitly defined by Eqs. 7.148, 7.151, and 7.150. From the derivative with respect to  $\omega$  of Eq. 7.150, we have

$$\frac{d\beta_g}{d\omega} = \left(\frac{\beta_{01}}{\beta_g}\right) \left(\frac{d\beta_{01}}{d\omega}\right) - \left(\frac{\beta_z}{\beta_g}\right) \left(\frac{d\beta_z}{d\omega}\right) = \frac{\beta_{01}^2}{\omega\beta_g} - \frac{\beta_z}{\beta_g} \left(\frac{d\beta_z}{d\omega}\right) \quad (7.164)$$

Because Fig. 7.33 or Eq. 7.160 shows that  $(d\beta_z/d\omega) \xrightarrow{\omega \rightarrow \infty} 0$  for any given mode, and in view of Eqs. 7.159 and 7.160, Eq. 7.164 tells us that

$$\left( \frac{d\beta_g}{d\omega} \right)_{\omega \rightarrow \infty} \rightarrow \frac{\beta_{01}}{\omega} = \sqrt{\epsilon_1 \mu_1} = \frac{1}{v_1} \quad (7.165)$$

The group velocity at high frequencies is dominated by the medium (medium 1) in which most of the energy is concentrated at these frequencies.

At the critical frequency, however, Eqs. 7.162 and 7.154 convert Eq. 7.164 to read

$$\begin{aligned} \left( \frac{d\beta_g}{d\omega} \right)_{\omega_{\text{crit}}} &= \frac{\beta_{01}}{\beta_{02}} \left( \frac{d\beta_{01}}{d\omega} \right)_{\omega_{\text{crit}}} - \left( \frac{\sqrt{\beta_{01}^2 - \beta_{02}^2}}{\beta_{02}} \right)_{\omega_{\text{crit}}} \left( \frac{d\beta_z}{d\omega} \right)_{\omega_{\text{crit}}} \\ \text{or} \\ \left( \frac{d\beta_g}{d\omega} \right)_{\omega_{\text{crit}}} &= \frac{v_2}{v_1} \left[ \frac{1}{v_1} - \sqrt{1 - \left( \frac{v_1}{v_2} \right)^2} \left( \frac{d\beta_z}{d\omega} \right)_{\omega_{\text{crit}}} \right] \end{aligned} \quad (7.166)$$

where it is understood that the derivatives are taken as limits for  $\omega \rightarrow \omega_{\text{crit}}$  only.

To compute  $d\beta_z/d\omega$ , note that from the right side of Eq. 7.148a we have on one hand

$$\frac{d}{d\omega} \left( \tan \frac{\beta_z a}{2} \right) = \frac{1}{\cos^2 [(\beta_z a)/2]} \frac{a}{2} \frac{d\beta_z}{d\omega} \quad (7.167a)$$

with a similar result for Eq. 7.148b:

$$\frac{d}{d\omega} \left( -\cot \frac{\beta_z a}{2} \right) = \frac{1}{\sin^2 [(\beta_z a)/2]} \frac{a}{2} \frac{d\beta_z}{d\omega} \quad (7.167b)$$

On the other hand, from the left side of Eqs. 7.148, making use of Eq. 7.151, we find

$$\frac{d(X_2'/Z_1')}{d\omega} = \frac{\epsilon_1(\beta_{01}^2 - \beta_{02}^2)}{\epsilon_2 r \beta_z^3} \left( \frac{\beta_z}{\omega} - \frac{d\beta_z}{d\omega} \right) \quad (7.168a)$$

with

$$r \equiv \sqrt{\left( \frac{\beta_{01}^2 - \beta_{02}^2}{\beta_z^2} \right)} - 1 \quad (7.168b)$$

That is, the value of  $d\beta_z/d\omega$  is computed by equating Eqs. 7.167 and 7.168a, which yields

$$\frac{d\beta_z}{d\omega} = \frac{\beta_z}{\omega} \left( \frac{1}{1 + \{(a \epsilon_2 \beta_z^3) / [2 \nu^2 \epsilon_1 (\beta_{01}^2 - \beta_{02}^2)]\}} \right) \leq \frac{\beta_z}{\omega} \quad (7.169a)$$

where

$$\nu = \cos(\beta_z a/2) \text{ or } \sin(\beta_z a/2) \quad (7.169b)$$

according to whether we are dealing with Eq. 7.148a or 7.148b respectively.

In the particular case  $\omega \rightarrow \omega_{\text{crit}}$ , we observe that  $v^2 \rightarrow 1$  and  $\beta_{z\text{crit}}$  is given by Eqs. 7.154 and 7.157. So Eq. 7.169a becomes

$$\left( \frac{d\beta_z}{d\omega} \right)_{\omega \rightarrow \omega_{\text{crit}}} = \sqrt{\epsilon_1 \mu_1 - \epsilon_2 \mu_2} = \frac{1}{v_1} \sqrt{1 - \left( \frac{v_1}{v_2} \right)^2} \quad (7.170)$$

which gives us in Eq. 7.136

$$\left( \frac{d\beta_g}{d\omega} \right)_{\omega_{\text{crit}}} = \frac{1}{v_2} \quad (7.171)$$

Again, the group velocity is dominated by the medium in which most of the field energy is concentrated.

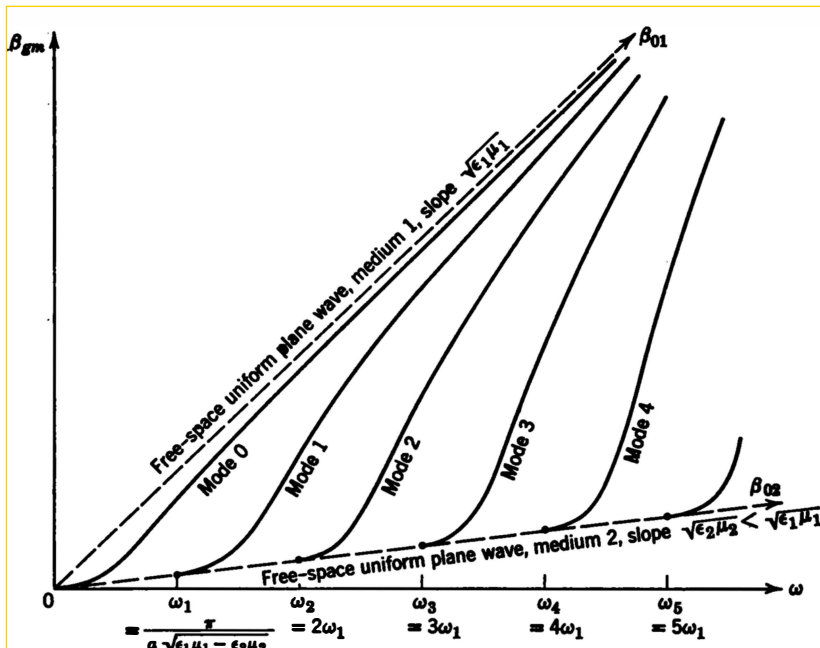


**Fig. 7.34.** Phase constants  $\beta_{gm}$  versus frequency  $\omega$  for TM modes for Figs. 7.32 and 7.33. Same general form, with same critical frequencies  $\omega_m$ , applies to TE waves. Even-order modes also apply to TM waves for Fig. 7.35. Odd-order modes also apply to TE waves for Fig. 7.35.

At intermediate frequencies  $\omega_{\text{crit}} < \omega < \infty$ , Eqs. 7.164, 7.169a, and 7.150 show that

$$\frac{d\beta_g}{d\omega} \geq \frac{\beta_{01}^2}{\omega\beta_g} - \frac{\beta_z}{\beta_g} \left( \frac{\beta_z}{\omega} \right) = \frac{\beta_g}{\omega} \quad (7.172)$$

which means that the group velocity cannot exceed the phase velocity in these modes.

Figure 7.34 shows the general form of  $\beta_{gm}(\omega)$  based upon all the preceding considerations. It should be compared with Fig. 7.31 for the rectangular metal wave guide. An analysis for TE modes (electric field parallel to the boundaries) yields similar results, with the same set of critical frequencies. This case is taken up in the Problems.

### 7.5.3 Combination Metal and Dielectric Wave Guide \*

As our final example, we ask whether a perfectly conducting metal surface, upon which is coated a layer of lossless dielectric, may serve to guide electromagnetic waves. The configuration is shown in Fig. 7.35a.

The TM case is most interesting, and we start again with the idea of successive total internal reflection from the boundary at  $z = 0$ . In this case, however, we shall have metallic reflection at  $z = -a/2$ , and the equivalent transmission-line picture relevant to the  $z$ -axis directions is shown in Fig. 7.35b. Compare Figs. 7.35 and 7.32.

Equation 7.144 with  $a/2$  in place of  $a$  expresses line conditions at  $z = -a/2$  looking to the right. This time, though, we wish  $E_{y1} = 0$  at  $z = -a/2$  on account of the metal surface. Looking to the left therefore, the metal requires  $\bar{\Gamma}'_{\text{left}}(-a/2) = -1$ , or looking to the right the metal demands the reciprocal  $\bar{\Gamma}'_{\text{right}}(-a/2) = (1/-1) = -1$ . Using Eq. 7.144 with this condition, and  $a/2$  for  $a$  yields

$$\bar{\Gamma}' \left( -\frac{a}{2} \right) = e^{j(\psi' - \beta_z a)} = -1 \quad (7.173)$$

which says simply that the metal surface must fall at a node of  $E_{y1}$ . Therefore

$$\psi' - \beta_z a = \pm(2n + 1)\pi \quad n = 0, 1, 2, \dots \quad (7.174)$$

or in view of Eq. 7.124

$$\frac{X_2'}{Z_1'} = \tan \left( \frac{\beta_z a}{2} \right) \quad (7.175)$$

where only positive values of  $\beta_z$  are of interest. The result (Eq. 7.175) is identical with Eq. 7.148a. All other considerations pertinent to the

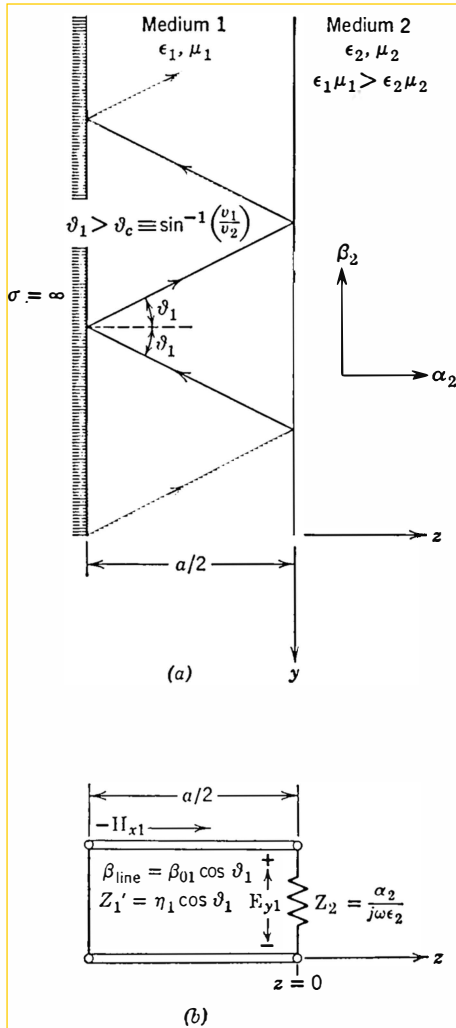


**Fig. 7.35.** Metal surface with dielectric coating (medium 1) as a wave guide. (a) Mechanism of successive reflections, alternately total internal ( $z = 0$ ) and metallic ( $z = -a/2$ ); (b) transmission-line representation with respect to  $z$ -axis (TM case, II parallel to boundaries).

details of solution, excluding Eq. 7.148b and Fig. 7.33c, but including Figs. 7.33a and 7.33b, apply to this case.

In the present problem, then, there are only half as many TM solutions as we had for the dielectric slab alone. In particular, only the cases of  $m$  even in Eq. 7.157 apply here. This is reasonable because, if we consider the solutions to the dielectric slab problem, symmetry requires that half of them will have nodes of  $E_{y1}$  at the middle of the slab and the rest will have maximum values of  $E_{y1}$  at the middle. The

clearest picture of this situation occurs at the critical frequencies (Eq. 7.157) where the slab width  $a$  is seen to be an *even* multiple of  $(\lambda_z/2)$  for  $m$  even, but an *odd* multiple of  $(\lambda_z/2)$  for  $|m|$  odd. With the comments following Eq. 7.163b, it is clear that only those solutions with  $m$  even do in fact have  $E_{y1} = 0$  on the plane  $z = -a/2$ , and for these cases we could slip in an infinitely thin conducting sheet on this plane to achieve a solution to our present problem. The *even-order* curves of Fig. 7.34 (derived from Fig. 7.33a) apply to these TM waves. It is interesting that one of the solutions preserved is that with  $\omega_{\text{crit}} = 0$ ; thus, subject to the general power limitations discussed previously, the dielectric-coated metal sheet can support low-frequency guided waves of the TM type.

Since only Figs. 7.33a and 7.33b apply to the metal-and-dielectric-guide problem, there are evidently "gaps" in the values of  $(\beta_z a)/2$  covered by these TM solutions. For example  $\pi/2 < \beta_z a/2 < \pi$  is not possible. These gaps were "filled in" by Fig. 7.33c for the dielectric-sheet case. In the present configuration, however, a study of the TE waves (in the Problems) shows that they just fill in the gaps by leading to Fig. 7.33c. They lead correspondingly to the odd-order curves of Fig. 7.34. This means, of course, that the TE and TM waves do *not* have the same critical frequencies in this case, and that *there is no TE mode which propagates at very low frequencies (i.e., for which  $\omega_{\text{crit}} = 0$ )*.

An interesting application of the lowest TM mode for "one-wire transmission" was first made by Goubau<sup>1</sup> (Fig. 7.36a). He actually uses the similar solution which applies to a round metal wire coated with a dielectric layer (just rust or corrosion will suffice, though it is not the most efficient arrangement). The nature of the field is quite like that of Fig. 7.35a if we visualize the metal and dielectric sheet bent around so that the  $x$ -axis becomes the perimeter of a circle ( $\varphi$ -coordinate), the  $z$ -axis becomes the radial coordinate ( $\rho$ ), and  $y$  becomes the longitudinal direction ( $z$ ). The coating is thin, and the field usually spreads outward transversely by many wire diameters. Most of the power is carried *outside* the wire and coating. The "launching" arrangement (Fig. 7.36b) takes this spreading into account by employing a coaxial-line feed with the outer conductor flared into a horn. A similar "receiving" horn collects the power at the other end. The arrangement is especially good for straight unimpeded runs, as suggested by Fig. 7.36b, but it may be used under other circumstances where sharp bends or serious discontinuities do not occur too frequently.

<sup>1</sup> George Goubau, "Single-Conductor Surface-Wave Transmission Lines," *Proc. IRE*, 39, 6, June 1951, pp. 619-624.

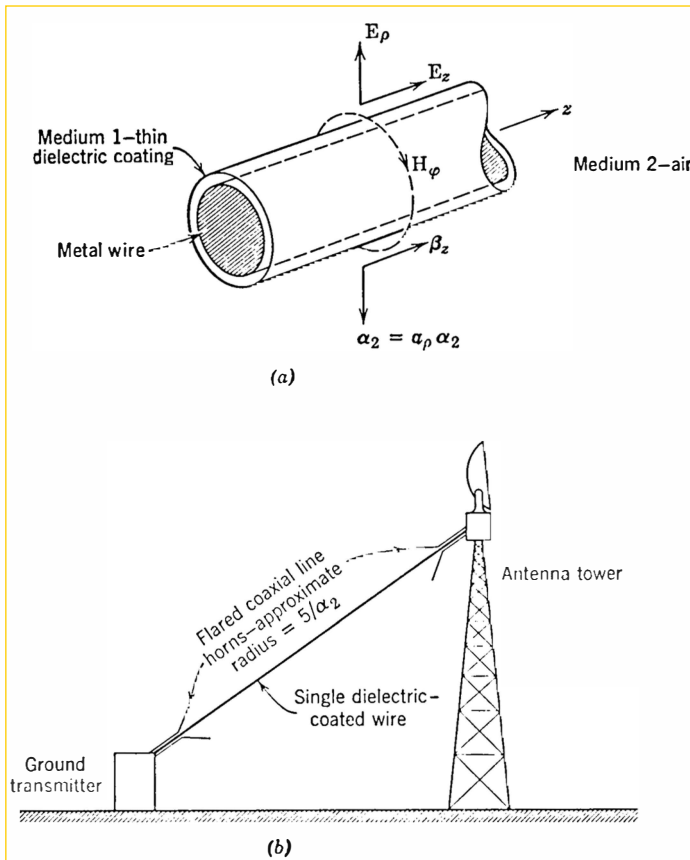


**Fig. 7.36.** Application of lowest TM mode on dielectric-coated metal surface to "one-wire" transmission. (a) Circular form of Fig. 7.35a; (b) use of single wire, showing flared coaxial horns to launch and receive TM mode.

quently. At these, the critical-reflection guidance feature of the system would fail, and some loss by radiation would result.

We have considered some of the simplest examples of waves guided by lossless media. In more complicated problems, the coordinate systems may become more elaborate, and mixtures of TE and TM waves together may be required to meet the boundary conditions. We have attempted to go only far enough with guided-wave concepts to introduce the major points of physical significance, and to place on firm ground our understanding of uniform and nonuniform plane

waves. Some further elaboration of guided waves is taken up in the Problems. To treat additional details here would quickly carry us into the realm of specialized methods and studies.

## PROBLEMS

**Problem 7.1.** (a) Write a complete set of Maxwell's equations for a source-free region with constant parameters  $\epsilon, \mu, \eta$ . Specialize the equations to the case in which the electromagnetic fields are independent of  $x$  and  $y$ . (b) Find the most general solutions to these equations for the  $z$  components of the fields and for the charge density. Under what conditions would  $\rho = \rho_0$ , a constant, be a suitable solution? (c) Find all the degenerate solutions for  $E_x$  and  $H_y$  which have the special forms: (i)  $E_x = E_x(z)$ ; (ii)  $E_x = E_x(t)$ ; (iii)  $H_y = H_y(z)$ ; (iv)  $H_y = H_y(t)$ . Repeat also for  $x$  and  $y$  interchanged in (i)–(iv) above. (d) Define the necessary and sufficient conditions to be placed upon Maxwell's equations so that *only* uniform plane waves will be solutions. (e) It has been suggested that because of the possibility of solutions (b) and (c), "light" is not necessarily a transverse wave phenomenon. Do you agree? Support your position with examples.

**Problem 7.2.** Make perspective sketches, corresponding to those of Figs. 7.1a and 7.1c, showing the orientations of the field vectors of two orthogonal plane waves traveling in the  $-z$  direction.

**Problem 7.3.** With reference to Sec. 7.1 of the text, consider in the time domain the pair of plane waves,  $E_{TA}^+ = aE_1^+ + bE_2^+$ ,  $H_{TA}^+ = \frac{1}{\eta} a_z \times E_{TA}^+$  and  $E_{TB}^+ = cE_1^+ + dE_2^+$ ,  $H_{TB}^+ = \frac{1}{\eta} a_z \times E_{TB}^+$ , in which  $a, b, c$ , and  $d$  are real constants and  $E_1^+$  and  $E_2^+$  are oriented respectively in the  $a_x$  and  $a_y$  directions. (a)  $E_1^+$  and  $E_2^+$  are linearly independent vectors because they lie in different (in fact, perpendicular) directions. Are  $E_1^+$  and  $E_2^+$  always linearly independent? Give examples. (b) Determine necessary and sufficient conditions for  $E_{TA}^+$  and  $E_{TB}^+$  to be linearly independent. Describe your results in words. (c) Waves  $A$  and  $B$  (described respectively by  $E_{TA}^+$  and  $E_{TB}^+$ ) are said to be orthogonal in the time domain if the instantaneous power density carried by waves  $A$  and  $B$  together equals the sum of the power densities of the individual waves. What restrictions must be imposed on  $E_{TA}^+$  and  $E_{TB}^+$  if the two waves are to be orthogonal in the time domain? State your result in words. (d) Express the restrictions found in (c) in terms of the components  $E_1^+$  and  $E_2^+$  of  $E_{TA}^+$  and  $E_{TB}^+$ , and interpret the results for all possible circumstances regarding  $E_1^+$  and  $E_2^+$ .

**Problem 7.4.** The components of the complex electric field of a uniform plane wave propagating in the  $+z$  direction are  $E_{x0}^+ = |E_{x0}^+| e^{j\vartheta_z}$ ,  $E_{y0}^+ = |E_{y0}^+| e^{j\vartheta_y}$ . (a) Show that the locus in time of the tip of the electric field vector satisfies the equation

$$\left(\frac{E_x^+}{|E_{x0}^+|}\right)^2 - 2 \frac{E_x^+ E_y^+}{|E_{x0}^+| |E_{y0}^+|} \cos \delta + \left(\frac{E_y^+}{|E_{y0}^+|}\right)^2 = \sin^2 \delta$$

where  $\delta = \vartheta_y - \vartheta_x$ . (b) Show that the coordinate axes, which in general do not

coincide with the principal axes of the ellipse obtained above, can be brought into coincidence with them by a rotation about the  $z$ -axes through an angle  $2\varphi$  where

$$\tan 2\varphi = \frac{2|E_{x0}^+| |E_{y0}^+|}{|E_{x0}^+|^2 - |E_{y0}^+|^2} \cos \delta$$

- (c) Under what conditions does the ellipse degenerate into a straight line? a circle?  
 (d) A uniform method of describing the sense in which the  $\mathbf{E}$ -vector traces out the polarization ellipse has not been adopted in the scientific literature. The most common practice is to view the fields looking in the direction *opposite* to the direction of propagation, i.e., in the negative  $z$  direction here, and then describe the polarization as being "right-handed" or "left-handed," depending on whether it is clockwise or counterclockwise respectively in this view. Under what analytical conditions is the polarization right-handed?

**Problem 7.5.** The components in the  $x, y$ -plane of the complex electric field of a plane wave are  $E_x$  and  $E_y$ . The complex ratio  $R_E = E_y/E_x$ , which can be represented as a point in a complex plane, determines the polarization in the  $x, y$ -plane. In other words, each point of what may be called the R-plane has associated with it a different elliptic polarization. (a) Prepare a sketch of the R-plane in which at representative points (e.g., points on the unit,  $\sqrt{3}$  and 2 circles which intersect the axes and the  $45^\circ$  lines) a small ellipse is drawn showing (roughly) the inclination and relative ratio of the axes of the polarization ellipse as well as the direction of rotation about the ellipse. See Prob. 7.4. (b) If the  $E_x$  and  $E_y$  are components of a uniform plane wave propagating in the  $+z$  direction, what is the ratio  $R_H$  of the complex magnetic field components in terms of  $R_E$ ? Describe how the diagram constructed in (a) can be used to obtain the polarization ellipse of the magnetic field corresponding to a given polarization of the electric field. (c) A certain medium has the characteristic that it propagates plane waves in pairs, such that to each wave with polarization in the  $x, y$ -plane described by the ratio  $R_E$  corresponds another wave with ratio  $R_{E2} = 1/R_E$ . Describe how the sketch prepared in (a) can be used to relate the polarizations of corresponding waves.

**Problem 7.6.<sup>1</sup>** Two statistically independent noise voltages, each of zero mean value, are applied respectively to the horizontal and vertical plates of an oscilloscope. (a) Sketch one of the patterns that might be traced on the scope face in a short observation interval. (b) Suppose that the two noise voltages have equal rms values and that each is characterized by a Gaussian amplitude distribution. Show that, if these voltages are regarded as the  $x$  and  $y$  components of the electric field of a uniform plane wave, this wave will be "randomly" polarized, as defined in the text. (c) Is the polarization still "random" if the two noise voltages are Gaussian, but have different rms values? Explain. (d) Let the probability densities of the two noise voltages be  $p(x)$  and  $q(y)$  respectively. Find all pairs of densities  $[p, q]$  such that the polarization of the uniform plane wave discussed in (b) is "random."

**Problem 7.7.** The complex electric field vector of an electromagnetic wave in free space (vacuum) is given by the expression  $\mathbf{E} = 10^{-4}(a_x - ja_y)e^{-j20\pi z} \text{ v/m}$ . (a) Find the frequency. (b) Sketch the instantaneous electric field vector  $\mathbf{E}(t, z)$  at  $z = 0$ .

<sup>1</sup>This problem requires a little familiarity with the principles of probability and statistics.

showing on a single diagram its magnitude and orientation at times  $t = 0$ ,  $t = 1/4\lambda$ ,  $t = 1/2\lambda$ , and  $t = 3/4\lambda$ . (c) Repeat (b) at  $z = 0.025 \text{ m}$ . (d) What is the type of polarization of the wave? (e) Find the complex magnetic field  $\mathbf{H}$ . (f) Repeat (b) and (e) for the instantaneous magnetic field vector  $\mathbf{H}(t, z)$ . (g) Find the complex Poynting vector  $\mathbf{S}$  and the instantaneous Poynting vector  $\mathbf{S}$  for the wave.

**Problem 7.8.** Given the following complex amplitude for a sinusoidal electric field in a vacuum  $\mathbf{E} = 10(a_x + j0.4a_y + j0.3a_z)e^{+j0.6\theta}e^{-j0.8z}$ . (a) What kind of disturbance is represented by this field and what is its frequency? (b) What is its direction of propagation? (c) What is its state of polarization? Explain. (d) Find the associated magnetic field. (e) Find the average power flow per square meter normal to the direction of propagation.

**Problem 7.9.** A traveling uniform plane wave propagates in air in a direction making equal acute angles with the  $+x$ -,  $+y$ -, and  $+z$ -axes. The electric field vector lies at all times in a plane parallel to the  $x$ ,  $y$ -plane, and at  $x = y = z = 0$  has a magnitude,  $|E_1(0, 0, 0, t)| = f(t)$ . (a) Express analytically the electric and magnetic fields,  $E_1(x, y, z, t)$  and  $H_1(x, y, z, t)$ , of the wave. (b) Express analytically the electric and magnetic fields,  $E_2(x, y, z, t)$  and  $H_2(x, y, z, t)$ , of a second traveling uniform plane wave that is propagating in the same direction as wave 1, has  $|E_2(0, 0, 0, t)| = f(t)$ , but is orthogonal to wave 1.

**Problem 7.10.** A uniform plane wave is moving in the  $z$  direction with  $\mathbf{E} = a_x 100 \sin(\omega t - \beta z) + a_y 200 \cos(\omega t - \beta z)$ . (a) Express  $\mathbf{H}$  by use of Maxwell's equations. (b) If the wave encounters a perfectly conducting  $x$ ,  $y$ -plane at  $z = 0$ , express the resulting  $\mathbf{E}$  and  $\mathbf{H}$  for  $z < 0$ . (c) Find the magnitude and direction of the surface current density on the perfect conductor.

**Problem 7.11.** A uniform plane wave in free space strikes normally a semi-infinite slab of lossless material. In the free space, the standing wave ratio is 3. In the material, the wave length is shorter by a factor of 6 than it is in free space. Find the relative permeability  $\mu/\mu_0$  and relative permittivity  $\epsilon/\epsilon_0$  of the material.

**Problem 7.12.** A uniform plane wave,  $f = 3.75 \times 10^7 \text{ cps}$ ,  $x$ -polarized, strikes normally a slab of lossless dielectric backed by a perfectly conducting layer. The dielectric has  $\epsilon/\epsilon_0 = 4$  and is 1.0 m thick. (a) What is  $\Gamma$  at the air-dielectric interface? (b) Sketch to scale the amplitudes  $|E_x|$  and  $|H_y|$  as functions of  $z$  outside and inside the dielectric. (c) If the thickness of the dielectric is 2.0 m, what change occurs in (b)?

**Problem 7.13.** (a) Find the three lowest frequencies at which all the incident power in Fig. 7.37 will be transmitted. The permeability of all media is  $\mu_0$ . (b) If complete

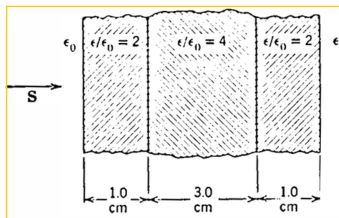


Fig. 7.37. Problem 7.13.

transmission is required for *any* thickness of the center medium, what is the lowest usable frequency? (c) For the situation shown in the figure, find the bandwidth of the transmission between its two lowest percentage values adjacent to and on either side of the frequency of (b). Find also these lowest percentage values of the transmission. (d) Why does the reflection from the modern coated optical lenses tend to be purple in color?

**Problem 7.14.** A slab of lossless dielectric has constant parameters  $\epsilon_1$ ,  $\mu_1$ , and thickness  $l$ . It is interposed normal to the direction of propagation of a uniform plane wave in free space. (a) Sketch the transmission-line analog of the system. (b) Sketch the transmission efficiency of the sheet versus its thickness measured in *free space* wave lengths. Take  $\mu_1 = \mu_0$  and  $\epsilon_1 = 2.25\epsilon_0$  as an example. Sketch on the same axes the reflection efficiency. (c) Under what conditions (on  $\epsilon_1$ ,  $\mu_1$ ,  $l$ , and the frequency) does the slab behave with respect to points outside it like a lumped capacitor shunted across a free-space transmission line? (d) The results of (a) suggest that a pane of window glass (for which  $\epsilon \cong 2.25\epsilon_0$  at optical frequencies) can distort the color of a scene viewed through it, and, particularly, of a scene reflected in it! Why is this suggestion false? Calculate the number of maxima of the transmission or reflection efficiency of a  $\frac{1}{4}$ -in. sheet of glass for normal incidence in the wave-length range of visible light ( $4 \times 10^{-7} \text{ m} < \lambda_0 < 7 \times 10^{-7} \text{ m}$ ). (e) Make a rough estimate of the thickness of a film of oil floating on water if parts of the film appear blue and parts appear red when viewed with reflected light. The optical properties of the oil are roughly the same as those of the window glass.

**Problem 7.15.** (a) A parallel-faced slab of dielectric (medium *b*) of thickness *l* separates two different dielectric regions (media *a* and *c*). Calculate the squared magnitude of the reflection coefficient,  $|\Gamma_{12}|^2$ , for a monochromatic uniform plane wave at normal incidence from medium *a*. Assume there is no reflected wave in medium *c*. Express your result in terms of  $\Gamma_1$ , the reflection coefficient that would apply at boundary 1 between media *a* and *b* if this were the only boundary in existence, and  $\Gamma_2$ , the corresponding reflection coefficient at boundary 2 between media *b* and *c*. Interpret  $1 - |\Gamma_{12}|^2$  physically. (b) A source of broadband visible light, whose continuous power density spectrum is fairly flat over many periods of the function  $|\Gamma_{12}|^2$  found above, illuminates the slab. Assuming that the eye or other optical instrument responds to the mean square value of the reflected field strength, deduce the optical reflection efficiency  $(|\Gamma_{12}|^2)$  of the slab thus measured. Express the answer in terms of parameters  $g_1 = \Gamma_1^2$  and  $g_2 = \Gamma_2^2$ . (c) Derive the result of (b) by adding up the *powers* of the various multiply reflected components of the composite reflected wave. Calculate the optical transmission efficiency of the double boundary in the same way. (d) Optically, in situations like that discussed above, *n* parallel sheets of glass separated by air constitute  $2n$  equally reflecting boundaries in cascade. The sheet thicknesses and spacings are irrelevant. From your result of (b), calculate the optical transmission and reflection efficiencies at normal incidence of such a multiple boundary.

**Problem 7.16.** A dielectric slab (medium 2 of Fig. 7.38*a*) extends over the entire  $x$ ,  $y$ -plane. The system between the "input" and "output" planes is to be regarded as a filter whose instantaneous input and output functions are  $E_{xi}$  and  $E_{xo}$ , respectively. The filter input is a normally incident uniform plane wave. (a) For  $\epsilon_2 = 36\epsilon_0$ , find the impulse response of the system. (b) It is desired to modify the filter so that it has the new impulse response shown in Fig. 7.38*b*, in which *A* can be any

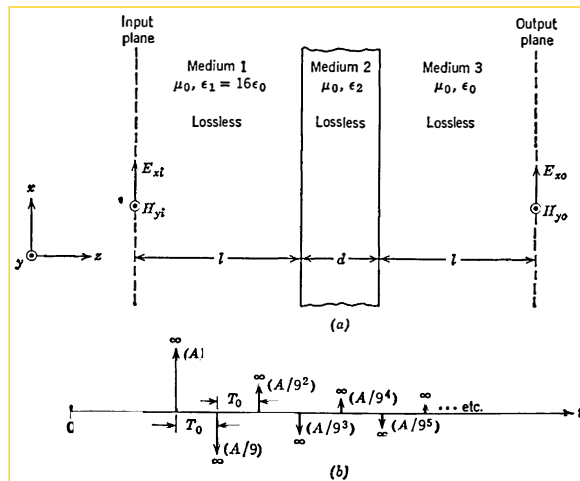


Fig. 7.38. Problem 7.16.

positive constant and  $T_0 = \frac{1}{3} \times 10^{-8}$  sec. The time interval between  $t = 0$  and the first output impulse is of no concern. Find the thickness  $d$  and the permittivity  $\epsilon_2$  of the dielectric slab required to obtain the desired impulse response.

**Problem 7.17.** In the sinusoidal steady state at frequency  $\omega$ , a linearly polarized uniform plane wave is incident at angle  $\vartheta$  upon a perfect conductor whose surface defines the  $z, y$ -plane. The incident magnetic field is parallel to the conductor, and has an amplitude  $H_0$  which it attains in the  $+x$  direction at  $x = y = z = t = 0$ .  
 (a) Write expressions for the complex-vector electric and magnetic fields  $E_i(x, y, z)$  and  $H_i(x, y, z)$  of the *incident* wave. (b) Write expressions for the complex-vector electric and magnetic fields  $E(x, y, z)$  and  $H(x, y, z)$  of the complete field solution to the problem. (c) Write the expression for the real instantaneous surface current density vector  $K(x, y, t)$  amp/m on the metal. (d) Write the expression for the real instantaneous surface-charge density  $Q_s(x, y, t)$  coulombs/m<sup>2</sup> on the metal.  
 (e) Repeat for a circularly polarized incident wave for which  $H(0, 0, 0, 0) = a_z H_0$ .  
 (f) For the case (e), when  $\vartheta = 0$ , determine the instantaneous and complex Poynting vectors,  $S(x, y, z, t)$  and  $\bar{S}(x, y, z)$  respectively, and interpret them.

**Problem 7.18.** A uniform plane wave is incident at angle  $\vartheta_1$  upon the interface between two lossless dielectrics. The (real) angle of refraction is  $\vartheta_2$ . When the polarization is parallel to the interface, the reflection coefficient is  $\gamma_2$ . (a) Find the numerical value of the transmission coefficient. (b) If the propagation direction of the transmitted wave is reversed, thus making this wave become a new incident wave with the same polarization as before, what will be the numerical values of the reflection and transmission coefficients? (c) If  $\vartheta_1 = 60^\circ$  and  $\vartheta_2 = 30^\circ$  above, repeat (a) and (b) for these same values of  $\vartheta_{1,2}$ , but with the polarization rotated  $90^\circ$ .

**Problem 7.19.** A uniform plane wave of frequency  $\omega$  polarized in the plane of incidence is obliquely incident at angle  $\vartheta$  from air onto a lossless dielectric with  $\mu = \mu_0$  and  $\epsilon > \epsilon_0$ . Measurement of standing wave ratio  $s$  is made with a probe

sensitive only to *tangential* components of electric field, and moving normal to the interfaces, for the following two cases: Case 1— $\vartheta = 30^\circ$ ,  $s = s_1$ ; Case 2— $\vartheta = 45^\circ$ ,  $s = s_2$ . It is found that  $s_2/s_1 = \sqrt{3}$ . Find: (a) The specific permittivity  $\epsilon/\epsilon_0$ , (b) The value of  $s_1$ .

**Problem 7.20.** (a) A flat plastic plate ( $\epsilon/\epsilon_0 = 2.25$ ) is 2 in. thick. A uniform-plane electromagnetic wave of frequency 10 kmc is incident on the plate at an angle  $\vartheta_1$  (from the normal). The polarization is parallel to the surface. Find all values of the angle  $\vartheta_1$  for which reflections are eliminated. (b) Repeat part (a) with the wave polarized in the plane of incidence.

**Problem 7.21.** An experiment is being designed to illustrate clearly Brewster's angle for a given plastic [ $(\epsilon/\epsilon_0) = 2.25$ ,  $\mu = \mu_0$ ,  $\sigma = 0$ ]. The method consists of measuring directly the reflected uniform plane wave field from a sheet of the material, as a function of incident angle, at a microwave frequency  $f = 10$  kmc. The plastic is very expensive, so minimum thickness is desirable. On the other hand, if the reflections are never very strong at any angle, the sensitivity of the null is poor. There is also the problem of avoiding "false" nulls (see Prob. 7.20) within the angle range considered practical (say,  $0^\circ$ – $85^\circ$ ). (a) Determine reasonable limits upon the thickness of the plastic sheet. (b) Discuss the effect upon the experiment if the incident plane wave source actually emits a pencil of waves with directions lying in a cone of small half-angle  $\alpha$  rad, and if the receiver for the reflected wave can be twisted about its own axis by  $\pm\alpha$  without changing its indication of a given uniform plane wave directed at it (twisting by more than  $\pm\alpha$  rad gives zero indication). Consider the relationships between the transverse sheet dimensions and the distances between source, sheet, and receiver. Comment also on what factors fix the angle range usable in the experiment.

**Problem 7.22.** A plane wave which in air has a 10 cm wave length is incident on an air-dielectric interface from the dielectric side. The permeability of the dielectric is equal to that of air, and  $\epsilon_1 = 4\epsilon_0$ . (a) What is the critical angle for no transmitted power into the air? (b) A nonmagnetic coating is to be added to the dielectric to make the interface nonreflecting at normal incidence, again from the dielectric side. What thickness  $d$  and dielectric constant  $\epsilon_2$  should this coating have? (c) Repeat (a) with the coating determined in (b) in place.

**Problem 7.23.** Prove or disprove: There is always one and only one angle of incidence of a randomly polarized uniform plane wave on a boundary between two lossless media, characterized by constant parameters  $(\epsilon_1, \mu_1)$  and  $(\epsilon_2, \mu_2)$ , at which the reflected wave is linearly polarized. (Caution: Bear in mind that if the angle of incidence exceeds the critical angle, the incident wave is totally reflected.) Relate the polarization of the reflected wave to the parameters of the two media for those cases in which the reflected wave is linearly polarized.

**Problem 7.24.** The boundary between two lossless dielectrics is the plane  $z = 0$ . The wave impedance and speed of light in the left-hand ( $z < 0$ ) dielectric are  $\eta_1$  and  $v_1$ ; in the right-hand dielectric these quantities are  $\eta_2$  and  $v_2$  respectively. A traveling wave having the electric field

$$E_i = a_x f \left( t + \frac{y \sin \vartheta_1 - z \cos \vartheta_1}{v_1} \right) \quad z \leq 0$$

is incident on the boundary from the left. (a) Express both electric and magnetic

fields of the incident, reflected, and transmitted waves if  $\vartheta_1$  is less than the critical angle. (b) Let  $f(\tau)$  be the rectangular pulse

$$f(\tau) = \begin{cases} 1, & |\tau| \leq \frac{1}{2} \\ 0, & |\tau| > \frac{1}{2} \end{cases}$$

and let  $\vartheta_1 = 60^\circ$ ,  $v_2 = \frac{1}{2}v_1$ , and  $\eta_2 = \eta_1$ . Sketch and dimension the contours in the  $y$ ,  $z$ -plane: amplitude of total electric field = constant. Make your contour "map" at the instant  $t = 0$ , and indicate with arrows how these contours change as time advances. (c) Now suppose  $v_2 > v_1$ , and the angle of incidence exceeds the critical angle. The electric field of the incident traveling wave is expressed in terms of the Fourier transform  $F(\omega)$  of the function  $f(\tau)$ :

$$\mathbf{E}_i = \frac{1}{2\pi} \int_{-\infty}^{+\infty} \mathbf{a}_x F(\omega) e^{i\omega(t + [(\eta \sin \vartheta_1 - z \cos \vartheta_1)/v_1])} d\omega$$

or

$$\mathbf{E}_i = \frac{1}{2\pi} \int_0^{+\infty} 2 \operatorname{Re} [\mathbf{a}_x F(\omega) e^{i\omega(t + [(\eta \sin \vartheta_1 - z \cos \vartheta_1)/v_1])}] d\omega$$

since  $\mathbf{E}_i$  is a real vector. Express similarly both the electric and magnetic fields of the reflected and transmitted waves. (d) If you had used the first given form in answering (c), would your transmission and reflection coefficients depend on frequency? How? What if you had used the second given form? What about the coefficient of  $z$ , corresponding to  $-\cos \vartheta_1/v_1$  above, in the expressions for the transmitted fields? Find two different arguments to support your answers to these questions. (e) Let  $f(\tau)$  be a unit impulse at  $\tau = 0$ . From your answer to (c), calculate, by actually performing the integrations, the electric field in the  $x$ ,  $z$ -plane on the right of the boundary. Does your calculation show this field to be zero before the arrival of the incident wave at the origin? Explain.

**Problem 7.25.** Consider Maxwell's equations for a lossless source-free region with constant permittivity  $\epsilon$  and permeability  $\mu$ . (a) Show that the rectangular vector components of the steady-state complex electric field  $\mathbf{E}$  obey the equation  $\nabla^2 \mathbf{E} + k^2 \mathbf{E} = 0$  ( $k = \omega\sqrt{\epsilon\mu}$ ) and that  $\mathbf{H}$  obeys the same equation. (b) Under what conditions on the complex constants  $\tilde{\gamma}_x$ ,  $\tilde{\gamma}_y$ , and  $\tilde{\gamma}_z$  is  $\mathbf{E}(x, y, z) = \mathbf{E}_0 e^{-(\tilde{\gamma}_x z + \tilde{\gamma}_y y + \tilde{\gamma}_z z)}$  a solution to the equation in (a), with  $\mathbf{E}_0$  a constant complex vector?

**Problem 7.26.** The complex fields produced in a certain isotropic, homogeneous, linear, time-invariant, source-free medium by a 100-mc sinusoidal source are

$$\begin{aligned} \mathbf{E} &= E_{0x} \mathbf{a}_x - 20\pi[(13 - j45)a_y + (26 + j60)a_z] e^{-\pi[(1+j5)x - (3+j)y + (4-j2)z]} \\ \mathbf{H} &= (H_{0x} \mathbf{a}_x + H_{0y} \mathbf{a}_y + H_{0z} \mathbf{a}_z) e^{-\pi[(1+j5)x - (3+j)y + (4-j2)z]} \end{aligned}$$

and it is known that  $|H_{0z}| = 7$ . (a) What can be said about the medium from the space variation of the fields? (b) Where is the source? Give a unit vector normal to a plane which separates a region in space where the fields are bounded from one where the fields are arbitrarily large. Let the unit vector point toward the strong-field region. (c) Determine the unspecified field components,  $E_{0x}$ ,  $H_{0x}$ ,  $H_{0y}$ , and  $H_{0z}$ . (d) What are the conductivity, relative permeability, and dielectric constant of the medium? (e) Describe the fields in words. Exactly what kind of wave do they represent? (f) Determine the (complex) polar angles  $\theta$  and  $\phi$  of the direction of propagation of the equivalent uniform plane wave.

<sup>1</sup> The considerable algebra required for this part should be done carefully or not at all.

**Problem 7.27.** A 900-mc nonuniform TE plane wave propagates in air in such a manner that its phase *increases* most rapidly with position in a direction parallel to, and lying in the first quadrant of, the  $x, y$ -plane. The amplitude of the  $x$ -component of the electric field is 3 v/m throughout the plane  $x - 2y + 2z = 0$ ; in the plane  $x - 2y + 2z = 1/\pi$  m, it is  $3e$  v/m. (a) Determine the (complex) propagation vector of the wave. (b) Express the most general fields that fit the problem statement. (c) Show that the complex polar angles for the direction of propagation of the equivalent uniform plane wave are  $\vartheta = \pi/2 - j \sinh^{-1} \frac{1}{3}$  and  $\tilde{\varphi} = \tan^{-1} \frac{1}{2} + j \tanh^{-1} \frac{1}{3}$ , with  $\text{Re}(\tilde{\varphi})$  in the third quadrant. Do not use a slide rule or tables.

**Problem 7.28.** Consider fields of the form  $\mathbf{E} = \text{Re}[\mathbf{E} e^{-\Omega t}]$ ,  $\mathbf{E} = \mathbf{E}_0 e^{-\tilde{\gamma} \cdot \mathbf{r}}$ ,  $\mathbf{H} = \text{Re}[\mathbf{H} e^{-\Omega t}]$ ,  $\mathbf{H} = \mathbf{H}_0 e^{-\tilde{\gamma} \cdot \mathbf{r}}$  in a lossless medium with  $\Omega$  a pure real number and  $\mathbf{E}_0, \mathbf{H}_0$  complex vectors. (a) If these fields are to satisfy Maxwell's equations, what constraints must be imposed on  $\mathbf{E}_0, \mathbf{H}_0$ , and  $\tilde{\gamma}$ ? On  $\mathbf{E}_0$  and  $\tilde{\gamma}$ ? On  $\mathbf{H}_0$  and  $\tilde{\gamma}$ ? On  $\tilde{\gamma}$  alone? (b) Express  $\mathbf{E}$  and  $\mathbf{H}$  in the case  $\tilde{\gamma}_x = \tilde{\gamma}_y = E_{0y} = H_{0z} = 0$ . Describe these fields in words. How could they be excited? Could a "uniform plane wave source" be used? (c) Examine  $\mathbf{E}$  and  $\mathbf{H}$  in the more general case,  $\tilde{\gamma} = \alpha + j\beta$ . Interrelate  $\alpha$  and  $\beta$ . Describe these fields in words. How could they be excited? (Hint: Study Sec. 7.4.3.)

**Problem 7.29.** As illustrated in Fig. 7.39, two perfectly conducting and infinitesimally thin sheets in air form a *semi*-infinite parallel-plate wave guide, with mouth in the plane  $z = 0$  and sides parallel to the  $y$ ,  $z$ -plane. Two  $y$ -polarized, steady-state uniform plane waves (1 and 2) of equal strength are incident upon the mouth of the guide at angles  $\vartheta$  shown, and their separate equiphasic surfaces of the same phase intersect in lines lying in the  $y, z$ -plane. (a) If the wave length  $\lambda$  of the incident waves is such that  $\sin \vartheta = \lambda/2a = \sqrt{3}/2$  and the peak field strength in each is 1 v/m, find the time-average power flowing down the *inside* of the guide, per meter of the  $y$  dimension. (b) Repeat (a) if wave 2 is turned off. (c) Repeat (a) if wave 2 is present but reversed in time phase. Check your result by verifying the relationships between the answers to (a), (b), (c) by a different method than the one used to get them. (d) Suppose  $\vartheta$  has a given arbitrary real value, not specially related to  $\lambda$ , and we determine by measurement that power  $\langle P_A \rangle$  goes down the inside of the guide (per meter of  $y$  dimension) when wave 1 *alone* is incident at power density level  $\langle S_1 \rangle$ . In terms of  $\langle P_A \rangle$  find: (i) The power down the guide if wave 2 is turned on with  $\langle S_2 \rangle = \langle S_1 \rangle$  and with identical phase at the origin; (ii) The result of (i) if wave 2 has reversed time phase.

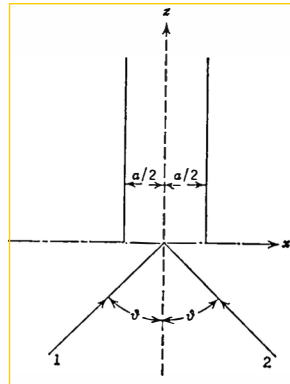


Fig. 7.39. Problem 7.29.

**Problem 7.30.** A long piece of 3-cm rectangular wave guide (inside dimensions 0.4 in.  $\times$  0.9 in.) is filled with polystyrene blocks ( $\epsilon = 2.5\epsilon_0$ ) so that the TE<sub>1,0</sub> mode will now propagate in the guide at 5 km/s. One end of the guide is connected to a matched load and the other to a 5-kmc source. In assembling the equipment, two of the blocks are separated so that there is a rectangular air-filled section of guide, having a length  $l$  and located halfway between source and load. You are

to determine fields and power flow in the vicinity of the air gap. (a) Show that only the  $\text{TE}_{1,0}$  mode transverse pattern is needed to meet boundary conditions in each of the three sections, and that the longitudinal parts of the problem may be solved by transmission-line analogy. (b) The fields in the air-filled section can be decomposed into two waves—one that decays exponentially with distance along the guide as it approaches the load end of the section, and one that decays exponentially as it approaches the source end. How much mean power is carried toward the load by each of these waves separately? Can any power reach the load when both are present together? (See Prob. 3.49.) (c) Calculate the ratio of the total electric field in the center of the guide at the boundary of the air-filled section nearest the load to the corresponding quantity at the boundary nearest the source. Show that the magnitude of this ratio does not exceed 1. (d) Calculate and sketch, as a function of  $l$ , the ratio of the load power to the power of the source wave that is *incident* on the air-filled section from the dielectric-filled one. (e) Calculate the VSWR, for  $l = 1$  in., in those sections of the guide in which the VSWR concept applies. From these results, and those of (d), discuss the electrical limitations to making out of this device an attenuator for which loss in decibels will be directly proportional to length  $l$ .

**Problem 7.31.** Consider a  $\text{TE}_{m,0}$  (+)-wave in a lossless rectangular wave guide of wide dimension  $a$  and narrow dimension  $b$ . Define "voltage"  $V_+$  as the line integral of the electric field up the center of the cross section, along a line parallel to the narrow side. Define current  $I_+$  so that  $\frac{1}{2}V_+I_+^*$  gives correctly the total complex power carried longitudinally through the cross section (as determined from the complex Poynting vector). (a) From the values of  $\gamma$  and  $Z_0 \equiv V_+/I_+$ , determine the series impedance per unit length  $Z_s$  and the shunt admittance per unit length  $Y_p$  of an equivalent transmission line for this mode. (b) Make a circuit diagram representing a length  $dz$  of the line in (a). In this diagram *all* element values must be *independent* of frequency. How does the cutoff frequency show in the equivalent circuit? (c) Identify the energy stored in each element of the equivalent circuit with that stored in the actual mode by one space component of the electric or magnetic field. (d) If a different line integral is taken to define  $V_+$ , so that  $V_+^* = KV_+$  but we still choose  $I_+$  such that  $\frac{1}{2}V_+^*I_+^*$  represents the correct complex power, reconsider your results in (a)–(c). (e) Could we choose to define "voltage" proportional to transverse magnetic field and "current" proportional to transverse electric field? Illustrate. (f) If we chose "current" proportional to *longitudinal* magnetic field, what choices are open for "voltage"? Repeat if "voltage" is chosen proportional to *longitudinal* field. Illustrate.

**Problem 7.32.** In the rarefied upper atmosphere several hundred kilometers above the earth's surface there exists a region of dense, horizontally stratified ionization caused by solar radiation. The several ionized layers are known collectively as the ionosphere. The parameters of an ionospheric layer may be taken to be  $\sigma = 0$ ,  $\mu = \mu_0$ ,  $\epsilon = \epsilon_0[1 - (\omega_p/\omega)^2]$  where  $\omega_p$ , the plasma frequency, is proportional to the square root of the electron density. (a) Obtain the propagation constant  $\gamma$  and the wave impedance  $\eta$  of a uniform plane wave in such an ionospheric layer. (b) A uniform plane wave in air of electric field  $E_1 = a_x \operatorname{Re}[E_1 e^{j(\omega t - k_z z)}]$  strikes a hypothetical abrupt boundary  $z = 0$  of an ionospheric layer from below. Neglecting reflections from the upper boundary of the layer, express the transmitted and reflected fields in the cases  $\omega > \omega_p$  and  $\omega < \omega_p$ . Sketch the squared magnitude of the reflection coefficient as a function of frequency for  $0 < \omega < 2\omega_p$ . (The re-

fection coefficient of an actual ionized layer which does not have abrupt boundaries diminishes much more rapidly with frequency when ( $\omega > \omega_p$ ) (c) On a particular date and time of day, and above a particular geographical location, the densest ionization occurs at an altitude of 400 km, and the plasma frequency of this dense ionization is  $\omega_p/2\pi = 5$  m $\mu$ . Neglecting ionization below this densest layer, determine the greatest possible angle of incidence  $\vartheta$  (Fig. 7.40) at which radiation from a ground-based transmitter could possibly strike the layer. (d) How far away from the transmitter will the reflected radiation return to earth? (e) What is the highest frequency at which this obliquely incident radiation will be totally

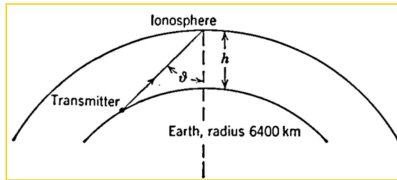


**Fig. 7.40.** Problem 7.32.

reflected? (f) A radar set is used to measure the distance to the moon at a time when the moon is at the zenith. The bandwidth of the radar signal is small compared with the difference between the center frequency of the radar signal and the plasma frequency of the ionosphere. Calculate and sketch, as a function of the radar signal center frequency, the discrepancy between the measured and actual distances to the moon caused by passage of the radar signal through a uniformly dense layer of ionization 100 km thick. What range of center frequencies may be used if this discrepancy is to be less than 1 km? Note that the model of the ionosphere implied by the problem statement has abrupt boundaries and thus would support multiple reflections of the transmitted signal and of the moon echo, both inside the ionized layer and between its lower boundary and the earth. For the purposes of this problem, it may be supposed that the radar signal is a pulsed sinusoid of short enough duration so that the first-arriving moon echo may be selected from the array of other echoes caused by unwanted or multiple reflections.